Interaction of a G protein-coupled receptor (Ste2p) of *Saccharomyces cerevisiae* with its ligand and its G-protein alpha subunit

A Dissertation Presented for the
Doctor of Philosophy Degree
The University of Tennessee, Knoxville

Li-Yin Huang
December 2011

Dedication

This dissertation is dedicated to my parents, Zen-Jun Huang and Zon-Hua Tsai, for their endless love and support. I would not be able to achieve any of this without the sacrifices they made in order for me to receive the best education possible.

Acknowledgments

I would like to thank many people who helped me throughout my studies. My first and deepest appreciation goes to my mentor Dr. Jeffrey M. Becker. He is such an enthusiastic scientist who always has great insights about research. I am thankful that he was so patient and supportive during the time I was struggling with my projects. His critical suggestions and guidance helped me overcome lots of setbacks that I would not even try without him. It is a great pleasure and honor to work for him.

I also would like to give my very appreciation to my committee members: Dr. Chunlei Su, Dr. Todd B. Reynolds, Dr. Elizabeth E. Howell, Dr. Timothy E. Sparer, and Dr. Ana Kitazono. Their extraordinary patience and encouragement motivated me. With their guidance and support, I finally learned how to become a good scientist.

I would like to thank Dr. Fred Naider for his support and valuable ideas on critical decisions throughout these studies. I also want to thank all the Dr. Naider laboratory members for the peptide syntheses that made this study possible.

I really appreciate all the lab members in Dr. Becker's laboratory: Special thanks to Dr. Melinda Hauser, Dr. Byung-Kwon Lee, and Dr. Tom Masi for their guidance and help on my study. I also want to thank Sarah Kauffman, Elena Ganusova, Steve Minkin, Heejung Kim, Giljun Park, Kyung Sik, Amanda Deyo, Madelyn Crawford, Jordan Kim, Brandon Sidney, and Seraj Uddin, who made Becker lab such an enjoyable and fun place to work at. I appreciate the help from Julie Maccarone in the biological experiments. My very special thanks belong to George Umanah for being my best friend and a great partner in the lab. Our reseach thrived on all the arguments and good discussions.

I also want to thank my favorite teachers: Lisa Meidl and Julie Moore, who helped me a lot to improve my English and lead me to know God. Thanks to Meidl boys (Bill, Peter, Nate, and Timothy), Ron and Marti Holder, Life Focus group at Sunday school, and the choir in Cedar Springs Presbyterian Church. I really appreciate all the cares from the church family, who made it feel just like home.

Last, but not the least, I would like to thank my very best friend, Jui-He Tsai (Ray). Since college to graduate school, we had been studying together for a long time. Ray is optimistic and has great personalities. It was very nice to always have him to share my struggles, laughters, tears, memories, and all the ups and downs in life. I really appreciate him.

Abstract

The G protein-coupled receptor (GPCR) family is composed of hundreds of members and is expressed in eukaryotes. Each GPCR has seven transmembrane domains and is in charge of sensing changes from the environment, transducing signals, and activating a series of biological responses. The signal transduction pathway of the receptor starts from sensing outside signal and then activates G proteins. This signaling requires a tight control for activation without which impaired cellular function leads to pathology. We have used the pheromone alpha-factor receptor (Ste2p) of the yeast *Saccharomyces cerevisiae* as a model system to understand ligand binding, receptor activation, and G protein interaction. One method we have used to study ligand binding is to incorporate the photo-reactive crosslinker p-benzoyl-L-phenylalanine (Bpa) into Ste2p to capture alpha-factor. This powerful tool requires the incorporation of Bpa, an unnatural amino acid, into Ste2p by a special genetic manipulation designed in the lab of Peter Schulz (Scripps Institute) and adapted by our lab for Ste2p. Another method to study ligand binding that we have adapted for use in our system is to incorporate a chemical crosslinker [3,4-dihydroxylphenylacetyl (DHPA)] into alpha-factor for periodate-mediated crosslinking to Ste2p. The interacting domain between alpha-factor and transmembrane domain 2 to 3 of Ste2p was identified after DOPAC crosslinking, cyanogen bromide digestion and MALDI-TOF mass spectrometry. After ligand binding, signal transduction is mediated by the interaction of activated Ste2p with its G protein (Gpa1p). We studied this interaction by replacing natural residues in the intracellular loop 3 of Ste2p and C-terminal end of Gpa1p with cysteine and then determining disulfide crosslinking between Ste2p and Gpa1p. Some residues were found to be in close proximity and displayed different interacting patterns due to conformational changes of the receptor upon ligand binding. The information we gathered here allows us to understand more about the physical interactions of alpha-factor, Ste2p, and Gpa1p and provides us insights about the initiation and activation of the signal transduction pathway of a peptide ligand receptor.

TABLE OF CONTENTS

CHAPTER **PAGE**

LIST OF FIGURES

PART I: General Introduction

PART II: Unnatural Amino Acid Replacement in a Yeast G Protein-Coupled Receptor in its Native Environment (Published previously as: TYPE IN FULL REF)

PART III: Changes in Conformation at the Cytoplasmic Ends of the Fifth and Sixth Transmembrane Helices of a Yeast G Protein-Coupled Receptor in Response to Ligand Binding

PART IV: Residue-to-Residue Interactions Between a G Protein-Coupled Receptor (GPCR) and its Gα Protein in the *Saccharomyces cerevisiae* Model System

PART V: Crosslinking of an α-factor Analog [K^0(BioACA), K^7(DHPA), Nle^{12}]α-factor (Bio-DHPA^7-α-factor) into its G Protein-Coupled Receptor, Ste2p

PART VI: General Conclusions and Future Studies

LIST OF TABLES

PART III: Changes in Conformation at the Cytoplasmic Ends of the Fifth and Sixth Transmembrane Helices of a Yeast G Protein-Coupled Receptor in Response to Ligand Binding

PART IV: Residue-to-Residue Interactions Between a G Protein-Coupled Receptor (GPCR) and its Gα Protein in the *Saccharomyces cerevisiae* Model System

PART I

General Introduction

Chapter 1

G Protein-Coupled Receptors: An Overview

Basic Information about G-Protein-Coupled Receptors

G protein-coupled receptors (GPCRs) are characterized by seven transmembrane domains with an extracellular N-terminus and intracellular C-terminus (*1*). The main function of a GPCR is to transduce extracellular signals into the cytoplasm of the cells and activate a variety of cellular responses according to different environmental stimuli. GPCRs control our sensations of vision, smell, taste, and pain (*2*), as well as responses to hormones and neurotransmitters (*3*). They are among the largest and most diverse protein families in mammalian genomes and represent targets for approximately 40% of all marketed drugs.

GPCRs serve as regulators with special structural motifs to interact with both extracellular ligands and intracellular proteins (*4*). A study examining the structure domains of three GPCRs, rhodopsin, thyrotropin stimulating hormone (TSH) receptors, and vasopressin 2 (V2) receptors, has revealed that genetic variations affect the receptors in ligand binding and G protein coupling (*5*). As the matter of relationships between GPCR structures and functions, the N-terminus and extracellular domains of GPCRs are suggested to play roles in ligand binding, intracellular trafficking, and down-regulation (*6*). Helix-helix interactions in the transmembrane domains are important to maintain the stability of the receptors in preferred structures for ligand binding and activation (*7*). Intracellular loop domains are essential for G protein interactions and signal transduction (*8-10*). Some receptors appear to exist as homodimers and heterodimers (*11*), such as the

$GABA_B$ receptor (*12*), and oligomeric assembly affects the receptor biosynthetic steps of maturation and trafficking and internalization internalization during down-regulation after signaling occurs.

GPCR Crystal Structure

Rhodopsin was the first GPCR structure to be crystallized (*13*), which set up the cornerstone for providing insights about receptor activation and interactions with ligand and G proteins. In addition to rhodopsin, crystal structures of β1 and β2-adrenergic receptors (*14-16*), adenosine receptor (*17*), CXCR4 chemokine receptor(*18*), Dopamine D3 receptor (*19*), and Histamine H1 receptor (*20*) have also been recently obtained. With the increasing availability of GPCR crystal structures, some of the key issues in GPCR biology, such as the ligand-binding pocket, extracellular disulfide bridges, and transmembrane domains orientations, have been elucidated (*21*). The information of three-dimensional GPCR structure supports homology modeling studies and benefits structure-based drug design (*22*).

Lignand binding domain of GPCR crystal structures

Rhodopsin consists of the chromophore 11-*cis*-retinal covalently linked with the protein opsin at the lysine residue at position 296 (*13*). Absorption of a photon changes the conformation of chromophore to all-*trans*-retinal and results in activation of Rhodopsin. According to the crystal structure of rhodoposin, several residues (Tyr^{43}, Met^{44}, Leu^{47}, Thr^{94}, Glu^{113}, Gly^{114}, Ala^{117}, Thr^{118}, Gly^{120}, Gly^{121}, Glu^{122}, Cys^{167}, Ser^{186},

Cys^{187}, Gly^{188}, Ile^{189}, Tyr^{191}, Met^{207}, His^{211}, Phe^{212}, Phe^{261}, Trp^{265}, Tyr^{268}, Ala^{269}, and Phe^{293}) from extracellular loops and transmembrane domains form the binding pocket for the chromophore.

The β_1-adrenergic receptor couples to the G_s pathway (adenylyl cyclase, cAMP, and protein kinase A) in cardiac cells, which when activated increases the heart rate (*23*) and induces myocyte hypertrophy and apoptosis by G_s-protein kinase A-independent activation of calmodulinkinase II signaling. The β_2-adrenergic receptor couples to G_s and G_i pathway and protects cardiomyocytes from apoptosis via a G_i–phosphatidylinositol 3 kinase (PI3K) pathway (*24*). The crystal structure of human β_2-adrenergic receptor (*14*) reveals extensive interactions between the receptor and the ligand, carazolol, at positions Trp^{286}, Phe^{289}, and Phe^{290}. The direct interaction between the receptor and carazolol is through an aromatic interaction with Phe^{193} at extracellular loop 2 (EL2) (*25*). The common binding pocket for timolol and carazolo includes Asp^{113}, Asn^{312}, and Tyr^{316}. Timolol binds deeper into the receptor pocket and forms a polar interaction with Asn^{293}, which allows an additional hydrogen bonding interaction with Thr^{118} (*26*). In human β_1-adrenergic receptor, similar to that of carazolol in β_2-adrenergic receptor, the ligand biding pocket includes Asp^{121}, Phe^{201}, Thr^{203}, Ser^{211}, and Asn^{329} (*15*). The Ser^{211} residue displays ligand-induced rotamer conformational changes to stabilize the binding pocket.

Adenosine receptors play an essential role in responding to adenosine in the central nervous system and are major targets of caffeine (*27*). The ligand binding pocket of A_{2A} Adenosine receptor for the antagonist theophylline (ZM241385) has been identified (*17*) to reside at Phe^{168}, Glu^{169}, Trp^{246}, Leu^{249}, His^{250}, Asn^{253}, His^{264}, Leu^{267},

Met^{270}, and Ile^{274}. The agonist (UK-432097) binds into the A_{2A} Adenosine receptor at Tyr^{9}, Ala^{63}, Val^{84}, Leu^{85}, Thr^{88}, Glu^{169}, Met^{177}, Trp^{246}, Leu^{249}, His^{250}, Asn^{253}, His^{264}, Leu^{267}, Met^{270}, Tyr^{271}, Ser^{277}, and His^{278} (*28*). The residues Glu^{169} (EL2), Tyr^{197} (TM6), and Phe^{201} (TM6) function as switches for rotamer conformation after ligand binding.

Transmembrane domain (TM) interaction of GPCR crystal structures

According to the crystal structure of rhodopsin (*13*), interactions among transmembrane domains (Leu^{40}-Phe^{293}-Phe^{294}- Cys^{264}, Asn^{55}-Asp^{83}-Ala^{299}, Asn^{73}- Tyr^{306}, Asn^{78}- Ser^{127}-Thr^{160}-Trp^{161}, Asp^{83}-Gly^{120}, Cys^{110}-Cys^{187}, Glu^{122}-Met^{163}-His^{211}, Glu^{134}-Arg^{135}-Glu^{247}-Thr^{251}) was observed to stabilize the inactive structure. The (D/E)R(Y/W) motif (Glu^{134}-Arg^{135}-Tyr^{136}) forms hydrogen bonds with surrounding residues. The tripeptide sequence Val^{137}-Val^{138}-Val^{139} covers the cytoplasmic side of Glu^{134} and Arg^{135} and maintains the conformation of rhodopdin. Photoactivation is likely to interfere with the transmembrane constrains, such as Phe^{294}, Ala^{299}, Asn^{302}, and Tyr^{306}, and unfold the active conformation.

In human β_2-adrenergic receptor (*14*), there are two disulfide bonds (Cys^{184}-Cys^{190} and Cys^{191}-Cys^{106}) stabilizing extracellular loop 2. The interactions among Trp^{286}, Phe^{289}, and Phe^{290} constrain the inactive state of the receptor. There are ionic interactions and salt bridges between residues at different TM domains (Lys^{60}-Glu^{338} and Lys^{305}-Asp^{192}) to maintain the receptor structure (*25*). Upon ligand binding in the β_1-adrenergic receptor, Ser^{212} forms a hydrogen bond with Asn^{310} (*29*) and the rotamer change of Ser^{215} appears to break the interaction of Val^{172}-Ser^{215}. Also Tyr^{149} forms a

hydrogen bond with Asp^{138} (*15*). A short α-helix in intracellular loop 2 interacts directly with the highly conserved Asp^{138}-Arg^{139}-Tyr^{140} (DRY) motif in TM3 (*15*).

Adenosine receptor forms hydrogen bonds in Asp^{101}-Tyr^{112}-Thr^{41} and disulfide bonds at Cys^{71}-Cys^{159}, Cys^{74}-Cys^{146}, Cys^{77}-Cys^{166}, and Cys^{259}-Cys^{262} (*17*). The D/ERY (Asp^{101}-Arg^{102}-Tyr^{103}) motif plays a role in stabilizing the polar interactions with TM2 (Thr^{41}), IL2 (Tyr^{112}), and TM6 (Glu^{228}), which possibly modulates G protein activation. There are interactions at IL2 (Tyr^{112}-Asp^{138}) and Thr^{88}-Ser^{277}-His^{278}. Upon ligand binding, the residue His^{250} moves ~1.8 Å inward and Trp^{246} indole moves ~1.9 Å to avoid the steric clash with the ligand (*28*). The conserved NPxxY motif composed of Asn^{284}, Pro^{285}, Phe^{286}, Ile^{287}, and Tyr^{288} at the cytoplasmic end of TM7 shifts about 4 to 5 Å inward, resulting in reorganizations of these side chains, especially at the residue Tyr^{288}.

G protein interaction of GPCR crystal structures

In all GPCRs, intracellular loops, especially IL2 and IL3, are critical to activate and provide variability among related GPCRs as a result to specific G-protein activation (*13, 15*). The C-terminal end of rhodopsin is surrounded by hydrophobic residues from TM2 (Pro^{71}, Leu^{72}), intracellular loop 2 (Phe^{148}), TM5 (Leu^{226}, Val^{230}), and TM6 (Val^{250}, Met^{253}), forming the binding site for a G protein (*13*). In the β_1-adrenergic receptor (Warne 2008 Nature 486), intracellular loop 2 is proposed to play a key role in G-protein coupling and activation (*15*).

Chapter 2

Alpha-factor Pheromone and its G Protein-coupled Receptor (Ste2p) of *Saccharomyces cerevisiae*

Yeast Mating Pheromone Response Pathway

In yeast two distinct GPCR systems have been identified: one is for pheromone signaling (Figure 1.1) and the other is for glucose sensing (*30*). Our lab uses the pheromone response pathway in *Saccharomyces cerevisiae* as a model system for the study of GPCR-ligand interaction. The MATα cell generates the 13-residue peptide [WHWLQLKPGQPMY] α-factor, which activates the Ste2p receptor on the MAT**a** cell. The MAT**a** cell generates the 12-residue lipopeptide [YIIKGVFWDPAC(farnesyl)OCH3] **a**-factor, which targets the Ste3p receptor on the MATα cell (*31*). The two mating peptides bind to residues on the extracellular side of receptors and cause conformational changes that transmit a signal to the G proteins inside the cells.

G protein subunits serve as intermediate modulators between the cell surface receptors and the intracellular effectors (*32*), transducing pheromone binding signal into cytoplasmic response. Upon ligand binding, Gpa1p (Gα subunit) bound GDP is replaced by GTP, and Ste4p/Ste18p (Gβγ subunits) are then released, which in turn transmits the signal required for mating. Recent studies have shown that Gpa1p can also stimulate downstream signaling. A GTPase-deficient mutant (GDP-bound form) of Gpa1p was found to couple with an RNA binding protein Scp160 (*33*) and endosomal phosphatidylinositol 3-kinase Vps15/Vps34 subunits (*34*), suggesting a role of Gpa1p not

only as a negative regulator of Ste4p/Ste18p (*35*, *36*), but also as an inducer of the mating signal pathway.

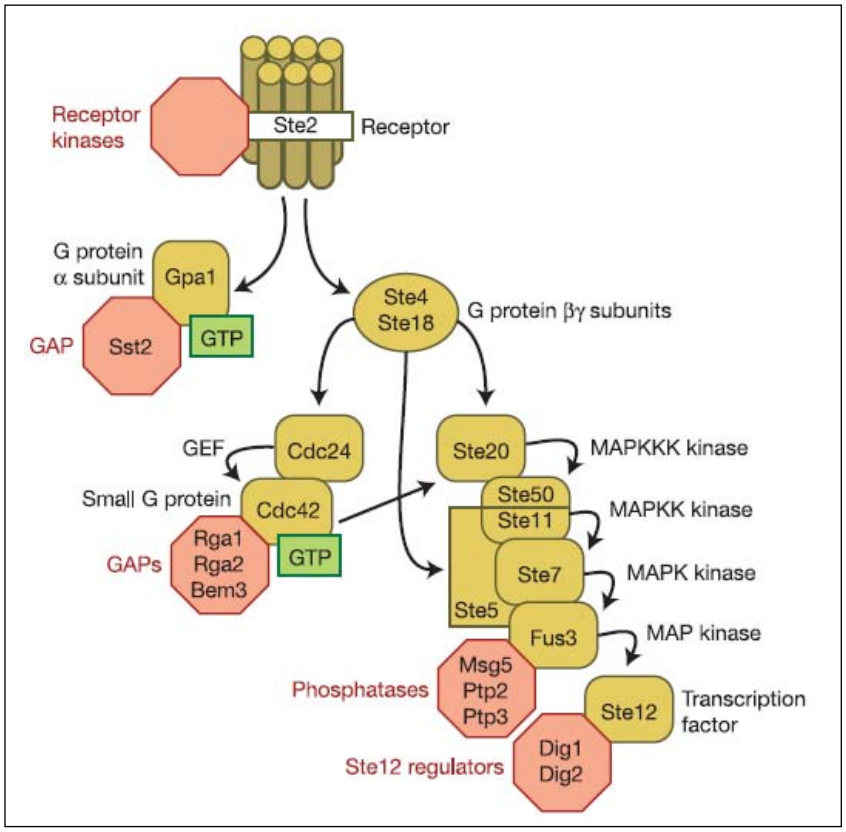

Figure 1.1 Components of the pheromone response pathway in yeast. This figure was taken from reference (*37*).

Released Ste4p/Ste18p subunits transmit the signal to a mitogen-activated protein (MAP) kinase cascade through at least three effector proteins (*32*): a guanine-nucleotide exchange factor Cdc24p (*38*), a protein kinase Ste20p (*39*), and a kinase scaffolding protein Ste5p (*40*). Cdc24p is the guanine nucleotide exchange factor for the Rho G-protein Cdc42p (*41*); Cdc42p regulates MAP kinase signaling through PAK (p21-

activated kinase)-family kinase Ste20p (*42*). After binding with Ste4p/Ste18p and Cdc42p (*43, 44*), Ste20p activates the downstream MAP kinase cascade. Pheromone response protein Ste5p serves as a scaffold (*45, 46*) to facilitate interactions among member of the MAP kinase cascade: Ste11p (MAPKKK), Ste7p (MAPKK) and Fus3p (MAPK). MAP kinase kinase kinase Ste11p phosphorylates MAP kinase kinase Ste7p, and Ste7p phosphorylates MAP kinase Fus3p. Mating specific Fus3p then phosphorylates Far1p (*47*) and Ste12p, a transcription factor (*48*). Far1p inhibits Cdc28-G1 cyclin complex and promotes G1 cell cycle growth arrest (*49*). The transcriptional transactivatior Ste12p binds to the pheromone response element (PRE) at the promoter region of target genes (*50*), such as *FUS1, FUS2, FIG1, FIG2, AGA1* that are induced for cell fusion. MAT**a** and MATα cells form shmoos with the apical tips directing toward each other (*51*). Eventually at the contact points of two opposite mating types, degradation of the cell wall and plasma membrane followed by nuclear fusion allow two haploid cells to become one **a**/α diploid zygote (*52*).

Regulation of Mating Pheromone Response Pathway

Figure 1.2 summarizes the activation, desensitization, and internalization of the Ste2p signaling pathway (*53*). Yeast cells start a mating cell cycle and trigger G1 growth arrest when there is nutrient starvation or the presence of mating factor from the other mating type (*54*). Eventually yeast cells would have to recover from mating state and continue proliferation through the mitotic cell cycle (*32*). The MAT**a** cell produces an extracellular protease, Bar1p, which cleaves α-factor (*55*) and allow cells to recover from

α-factor induced growth arrest. Expression of RGS (regulator of G-protein signaling) Sst2p is highly induced by the activation of Ste2p. Membrane-associate Sst2p is a direct negative regulator (*56*) that interferes with GTP-bound Gpa1p and down-regulates mating signal. Yeast casein kinases, Yck1p and Yck2p, are involved in bud morphogenesis and internalization of pheromone receptors (*57*). Yck-mediated phosphorylation of the mating receptors is required for endocytosis at the cell membrane (*58*). Eventually phosphorylation at the C-terminus of the receptor leads to ubiquination, internalization and degradation (*32*).

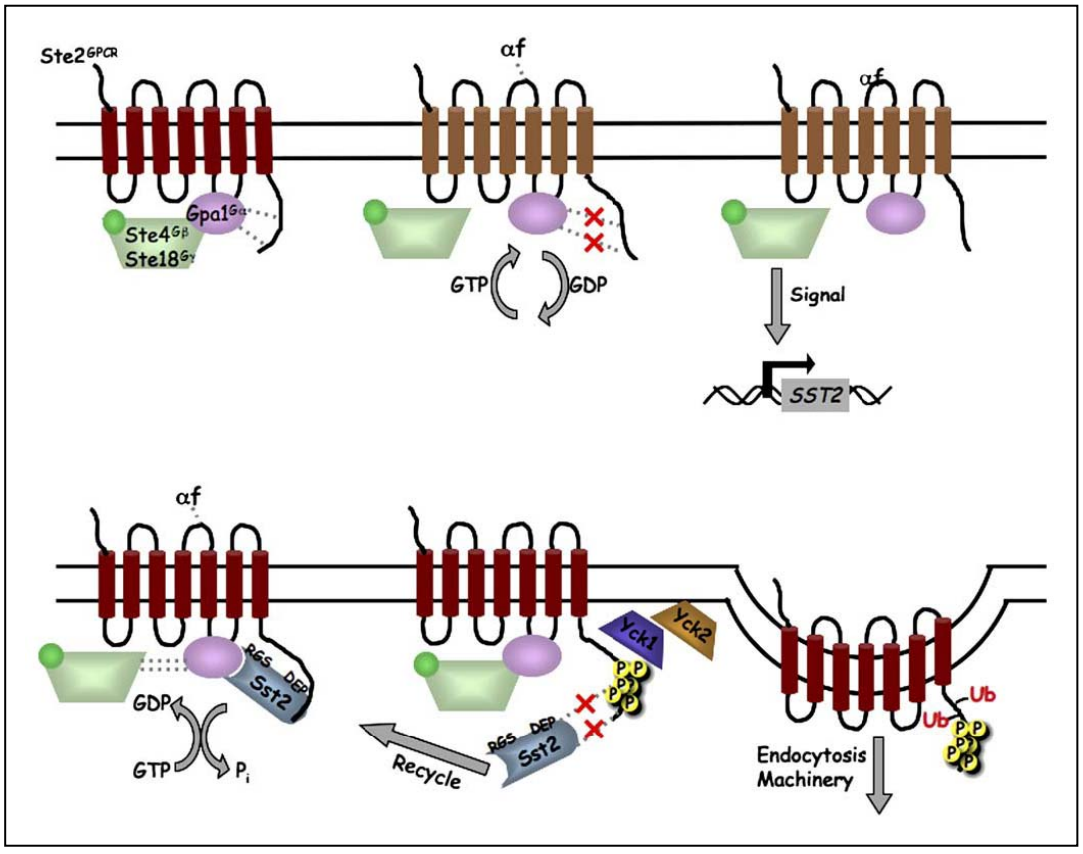

Figure 1.2 Sst2-mediated activation, desensitization, and internalization of Ste2p.

This figure was taken from reference (*53*).

Reference of Part I

1. Gether, U., and Kobilka, B. K. (1998) G protein-coupled receptors. II. Mechanism of agonist activation, *The Journal of biological chemistry 273*, 17979-17982.
2. Vaidehi, N., Floriano, W. B., Trabanino, R., Hall, S. E., Freddolino, P., Choi, E. J., Zamanakos, G., and Goddard, W. A., 3rd. (2002) Prediction of structure and function of G protein-coupled receptors, *Proceedings of the National Academy of Sciences of the United States of America 99*, 12622-12627.
3. Rohrer, D. K., and Kobilka, B. K. (1998) G protein-coupled receptors: functional and mechanistic insights through altered gene expression, *Physiological reviews 78*, 35-52.
4. Eglen, R. M., and Reisine, T. (2009) New insights into GPCR function: implications for HTS, *Methods Mol Biol 552*, 1-13.
5. Rana, B. K., Shiina, T., and Insel, P. A. (2001) Genetic variations and polymorphisms of G protein-coupled receptors: functional and therapeutic implications, *Annual review of pharmacology and toxicology 41*, 593-624.
6. Tuteja, N. (2009) Signaling through G protein coupled receptors, *Plant signaling & behavior 4*, 942-947.
7. Gether, U. (2000) Uncovering molecular mechanisms involved in activation of G protein-coupled receptors, *Endocrine reviews 21*, 90-113.
8. Hayashida, W., Horiuchi, M., and Dzau, V. J. (1996) Intracellular third loop domain of angiotensin II type-2 receptor. Role in mediating signal transduction and cellular function, *The Journal of biological chemistry 271*, 21985-21992.

9. Robbins, M. J., Calver, A. R., Filippov, A. K., Hirst, W. D., Russell, R. B., Wood, M. D., Nasir, S., Couve, A., Brown, D. A., Moss, S. J., and Pangalos, M. N. (2001) GABA(B2) is essential for g-protein coupling of the GABA(B) receptor heterodimer, *The Journal of neuroscience : the official journal of the Society for Neuroscience 21*, 8043-8052.

10. Shpakova, E. A., and Shpakov, A. O. (2011) Peptides corresponding to intracellular regions of somatostatin receptors with agonist and antagonist activity, *Doklady. Biochemistry and biophysics 437*, 68-71.

11. Terrillon, S., and Bouvier, M. (2004) Roles of G-protein-coupled receptor dimerization, *EMBO reports 5*, 30-34.

12. Bulenger, S., Marullo, S., and Bouvier, M. (2005) Emerging role of homo- and heterodimerization in G-protein-coupled receptor biosynthesis and maturation, *Trends in pharmacological sciences 26*, 131-137.

13. Palczewski, K., Kumasaka, T., Hori, T., Behnke, C. A., Motoshima, H., Fox, B. A., Le Trong, I., Teller, D. C., Okada, T., Stenkamp, R. E., Yamamoto, M., and Miyano, M. (2000) Crystal structure of rhodopsin: A G protein-coupled receptor, *Science 289*, 739-745.

14. Cherezov, V., Rosenbaum, D. M., Hanson, M. A., Rasmussen, S. G., Thian, F. S., Kobilka, T. S., Choi, H. J., Kuhn, P., Weis, W. I., Kobilka, B. K., and Stevens, R. C. (2007) High-resolution crystal structure of an engineered human beta2-adrenergic G protein-coupled receptor, *Science 318*, 1258-1265.

15. Warne, T., Serrano-Vega, M. J., Baker, J. G., Moukhametzianov, R., Edwards, P. C., Henderson, R., Leslie, A. G., Tate, C. G., and Schertler, G. F. (2008) Structure of a beta1-adrenergic G-protein-coupled receptor, *Nature 454*, 486-491.

16. Rasmussen, S. G., DeVree, B. T., Zou, Y., Kruse, A. C., Chung, K. Y., Kobilka, T. S., Thian, F. S., Chae, P. S., Pardon, E., Calinski, D., Mathiesen, J. M., Shah, S. T., Lyons, J. A., Caffrey, M., Gellman, S. H., Steyaert, J., Skiniotis, G., Weis, W. I., Sunahara, R. K., and Kobilka, B. K. (2011) Crystal structure of the beta2 adrenergic receptor-Gs protein complex, *Nature 477*, 549-555.

17. Jaakola, V. P., Griffith, M. T., Hanson, M. A., Cherezov, V., Chien, E. Y., Lane, J. R., Ijzerman, A. P., and Stevens, R. C. (2008) The 2.6 angstrom crystal structure of a human A2A adenosine receptor bound to an antagonist, *Science 322*, 1211-1217.

18. Wu, B., Chien, E. Y., Mol, C. D., Fenalti, G., Liu, W., Katritch, V., Abagyan, R., Brooun, A., Wells, P., Bi, F. C., Hamel, D. J., Kuhn, P., Handel, T. M., Cherezov, V., and Stevens, R. C. (2010) Structures of the CXCR4 chemokine GPCR with small-molecule and cyclic peptide antagonists, *Science 330*, 1066-1071.

19. Chien, E. Y., Liu, W., Zhao, Q., Katritch, V., Han, G. W., Hanson, M. A., Shi, L., Newman, A. H., Javitch, J. A., Cherezov, V., and Stevens, R. C. (2010) Structure of the human dopamine D3 receptor in complex with a D2/D3 selective antagonist, *Science 330*, 1091-1095.

20. Shimamura, T., Shiroishi, M., Weyand, S., Tsujimoto, H., Winter, G., Katritch, V., Abagyan, R., Cherezov, V., Liu, W., Han, G. W., Kobayashi, T., Stevens, R.

C., and Iwata, S. (2011) Structure of the human histamine H1 receptor complex with doxepin, *Nature 475*, 65-70.

21. Congreve, M., and Marshall, F. (2010) The impact of GPCR structures on pharmacology and structure-based drug design, *British journal of pharmacology 159*, 986-996.

22. Klabunde, T., and Hessler, G. (2002) Drug design strategies for targeting G-protein-coupled receptors, *Chembiochem : a European journal of chemical biology 3*, 928-944.

23. Xiang, Y., and Kobilka, B. K. (2003) Myocyte adrenoceptor signaling pathways, *Science 300*, 1530-1532.

24. Xiao, R. P., Zhu, W., Zheng, M., Chakir, K., Bond, R., Lakatta, E. G., and Cheng, H. (2004) Subtype-specific beta-adrenoceptor signaling pathways in the heart and their potential clinical implications, *Trends in pharmacological sciences 25*, 358-365.

25. Bokoch, M. P., Zou, Y., Rasmussen, S. G., Liu, C. W., Nygaard, R., Rosenbaum, D. M., Fung, J. J., Choi, H. J., Thian, F. S., Kobilka, T. S., Puglisi, J. D., Weis, W. I., Pardo, L., Prosser, R. S., Mueller, L., and Kobilka, B. K. (2010) Ligand-specific regulation of the extracellular surface of a G-protein-coupled receptor, *Nature 463*, 108-112.

26. Hanson, M. A., Cherezov, V., Griffith, M. T., Roth, C. B., Jaakola, V. P., Chien, E. Y., Velasquez, J., Kuhn, P., and Stevens, R. C. (2008) A specific cholesterol

binding site is established by the 2.8 A structure of the human beta2-adrenergic receptor, *Structure 16*, 897-905.

27. Jacobson, K. A., and Gao, Z. G. (2006) Adenosine receptors as therapeutic targets, *Nature reviews. Drug discovery 5*, 247-264.

28. Xu, F., Wu, H., Katritch, V., Han, G. W., Jacobson, K. A., Gao, Z. G., Cherezov, V., and Stevens, R. C. (2011) Structure of an agonist-bound human A2A adenosine receptor, *Science 332*, 322-327.

29. Warne, T., Moukhametzianov, R., Baker, J. G., Nehme, R., Edwards, P. C., Leslie, A. G., Schertler, G. F., and Tate, C. G. (2011) The structural basis for agonist and partial agonist action on a beta(1)-adrenergic receptor, *Nature 469*, 241-244.

30. Versele, M., Lemaire, K., and Thevelein, J. M. (2001) Sex and sugar in yeast: two distinct GPCR systems, *EMBO reports 2*, 574-579.

31. Naider, F., and Becker, J. M. (2004) The alpha-factor mating pheromone of Saccharomyces cerevisiae: a model for studying the interaction of peptide hormones and G protein-coupled receptors, *Peptides 25*, 1441-1463.

32. Dohlman, H. G., and Thorner, J. W. (2001) Regulation of G protein-initiated signal transduction in yeast: paradigms and principles, *Annual review of biochemistry 70*, 703-754.

33. Guo, M., Aston, C., Burchett, S. A., Dyke, C., Fields, S., Rajarao, S. J., Uetz, P., Wang, Y., Young, K., and Dohlman, H. G. (2003) The yeast G protein alpha

subunit Gpa1 transmits a signal through an RNA binding effector protein Scp160, *Molecular cell 12*, 517-524.

34. Slessareva, J. E., Routt, S. M., Temple, B., Bankaitis, V. A., and Dohlman, H. G. (2006) Activation of the phosphatidylinositol 3-kinase Vps34 by a G protein alpha subunit at the endosome, *Cell 126*, 191-203.

35. Coria, R., Ongay-Larios, L., and Birnbaumer, L. (1996) Separate roles for N- and C-termini of the STE4 (beta) subunit of the Saccharomyces cerevisiae G protein in the mediation of the growth arrest. Lack of growth-arresting activity of mammalian beta gamma complexes, *Yeast 12*, 41-51.

36. Hirschman, J. E., De Zutter, G. S., Simonds, W. F., and Jenness, D. D. (1997) The G beta gamma complex of the yeast pheromone response pathway. Subcellular fractionation and protein-protein interactions, *The Journal of biological chemistry 272*, 240-248.

37. Wang, Y., and Dohlman, H. G. (2004) Pheromone signaling mechanisms in yeast: a prototypical sex machine, *Science 306*, 1508-1509.

38. Toenjes, K. A., Sawyer, M. M., and Johnson, D. I. (1999) The guanine-nucleotide-exchange factor Cdc24p is targeted to the nucleus and polarized growth sites, *Current biology : CB 9*, 1183-1186.

39. Akada, R., Kallal, L., Johnson, D. I., and Kurjan, J. (1996) Genetic relationships between the G protein beta gamma complex, Ste5p, Ste20p and Cdc42p: investigation of effector roles in the yeast pheromone response pathway, *Genetics 143*, 103-117.

40. Dowell, S. J., Bishop, A. L., Dyos, S. L., Brown, A. J., and Whiteway, M. S. (1998) Mapping of a yeast G protein betagamma signaling interaction, *Genetics 150*, 1407-1417.

41. Mionnet, C., Bogliolo, S., and Arkowitz, R. A. (2008) Oligomerization regulates the localization of Cdc24, the Cdc42 activator in Saccharomyces cerevisiae, *The Journal of biological chemistry 283*, 17515-17530.

42. Takahashi, S., and Pryciak, P. M. (2007) Identification of novel membrane-binding domains in multiple yeast Cdc42 effectors, *Molecular biology of the cell 18*, 4945-4956.

43. Leeuw, T., Wu, C., Schrag, J. D., Whiteway, M., Thomas, D. Y., and Leberer, E. (1998) Interaction of a G-protein beta-subunit with a conserved sequence in Ste20/PAK family protein kinases, *Nature 391*, 191-195.

44. Moskow, J. J., Gladfelter, A. S., Lamson, R. E., Pryciak, P. M., and Lew, D. J. (2000) Role of Cdc42p in pheromone-stimulated signal transduction in Saccharomyces cerevisiae, *Molecular and cellular biology 20*, 7559-7571.

45. Printen, J. A., and Sprague, G. F., Jr. (1994) Protein-protein interactions in the yeast pheromone response pathway: Ste5p interacts with all members of the MAP kinase cascade, *Genetics 138*, 609-619.

46. Flotho, A., Simpson, D. M., Qi, M., and Elion, E. A. (2004) Localized feedback phosphorylation of Ste5p scaffold by associated MAPK cascade, *The Journal of biological chemistry 279*, 47391-47401.

47. Elion, E. A., Satterberg, B., and Kranz, J. E. (1993) FUS3 phosphorylates multiple components of the mating signal transduction cascade: evidence for STE12 and FAR1, *Molecular biology of the cell 4*, 495-510.

48. Blackwell, E., Kim, H. J., and Stone, D. E. (2007) The pheromone-induced nuclear accumulation of the Fus3 MAPK in yeast depends on its phosphorylation state and on Dig1 and Dig2, *BMC cell biology 8*, 44.

49. Olson, K. A., Nelson, C., Tai, G., Hung, W., Yong, C., Astell, C., and Sadowski, I. (2000) Two regulators of Ste12p inhibit pheromone-responsive transcription by separate mechanisms, *Molecular and cellular biology 20*, 4199-4209.

50. Bardwell, L. (2004) A walk-through of the yeast mating pheromone response pathway, *Peptides 25*, 1465-1476.

51. Melloy, P., Shen, S., White, E., McIntosh, J. R., and Rose, M. D. (2007) Nuclear fusion during yeast mating occurs by a three-step pathway, *The Journal of cell biology 179*, 659-670.

52. Philips, J., and Herskowitz, I. (1997) Osmotic balance regulates cell fusion during mating in Saccharomyces cerevisiae, *The Journal of cell biology 138*, 961-974.

53. Ballon, D. R., Flanary, P. L., Gladue, D. P., Konopka, J. B., Dohlman, H. G., and Thorner, J. (2006) DEP-domain-mediated regulation of GPCR signaling responses, *Cell 126*, 1079-1093.

54. Herskowitz, I. (1988) Life cycle of the budding yeast Saccharomyces cerevisiae, *Microbiological reviews 52*, 536-553.

55. MacKay, V. L., Welch, S. K., Insley, M. Y., Manney, T. R., Holly, J., Saari, G. C., and Parker, M. L. (1988) The Saccharomyces cerevisiae BAR1 gene encodes an exported protein with homology to pepsin, *Proceedings of the National Academy of Sciences of the United States of America 85*, 55-59.

56. Dohlman, H. G., Song, J., Ma, D., Courchesne, W. E., and Thorner, J. (1996) Sst2, a negative regulator of pheromone signaling in the yeast Saccharomyces cerevisiae: expression, localization, and genetic interaction and physical association with Gpa1 (the G-protein alpha subunit), *Molecular and cellular biology 16*, 5194-5209.

57. Babu, P., Bryan, J. D., Panek, H. R., Jordan, S. L., Forbrich, B. M., Kelley, S. C., Colvin, R. T., and Robinson, L. C. (2002) Plasma membrane localization of the Yck2p yeast casein kinase 1 isoform requires the C-terminal extension and secretory pathway function, *Journal of cell science 115*, 4957-4968.

58. Panek, H. R., Stepp, J. D., Engle, H. M., Marks, K. M., Tan, P. K., Lemmon, S. K., and Robinson, L. C. (1997) Suppressors of YCK-encoded yeast casein kinase 1 deficiency define the four subunits of a novel clathrin AP-like complex, *The EMBO journal 16*, 4194-4204.

PART II

Unnatural Amino Acid Replacement in a Yeast G Protein-Coupled Receptor in its Native Environment

Part II was published in its entirety as: Huang LY, Umanah G, Hauser M, Son C, Arshava B, Naider F, Becker J. M. (2008). *Biochemistry*, **47**(20):5638-48. Li-Yin Huang determined the expression conditions and biological activities of all mutants. George K. Umanah was responsible for the mass spectrometric and cross-linking studies. Boris Arshava in Dr. Naider's laboratory was responsible for synthesis and purification of the pheromone peptides used in the study.

Abstract for Part II

Ste2p is the G protein-coupled receptor (GPCR) for the tridecapeptide pheromone alpha factor of *Saccharomyces cerevisiae*. This receptor-pheromone pair has been used extensively as a paradigm for investigating GPCR structure and function. Expression in yeast harboring a cognate tRNA/aminoacyl-tRNA synthetase pair specifically evolved to incorporate p-benzoyl- l-phenylalanine (Bpa) in response to the amber codon allowed the biosynthesis of Bpa-substituted Ste2p in its native cell. We replaced natural amino acid residues in Ste2p with Bpa by engineering amber TAG stop codons into STE2 encoded on a plasmid. Several of the expressed Bpa-substituted Ste2p receptors exhibited high-affinity ligand binding, and incorporation of Bpa into Ste2p influenced biological activity as measured by growth arrest of whole cells in response to alpha factor. We found that, at concentrations of 0.1-0.5 mM, a dipeptide containing Bpa could be used to enhance delivery of Bpa into the cell, while at 2 mM, both dipeptide and Bpa were equally effective. The application of a peptide delivery system for unnatural amino acids will extend the use of the unnatural amino acid replacement methodology to amino acids that are impermeable to yeast. Incorporation of Bpa into Ste2p was verified by mass spectrometric analysis, and two Bpa-Ste2p mutants were able to selectively capture alpha factor into the ligand-binding site after photoactivation. To our knowledge, this is the first experimental evidence documenting an unnatural amino acid replacement in a GPCR expressed in its native environment and the use of a mutated receptor to photocapture a peptide ligand.

Chapter 1

Introduction

G protein-coupled receptors (GPCRs) are activated upon binding their cognate ligands. Ligand binding initiates a change in the conformation of these integral membrane proteins. This promotes signal transduction across the membrane and the activation of the G protein-mediated signal transduction cascade (*1, 2*). The interactions between ligands and their receptors are defined for a number of GPCRs (*3*). However, the ligand-induced changes in protein structure, which initiate signal transduction, are difficult to study. Although site-directed mutagenesis has been used to address the issue of GPCR activation, more methods for studying ligand-dependent conformational changes upon receptor activation are needed. One promising approach, which may be adapted to the study of the dynamics of the GPCR structure, is the use of orthogonal pairs of tRNA/aminoacyl-tRNA synthetases evolved and expressed in the target cell to incorporate unnatural amino acids (*4-7*).

Non-naturally occurring amino acids can be synthesized to contain a variety of chemical moieties for use as photoaffinity labels or fluorescent and/or spectroscopic probes. To autonomously incorporate unnatural amino acids into proteins in living cells, the mutated tRNA is designed to recognize a specific codon, usually a nonsense codon, such as the amber TAG stop. Provided that there is a sufficient quantity of the unnatural amino acid in the cytoplasm, the evolved cognate aminoacyl-tRNA synthetase specifically charges its orthogonal tRNA with this novel amino acid for delivery into the protein.

The genetic codes of Escherichia coli, yeast, and mammalian cells have been altered to allow for the translational insertion of more than 30 unnatural amino acids with a variety of novel properties useful in the study of protein structure and function(*5, 8*). Thus far, these applications have focused primarily on soluble proteins. With respect to eukaryotic membrane proteins expressed in mammalian cells, unnatural amino acids have been introduced into the nicotinic acetycholine receptor in both CHO and cultured neuronal cells (*9*) and in the epidermal growth factor receptor in HEK293 cells (*10*). A heterologous Xenopus oocyte expression system has also been used extensively to insert non-natural amino acids into the nicotinic acetylcholine receptor (*11*) the neurokinin-2 receptor (*12*), the GABAA receptor (*13*), the NMDA receptor (*14*), and numerous channel proteins, including the serotonin-gated ion channel (*15*), the inwardly rectifying potassium channel (*16*), and the voltage-sensitive sodium channel (*17*). In both the mammalian and Xenopus expression systems, a tRNA chemically charged with the non-natural amino acid is introduced into the cell along with the target mRNA. While these systems are useful for the short-term studies of protein properties, they are not amenable to large-scale production of proteins into which unnatural amino acids have been incorporated. Recently, it was demonstrated in CHO cells that unnatural amino acids could be introduced into green fluorescent protein (GFP) using specific orthogonal tRNA/aminoacyl-tRNA synthetase pairs (*6*). Because the yeast *Saccharomyces cerevisiae* provides a tractable system in which to develop this methodology, we report here the genetic incorporation of an unnatural amino acid into a polytopic membrane protein in its native eukaryotic host cell.

To date in *S. cerevisiae*, orthologous tRNA/aminoacyl-tRNA synthetase pairs have been used to incorporate a variety of unnatural amino acids, including the photoactivatable amino acid analogue *p*-benzoyl-$_L$-phenylalanine (Bpa) (*4*), the fluorescent amino acid dansyl alanine (*18*), and acetylene- and azide-containing amino acids (*7, 19*), into the soluble protein human superoxide dismutase. Here, we report the site-specific incorporation of Bpa into Ste2p, a yeast GPCR, using an orthologous tRNA/aminoacyl-tRNA synthetase pair. In this system, the amber TAG stop codon was engineered into specific sites within the STE2 coding region. Bpa was supplied to the cells either as the free amino acid analogue or as the dipeptide Met−Bpa. Upon translation of the message, Bpa was incorporated into the nascent Ste2p and ultimately expressed at the cell surface. Two of our Bpa−Ste2p receptors were used to selectively photocapture biotinylated α factor. To our knowledge, this is the first report of the expression in the native host cell of a GPCR containing a photoactivatable amino acid. The successful photocapture of α factor by novel Ste2p mutants shows that GPCRs containing unnatural amino acids can be used to capture ligand and study changes in domain−domain interactions during GPCR activation.

Chapter 2

Material and Methods

Media, Reagents, Strains, and Plasmids

S. cerevisiae strain DK102 (*MATa, ura3−52 lys2−801^{am} ade201^{oc} trp1-Δ63 his3-Δ200 leu2-Δ1 ste2::HIS3 sst1-Δ5*) was used for growth arrest and binding assays, and the protease-deficient strain BJS21 (*MATa, prc1−407 prb1−1122 pep4−3 leu2 trp1 ura3−52 ste2::Kan^{R}*) was used for protein isolation and immunoblot analysis. C-Terminal FLAG and His-tagged STE2 was PCR-amplified from plasmid pNED1 (*20*) and cloned into the plasmid p426-GPD (*21*) to yield plasmid pCL01. The plasmid pCL01 was engineered by single-stranded mutagenesis to incorporate TAG stop codons at eight specific positions within the STE2 coding region (Figure 2.1). The sequence of all TAG mutants was verified by DNA sequence analysis completed by the Molecular Biology Resource Facility located on the campus of the University of Tennessee. Mutagenic and sequencing primers were purchased from Sigma/Genosys (The Woodlands, TX) or IDT (Coralville, IA). The pCL01 TAG mutant plasmids were cotransformed by the method of Geitz (*22*) into DK102 and BJS21 cells along with plasmid pECTyrRS/tRNACUA, encoding the orthogonal amber suppressor tRNA synthetase−tRNA pair genetically modified to allow for incorporation of *p*-benzoyl-$_{L}$-phenylalanine (Bpa) (*4*). Transformants were selected by growth on minimal medium (*23*) lacking tryptophan and uracil (designated as MLWU) to maintain selection for the plasmids. Cells used in the assays described below were cultured in MLWU and grown to mid-log phase at room temperature with shaking (200 rpm) in the presence or absence of 2 mM Bpa, unless otherwise specified.

Methionyl-Bpa was synthesized by standard solution phase techniques (*24*) and purified by reverse-phase high-performance liquid chromatography (HPLC) to greater than 99% homogeneity. All media components were obtained from BD (Franklin Lakes, NJ) and were of the highest quality available. Bpa was purchased from Bachem (Torrance, CA) and was dissolved in NaOH (1 N) at a final concentration of 100 mM immediately before use.

Growth Arrest Assays

DK102 cells expressing the wild-type (WT) or TAG constructs were grown at 30°C in MLWU, harvested, washed 3 times with sterile water, and resuspended at a final concentration of 5×10^6 cells/mL. Cells (1 mL) were combined with 3.5 mL agar noble (1.1%) with or without the addition of Bpa (2 mM final concentration) and poured as a top agar lawn onto MLWU medium. Filter disks (BD, Franklin Lakes, NJ) impregnated with the tridecapeptide pheromone α factor (WHWLQLKPGQPNle12Y) synthesized and characterized as previously described (*25*) were placed on the top agar, and the plates were incubated at room temperature (23°C) for 48−72 h. The growth arrest assays were repeated a minimum of 3 times, and similar results were observed for each replicate.

Immunoblots

BJS21 cells expressing WT or TAG-STE2 constructs grown in the presence or absence of Bpa were used to prepare total cell membranes isolated as previously described (*20*). The protein concentration was determined (BioRad, Hercules, CA), and

membranes were solubilized in sodium dodecyl sulfate (SDS) sample buffer. Proteins (2 μg/lane for WT and 30 μg/lane for mutants) were fractioned by SDS−polyacrylamide gel electrophoresis (PAGE) and immunoblotted. Blots were probed with FLAG antibody (Sigma/Aldrich Chemical, St. Louis, MO) or an antibody directed against the N-terminal 100 amino acids of Ste2p generously provided by J. Konopka (*26*). The immunoblots were imaged, and band density was quantitated using Quantity One software (version 4.5.1) on a Chemi-Doc XRS photodocumentation system (BioRad, Hercules, CA). Multiple repeats of immunoblot experiments yielded the same results.

Binding Assays

Tritiated α factor (10.2 Ci/mmol, 12 μM) prepared as previously described (*25*) was used in saturation binding assays on whole cells. DK102 cells expressing WT or TAG constructs were harvested, washed 3 times with YM1 (*20*), and adjusted to a final concentration of 2×10^7 cells/mL. Cells (600 μL) were combined with 150 μL of ice-cold 5× binding medium (YM1 plus protease inhibitors [YM1i (*20*)] supplemented with [^{3}H]α factor) and incubated at room temperature for 30 min. The final concentration of [^{3}H]α factor ranged from 0.5×10^{-10} to 1×10^{-6} M. Upon completion of the incubation interval, 200 μL aliquots of the cell−pheromone mixture were collected in triplicate and washed over glass fiber filter mats using the Standard Cell Harvester (Skatron Instruments, Sterling, VA). Retained radioactivity on the filter was counted by liquid scintillation spectroscopy. DK102 cells lacking Ste2p were used as a nonspecific binding control for the assays. Binding assays were repeated a minimum of 3 times, and similar results were

observed for each replicate. Specific binding for each mutant receptor was calculated by subtracting the nonspecific values from those obtained for total binding. Specific binding data were analyzed by nonlinear regression analysis for single-site binding using Prism software (GraphPad Software, San Diego, CA) to determine the *Km* (in nanomolars) and B_{max} values (receptors/cell) for each mutant receptor.

Matrix-Assisted Laser Desorption Ionization−Time of Flight (MALDI−TOF)

BJS21 cells expressing either the WT or $G188^{TAG}$ Ste2p were grown in the presence or absence of Bpa and used to prepare total cell membranes as previously described (*20*). Approximately 3 mg of cell membranes was resuspended in ice-cold solubilization buffer [50 mM Tris-HCl at pH 7.4, 150 mM NaCl, 1 mM ethylenediaminetetraacetic acid (EDTA), and 1% Triton X-100] with protease inhibitors (PMSF, pepstatin A, and leupeptin), incubated overnight at 4°C with end-over-end mixing, and then centrifuged at 15000g for 30 min to remove nonsoluble material. The solubilized proteins were then mixed with FLAG resin (Sigma/Aldrich Chemical Co., St. Louis, MO) and incubated at 4°C with end-over-end mixing for 6 h. The resin was collected by centrifugation at low speed (800g for 1 min) and resuspended and collected 4 times in TBS buffer (25 mM Tris-HCl, 140 mM NaCl, and 3 mM KCl at pH 7.4). Ste2p was eluted by resuspending the resin in 1 mL of ice-cold elution buffer (0.1 M glycine HCl at pH 3.5) and incubated at 4°C with end-over-end mixing for 5 min. The resin was pelleted by centrifugation (2000g for 1 min), and the supernatant, containing the eluted Ste2p, was transferred to a fresh tube containing 20 μL of 0.5 M Tris-HCl at pH 7.4 and

1.5 M NaCl. Purity and concentration of samples was estimated by Coomassie Blue and silver staining of SDS−PAGE gels. The samples were also analyzed by immunoblotting using an antibody to the FLAG epitope on the C terminus of Ste2p.

Samples containing eluted Ste2p (50 μg) were dried by vacuum centrifugation (Thermo Scientific, Waltham, MA) and then dissolved in 100% trifluoroacetic acid (TFA) containing 10 mg/mL cyanogen bromide (CNBr). Deionized−distilled water (ddH2O) was then added to adjust the final TFA concentration to 70%, and the sample was incubated at 37°C in the dark for 18 h. The samples were dried by vacuum centrifugation and washed 3 times with ddH2O and resuspended in 0.1% TFA. The resulting CNBr peptide fragments were further washed and concentrated using ZipTip pipet tips (Millipore Corporation, Billerica, MA) following the directions of the manufacturer and resuspended in 70% acetonitrile/30% water (0.1% TFA). For MALDI−TOF analysis, α-cyano-4-hydroxy-trans-cinnamic acid (ACHA, Sigma/Aldrich Chemical Co., St. Louis, MO) at a concentration of 20 mg/mL in 50% acetonitrile/50% water (0.1% TFA) was used as the matrix. The digested samples (0.5 μL eluate from ZipTip) were either mixed with 0.5 μL of matrix before spotting on the target or 1.0 μL of matrix was spotted and allowed to dry before applying 1.0 μL of samples. MADLI−TOF spectra were acquired on a Bruker Daltonics (Boston, MA) Microflex using both reflector and linear methods.

Crosslinking

A biotinylated form of α factor, [K^7(biotinylamidocaproate), Nle^{12}]α factor, was prepared as previously described (*27*). Membranes prepared from BJS21 cells expressing the $F55^{TAG}$, $G188^{TAG}$, and $Y193^{TAG}$ receptors, grown at room temperature in the presence or absence of Bpa (1 mM), were suspended in PPBi buffer [0.5 M potassium phosphate at pH 6.2, 10 mM tert-amyl methyl ether (TAME), 10 mM sodium azide, 10 mM potassium fluoride, and 0.1% bovine serum albumin (BSA)], incubated with biotinylated pheromone (1 μM) in the presence or absence of nonbiotinylated pheromone (100 μM) for 30 min at room temperature, and then chilled to 4°C for the remainder of the procedure. Cross-linking was performed as previously described (*27*). Briefly, the membranes were exposed to UV light at 365 nm using a Stratalinker (Stratagene, La Jolla, CA) for three 15 min intervals. The cross-linked membranes were washed 3 times with CAPS buffer [10 mM N-cyclohexyl-3-aminopropanesulfonic acid (Sigma, St. Louis, MO) at pH 10] by centrifugation to remove noncross-linked biotinylated α factor, fractionated by SDS−PAGE and immunoblotted with antibody to Ste2p and with Neutravidin−horseradish peroxidase (HRP) conjugate (Pierce, Rockford, IL) to detect the biotinylated pheromone covalently linked to the receptor. The signal generated by the Neutravidin−HRP conjugate associated with the biotinylated ligand−receptor complex was quantitated by measurement of the band density using Quantity One software (version 4.5.1) on a Chemi-Doc XRS photodocumentation system (BioRad, Hercules, CA). Before fractionation by SDS−PAGE, the amount of protein in each sample was determined, and amounts specified in the text were loaded into each lane.

Chapter 3

Results

Effect of Bpa Incorporation on Ste2p Expression and Signal Transduction

The amber stop codon TAG was inserted into the STE2 coding sequence by site-directed mutagenesis at the eight sites indicated in Figure 2.1. On the basis of the latest information concerning Ste2p topology (*28-30*), the sites were located in the first transmembrane domain ($F55^{TAG}$), in the first ($S107^{TAG}$, $G115^{TAG}$, and $V127^{TAG}$) and second ($Y193^{TAG}$ and $F204^{TAG}$) extracellular loops, at the border between the fourth transmembrane domain and the second loop ($G188^{TAG}$) and in the sixth transmembrane domain ($Y266^{TAG}$). These residues were selected on the basis of several criteria: (i) location, either in an extracellular loop or near the interface between a TM and an extracellullar surface, (ii) prior site-directed mutagenesis studies indicating that the residues (S107, G115, V127, and G188) were tolerant to amino acid substitution (*31*), and (iii) conservation of the aromatic functional group (F55, F204, and Y266) (*32, 33*). The plasmids bearing these mutations and the plasmid pECTyrRS/tRNACUA, which encoded the tRNA/tRNA synthetase pair, were transformed into DK102 and BJS21 cells. Cell membranes isolated from strain BJS21 expressing the TAG mutant constructs and the tRNA/tRNA synthetase pair were immunoblotted and probed with antibodies directed against the C-terminal FLAG epitope tag and the N-terminal 100 amino acids of Ste2p (*26*) to determine the effect of the amber stop codon on protein synthesis in the presence and absence of Bpa.

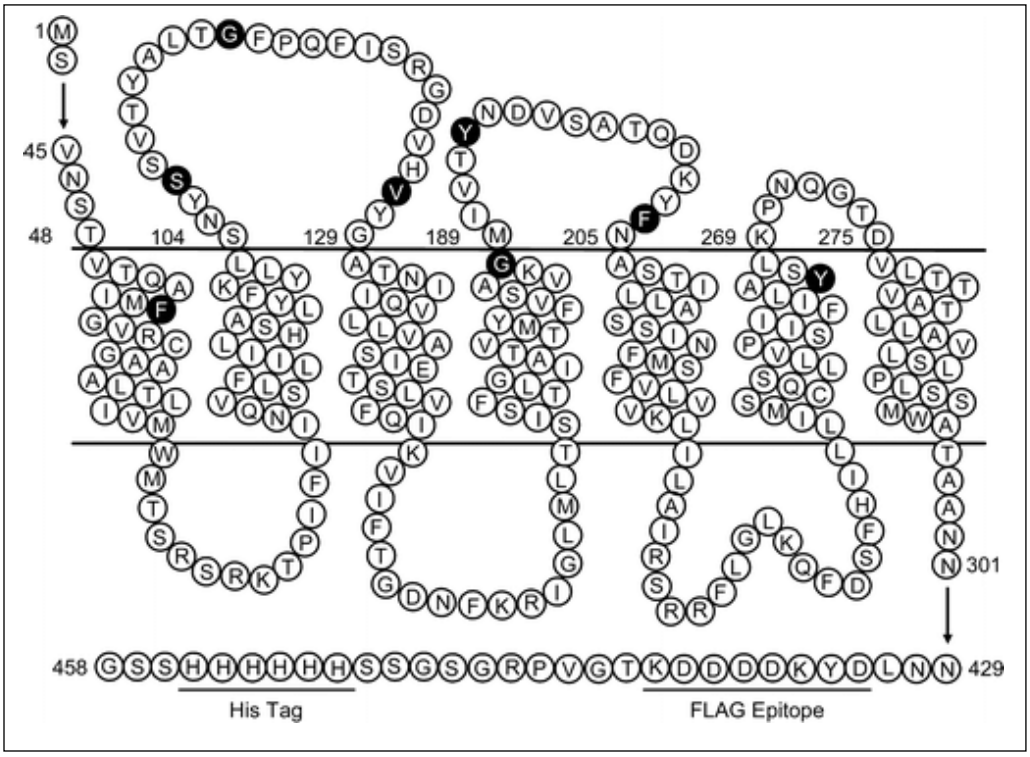

Figure 2.1 Sites targeted for Bpa insertion into Ste2p. The coding region of the STE2 gene was modified to introduce the amber TAG codon, resulting in the insertion of Bpa into Ste2p at the sites indicated in black (F55, S107, G115, V127, G188, Y193, F204, and Y266). The FLAG and His tags are underlined.

To determine if the Ste2p−Bpa mutant proteins were able to bind ligand and ultimately transduce the signal across the cell membrane, growth arrest or "halo" assays were conducted on these transformed cells. Disks impregnated with α factor were placed onto a top agar lawn of DK102 cells putatively expressing Ste2p−Bpa receptors, and the plates were incubated at room temperature for 48−72 h. The rationale to conduct these studies was 2-fold. In the absence of Bpa, the tRNA should not be charged, resulting in the production of truncated Ste2p. In this case, the cells should not respond to pheromone

and growth arrest should not occur. In the presence of Bpa, the TAG codon should be suppressed by the charged tRNA and full-length protein should be synthesized. If the incorporation of Bpa results in expression, the mutant Ste2p proteins might bind pheromone, resulting in the initiation of signal transduction ultimately resulting in growth arrest, indicated by the formation of a clear halo around the disk.

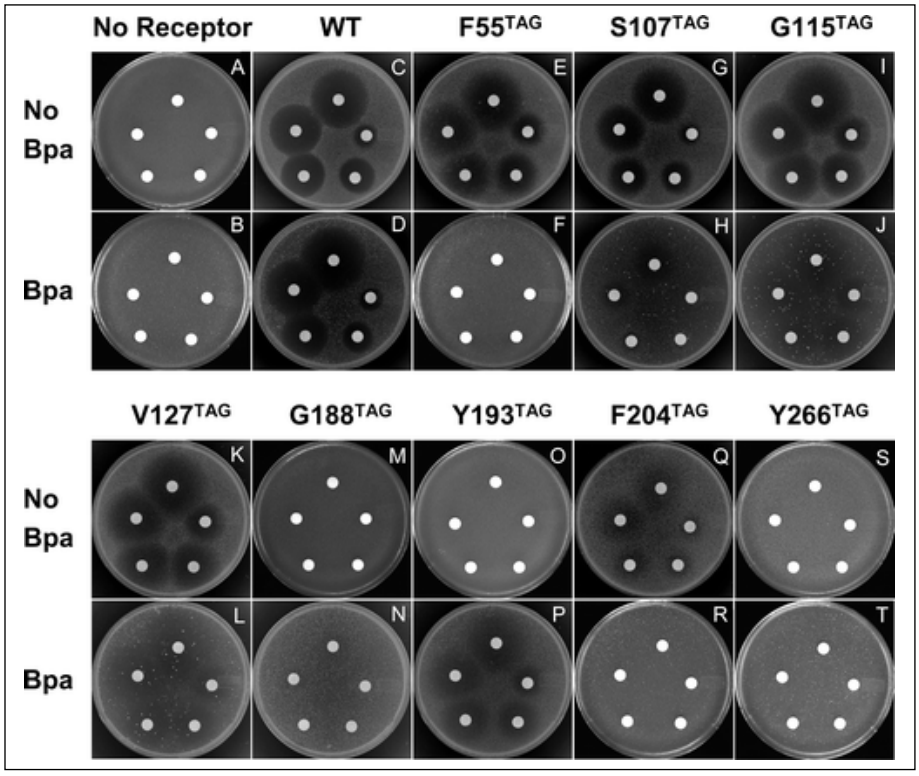

Figure 2.2 Halo assays of WT and Bpa mutant receptors. Cells lacking receptor (A and B), cells containing WT Ste2p (C and D), or cells with mutated Ste2p (E−T) were plated onto medium in the presence and absence of Bpa. Disks containing α factor (2, 1, 0.5, 0.2, and 0.1 μg/disk, starting at the 12 O'clock position on each plate and moving counter-clockwise) were placed onto the lawn of cells. The plates were incubated for 48−72 h at room temperature.

For cells expressing WT Ste2p, dose-dependent halos with well-defined borders and clear zones of inhibition were formed in both the presence and absence of Bpa, indicating that Bpa addition to growth medium did not affect the pheromone response (parts C and D of Figure 2.2). Full-length WT Ste2p was synthesized in both the presence and absence of Bpa and could be detected by both N-terminal (Figure 2.3A) and C-terminal (Figure 2.3B) antibodies. Cells that were deleted for Ste2p did not form halos in either the presence or absence of Bpa (parts A and B of Figure 2.2), and Ste2p was not detected on immunoblots (Figure 2.4).

The mutants $F55^{TAG}$ (Figure 2.2E) and $F204^{TAG}$ (Figure 2.2Q) formed dose-dependent halos in the absence of Bpa, although these halos were "fuzzy", referring to the poor definition of the borders and reduced clarity of the zone of inhibition compared to the WT control. The fuzzy nature of these halos is most likely due to a decreased receptor number or to more rapid desensitization of the Bpa mutant receptor, resulting in a recovery from the growth arrest response (*34, 35*). Immunoblot analysis indicated that, in the absence of Bpa, the protein expression level of the $F55^{TAG}$ mutant was below the limit of detection (Figure 2.3A) and the expression of the $F204^{TAG}$ mutant was very low (Figure 2.4). Despite the inability to visualize the $F55^{TAG}$ protein on the immunoblot, sufficient protein was made by read-through expression to produce the biological response and to be detected by the ligand binding assay (see below). The observation that low levels of Ste2p are sufficient to result in signal transduction was made previously (*36*). These investigators reported that only a fraction of the receptors in a normal cell are necessary for signaling and that reduction of the receptor level to below 5% of the normal

level led to smaller, turbid, fuzzy-edged growth arrest zones in response to α factor. The lack of receptor expression was required to completely block α-factor-induced growth arrest.

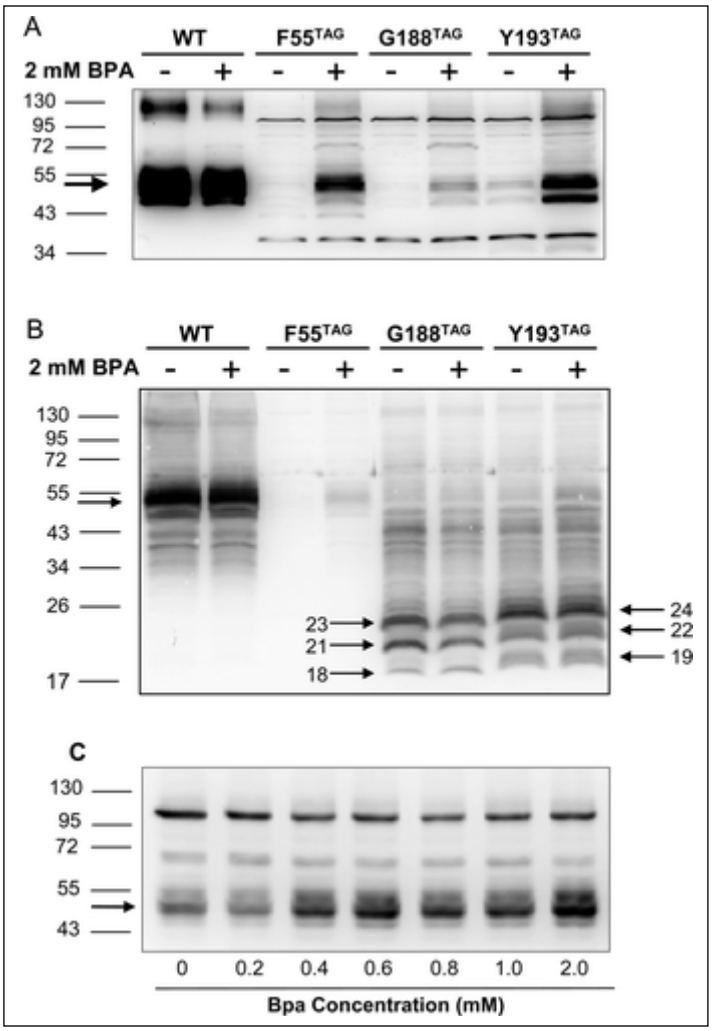

Figure 2.3 Immunoblots of membranes isolated from cells expressing Bpa mutant Ste2p. In each panel, the arrow at the left indicates the band corresponding to full-length Ste2p. (A) C-Terminal FLAG and (B) N-terminal anti-Ste2p immunoblots prepared from cells expressing the F55, G188, and Y193 receptors grown in the presence and absence of 2 mM Bpa. In B, the arrows in the lower portion of the figure indicate truncated forms of

Ste2p. (C) FLAG immunoblot of membranes prepared from cells expressing the F55^{TAG} receptor in the presence of increasing concentrations of Bpa.

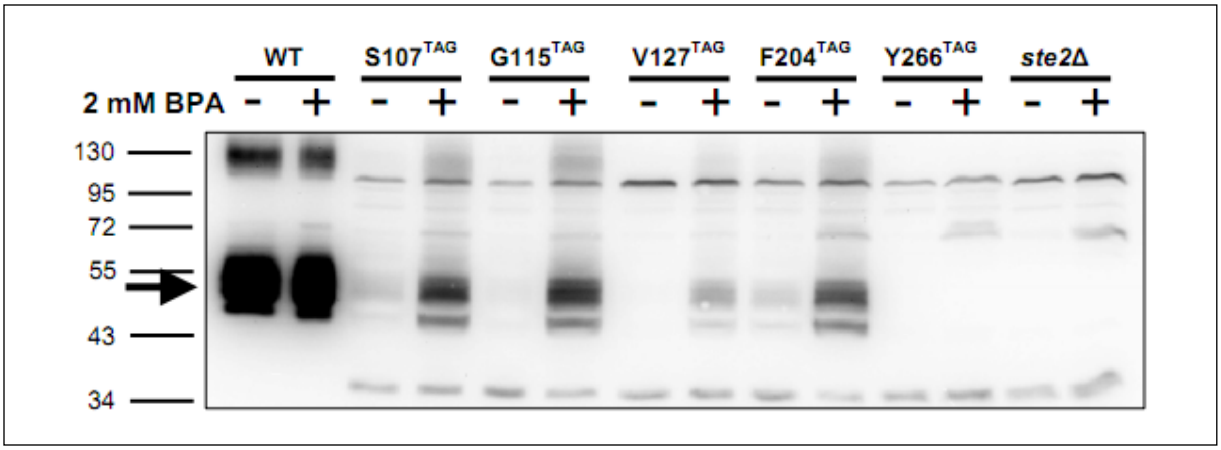

Figure 2.4 Immunoblots of membranes isolated from cells expressing Ste2p mutants with the TAG codon inserted at specific residues indicated in the figure. The arrow at the left indicates the band corresponding to full length Ste2p. The receptors were detected with an antibody to the C-terminal FLAG epitope. Membranes were prepared from cells grown in the presence (+) and absence (-) of 2 mM Bpa as indicated in the figure.

The presence of halos for the F55^{TAG} and F204^{TAG} receptors in the absence of Bpa indicates that there was “read-through” of the amber stop codon (allows translation to read through the amber stop codon and produces full-length protein), resulting in the production of a functional receptor. In contrast, in the presence of Bpa, these same mutants did not form halos (parts F and R of Figure 2.2). Subsequent immunoblot analysis indicated that the expression of the F55^{TAG} (Figure 2.3A) and F204^{TAG} receptors was enhanced in cells grown in the presence of Bpa (Figure 2.4), suggesting that Bpa was

incorporated into Ste2p but was not tolerated at those positions, resulting in nonsignaling receptors. The expression was at relatively low levels; 15 times more protein was loaded for the mutants to allow for detection by the immunoblot compared to that of the WT (30 versus 2 μg).

Receptors with mutations at positions S107 (Figure 2.2G), G115 (Figure 2.2I), and V127 (Figure 2.2 K) also exhibited read-through expression. Halos formed in the absence of Bpa, although they were fuzzy for the $G115^{TAG}$ and $V127^{TAG}$ receptors. Little or no protein was detected by immunoblot analysis for these three receptors when cells were grown in the absence of Bpa (Figure 2.4) indicating again, as in the case of $F55^{TAG}$, expression was below the limit of detection for the immunoblot even though sufficient protein was made by read-through expression to produce the biological response. In the presence of Bpa, expression of these three mutants resulted in halo formation, although the halos were not well-delineated (parts H, J, and L of Figure 2.2, respectively). Immunoblot analysis indicated that expression of these three proteins was enhanced in cells grown in the presence of Bpa (Figure 2.4). Thus, the decline in halo definition, despite the fact that there was an increase in Ste2p protein, indicates that Bpa was incorporated into these receptors but the function was compromised.

For the mutant at position Y193, no halos were formed in the absence of Bpa, suggesting that no functional Ste2p was expressed (Figure 2.2O), although a low-level full-length protein was detected by immunoblot analysis with the C-terminal antibody (Figure 2.3A). In contrast, in the presence of Bpa, dose-dependent fuzzy halos were formed, indicating that Bpa was inserted in response to the TAG codon, resulting in a

functional protein (Figure 2.2P). In parallel with this increase in Ste2p function, there was a concomitant increase in protein expression (Figure 2.3A) for cells grown in the presence of Bpa. The G188TAG mutant had a similar phenotype (parts M and N of Figure 2.2) but with less defined halos observed only at the highest amount of pheromone and only in the presence of Bpa. The poor definition of the halos suggested that Bpa was not well-tolerated at this position. For the G188 receptor, there was no detectable protein produced in the absence of Bpa and a weak but clearly discernible band was detected in membranes obtained from cells grown in the presence of Bpa (Figure 2.3A). Finally, the $Y266^{TAG}$ receptor was not functional in either the presence or absence of Bpa (parts S and T of Figure 2.2), and immunoblot analysis (Figure 2.4) indicated that this receptor was not expressed under either condition.

C-Terminally truncated forms of the receptor can be seen for the $G188^{TAG}$ and $Y193^{TAG}$ receptors using antibody to the N terminus (Figure 2.3B). Three major bands were detected at 23, 21, and 18 kDa for the $G188^{TAG}$ and at 24, 22, and 19 kDa for the $Y193^{TAG}$ receptor. These bands corresponded to the expected size of the nonglycosylated receptor and its two major glycosylated states truncated at the inserted stop codons (*37*). The origin of the bands of higher molecular weight (between 22 and 50 kDa) in the $G188^{TAG}$ and $Y193^{TAG}$ lanes (Figure 2.3B) was not investigated, although these bands are not related to the absence or presence of Bpa. Truncated forms of the $F55^{TAG}$ receptor were not detected with the N-terminal antibody (Figure 2.3B) on this immunoblot because the predicted receptor fragment (6 kDa) would not have been retained on the gel. Note that the full-length Ste2p band intensity (52 kDa) for the WT strain is less intense as

detected by the N-terminal antibody (Figure 2.3B) than that of the same membranes probed with the FLAG antibody (Figure 2.3A). In our hands, the FLAG antibody always yields a stronger signal than the N-terminal antibody. This provides an explanation for the observation that, although full-length Bpa-containing proteins can be detected with the FLAG antibody, they are barely discernible by the N-terminal antibody. Expression of the full-length $F55^{TAG}$ Bpa-containing receptor was enhanced in response to an increased Bpa concentration in the growth medium (Figure 2.3C). At a low concentration (0.2 mM Bpa), no increase over control (no Bpa) was observed, while at higher concentrations (2 mM), the signal corresponding to Ste2p on the immunoblot was enhanced, increasing by 2.6-fold over the control as measured by band intensity. Similar results were obtained for the $G188^{TAG}$ and $Y193^{TAG}$ mutants (data not shown), suggesting that entry of Bpa into the cell is one factor determining the efficiency of Bpa insertion into the protein.

Effect of Bpa-Containing Peptides on the Expression of Ste2p

The data for the $F55^{TAG}$, $G188^{TAG}$, and $Y193^{TAG}$ receptors described above suggests that the expression of Bpa-containing Ste2p could be enhanced if Bpa were more efficiently delivered into the cell. It is known that small peptides enter yeast cells intact through the di/tripeptide transporter Ptr2p (*38, 39*), and upon entry into the cell, these peptides are hydrolyzed to free amino acids. In an attempt to increase the delivery of Bpa into the cell, a Bpa-containing dipeptide (Met−Bpa) was synthesized. Methionyl di- and tripeptides are excellent substrates for the yeast peptide transport system (*40*).

Cells expressing the F55^{TAG}, G188^{TAG}, and Y193^{TAG} receptor constructs were grown in the presence and absence of Met−Bpa, and membranes were isolated and probed with the C-terminal FLAG antibody to detect full-length protein. The expression of full-length WT Ste2p was not affected by the presence of Met−Bpa, confirming that this compound did not interfere with normal Ste2p expression at the concentrations indicated (Figure 2.5A). The Y193^{TAG} mutant expressed minimal FLAG-reactive Ste2p in the absence of Bpa, but in the presence of Met−Bpa (Figure 2.5B), full-length protein was detected.

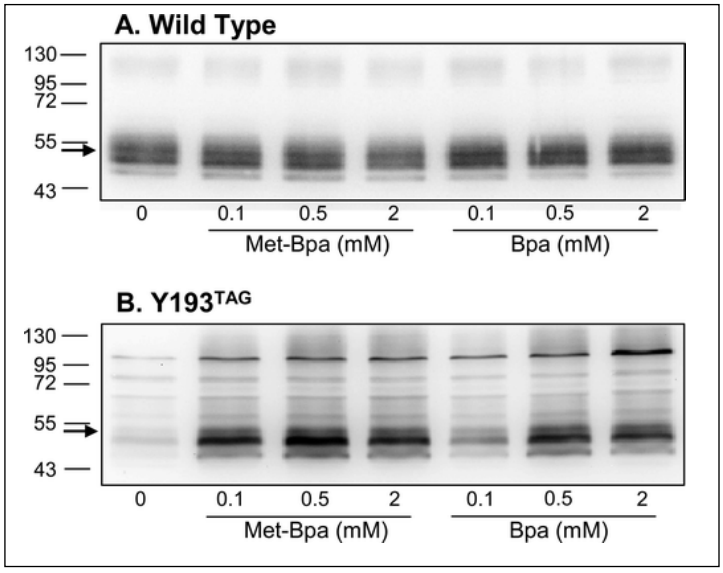

Figure 2.5 Use of a peptidyl form of Bpa. FLAG immunoblot analysis of membranes from cells expressing either WT (A) or Y193^{TAG} (B) Ste2p receptors grown in the presence of the dipeptide Met−Bpa or free Bpa at the concentrations indicated. Protein loads were 2 and 30 μg for the WT and Y193 mutant, respectively.

In comparison to the expression of Y193^{TAG} grown in the presence of 0.1 mM Met−Bpa to that grown in the presence of 0.1 mM Bpa (Figure 2.5B), expression was

greater for the dipeptide (3.1-fold increase). At higher concentrations (0.5 and 2 mM), growth on Met−Bpa and Bpa yielded similar levels of expression (1.4-fold increase at each concentration). Similar results were obtained for the $F55^{TAG}$ and $Y193^{TAG}$ mutants. Growth on dipeptide at 0.1 mM resulted in 2.4- and 2.0-fold increases in expression compared to growth on 0.1 mM Bpa for the $F55^{TAG}$ and $Y193^{TAG}$ mutants, respectively. At higher concentrations of peptide (0.5 mM and 2 mM), growth on Met−Bpa did not increase Ste2p expression when compared to the same concentration of Bpa.

Cell-Surface Expression of Bpa Mutants Determined by Saturation Binding Assay

To characterize the cell-surface expression and binding affinity of the Ste2p Bpa mutants, DK102 cells expressing the $F55^{TAG}$, $G188^{TAG}$, and $Y193^{TAG}$ receptors were used in whole-cell binding assays. Binding of radiolabeled α factor was detected for cells expressing the WT receptor when cultured in either the presence or absence of Bpa. In experiments using the WT receptor, Bpa did not have any significant effect on the B_{max} and binding affinity (B_{max} = 152,470 ± 6900 receptors per cell, K_d = 9.7 ± 1.4 nM) when compared to cells cultured in the absence of Bpa (B_{max} = 158,100 ± 6500 receptors per cell, K_d = 11.0 ± 1.0 nM). For the mutant receptors, binding was not detected for cells grown in the absence of Bpa (data not shown). However, for cells grown in the presence of Bpa, saturable binding was observed (Figure 2.6). The B_{max} values for the mutants were reduced by 10−20-fold compared to the WT receptor (Figure 2.5), which is consistent with the low level of expression observed in the immunoblots (Figure 2.3). The binding affinity (K_d) of the $Y193^{TAG}$ and $G188^{TAG}$ mutants (12.8 ± 4.9 and 17.5 ± 5.7

nM, respectively) were similar to that for the WT receptor, indicating that substitution of Bpa for the endogenous amino acid at these positions did not affect the interaction of the ligand with the receptor. In contrast, for the $F55^{TAG}$ mutant, the binding affinity was reduced to 78.9 ± 46.1 nM, indicating that the substitution of Bpa for phenylalanine at this position affected ligand binding, which correlates to the relative low signaling activity of this receptor.

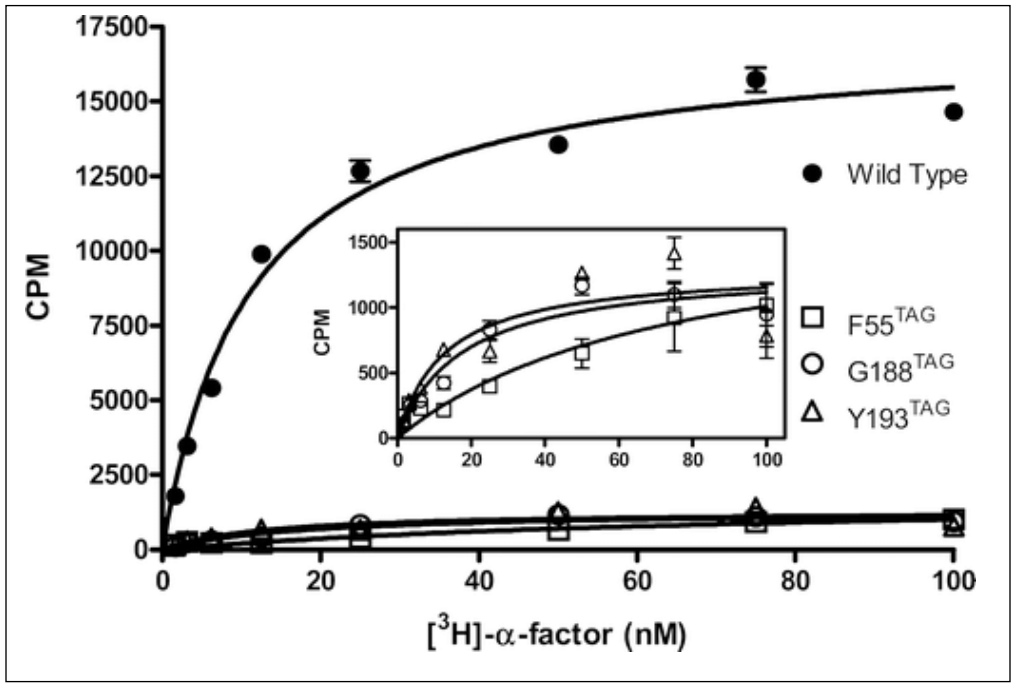

Figure 2.6 Whole cell saturation binding assay of [^{3}H]α factor to WT Ste2p and Ste2p−TAG mutant receptors. Cells expressing the WT receptor and the indicated Bpa mutants were grown in the presence of 2 mM Bpa. (Inset) Saturation binding assay for TAG mutant receptors plotted on an expanded scale. The data represent specific binding to cells as determined by subtracting the binding to an isogenic strain lacking the receptor from binding to cells containing WT or mutant Ste2p.

MALDI−TOF Indicates that Bpa Is Incorporated into Ste2p at Position G188

To confirm the incorporation of Bpa into Ste2p, MALDI−TOF mass spectrometric analysis of purified WT and $G188^{TAG}$ receptors was performed. The G188TAG receptor was chosen for this analysis based on nearby naturally occurring methionine sites in Ste2p that would yield a small peptide (residues 181−189) upon CNBr cleavage to facilitate mass spectroscopy. The substitution of glycine (75.07 Da) for Bpa (269.30 Da) at position 188 should result in a mass shift of 194 Da in the 188Bpa-containing peptide. To estimate purity and concentration of the samples prior to CNBr cleavage and MALDI−TOF analysis, Coomassie Blue and silver staining of SDS−PAGE gels was performed on the purified $G188^{TAG}$ and WT receptors. In the Coomassie-stained gel, only two bands, corresponding in molecular weight to the glycosylated and nonglycosylated forms of Ste2p (50−52 kDa), were observed. Using the more sensitive silver-staining technique on the same sample, the same two bands were detected, along with some very faint bands not corresponding to Ste2p. Immunoblot analysis confirmed that the two major bands were Ste2p (data not shown). After CNBr cleavage of WT and G188TAG receptors, we carried out a MALDI−TOF analysis of the peptide fragments generated, focusing on the molecular-weight region corresponding to the peptide with the putative Gly to Bpa substitution. Our analysis of the CNBr-cleaved WT and $G188^{TAG}$ receptors (Figure 2.7) revealed a mass shift from 954.154 Da in WT to 1146.46 Da in $G188^{TAG}$, corresponding to a 192 Da increase. Other peaks of identical mass corresponding to CNBr fragments of Ste2p were observed in both the WT (1473.81 and 1505.39 Da) and G188Bpa (1474.45 and 1506.19 Da) receptors. Some peaks not

corresponding to any of the theoretical masses of Ste2p CNBr fragments were also observed and are likely due to the degradation of Ste2p, which occurred during the overnight incubation at 37°C during CNBr cleavage, or the presence of other peptides in the preparation.

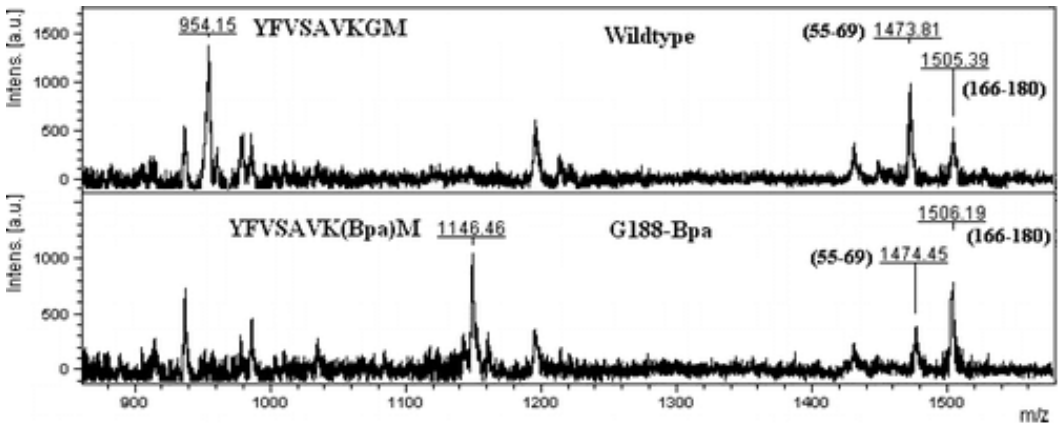

WT		G188^{TAG} (+Bpa)		
theoretical mass	observed mass	theoretical mass	observed mass	corresponding CNBr fragment (residues of Ste2p)
953.11	954.15	**1147.34**	**1146.46**	181–189
1474.82	1473.81	1474.82	1474.45	55–69
1506.77	1505.39	1506.77	1506.19	166–180

Figure 2.7 MALDI−TOF analysis of CNBr cleavage fragments of WT and G188^{TAG} receptors. A peak (954.15 Da) corresponding to residues 181−189 (YFVSAVKGM) in the WT receptor was not present in the G188^{TAG} receptor. The masses for the CNBr fragments indicated that the carboxyl-terminal methionine is converted to homoserine lactone. A new peak (1146.46 Da) corresponding to 181−189 with Bpa at position 188 was detected. Other peaks corresponding to residues 55−69 and 166−180 were observed for both WT and G188^{TAG} receptors.

Bpa at Positions F55 and Y193 Can Cross-link to the α-Factor Ligand

To determine if Bpa incorporated into Ste2p could be used to cross-link to and thus capture the α-pheromone, cells expressing the WT, $F55^{TAG}$, $G188^{TAG}$, and $Y193^{TAG}$ receptors as well as cells lacking Ste2p as a control were grown in the presence of Bpa. Membranes were prepared and incubated with or without [K^7(biotinylamidocaproate)]α factor, an α factor analogue that contains biotin on the position seven lysine of the pheromone and binds to the receptor with high affinity (*27*). Cross-linking was also evaluated in the presence or absence of 100-fold excess nonbiotinylated α factor. After incubation, the membranes were exposed to UV light to activate capture of pheromone to the Bpa-labeled receptor. The membranes were fractionated by SDS−PAGE, blotted, and then probed with FLAG antibody to detect Ste2p (Figure 2.8A) or Neutravidin−HRP to detect biotinylated ligand (Figure 2.8B). WT receptor was expressed at levels higher than any of the mutant receptors (Figure 2.7A) as seen in previous experiments (Figure 2.3). When the immunoblots were probed with Neutravidin−HRP (Figure 2.8B), a distinct band was detected at the size expected for Ste2p in the $F55^{TAG}$ and $Y193^{TAG}$ receptors, indicating that the biotinylated α factor was cross-linked. Despite the fact that at least 20 times as much WT Ste2p was expressed when compared to the $F55^{TAG}$ or $Y193^{TAG}$ receptors (Figure 2.8A), covalent labeling as detected with Neutravidin−HRP was significantly stronger for the mutants (Figure 2.8B). Moreover, labeling of the $F55^{TAG}$ and $Y193^{TAG}$ Bpa-containing receptors was reduced in the presence of excess nonbiotinylated α factor (Figure 2.8B) by 83 and 64%, respectively, as determined by quantitation of the band density. Similar results were observed in three independent

replicates of this experiment. For membranes prepared from cells lacking the receptor, as well as for the WT and the G188^{TAG} receptors, a faint band at approximately 50 kDa was observed (Figure 2.8B) that was dependent upon incubation of the membranes with biotinylated pheromone. The signal was not affected by the presence of nonbiotinylated pheromone. Thus, this signal is the result of nonspecific association of the biotinylated pheromone with the membranes in a Ste2p-independent manner.

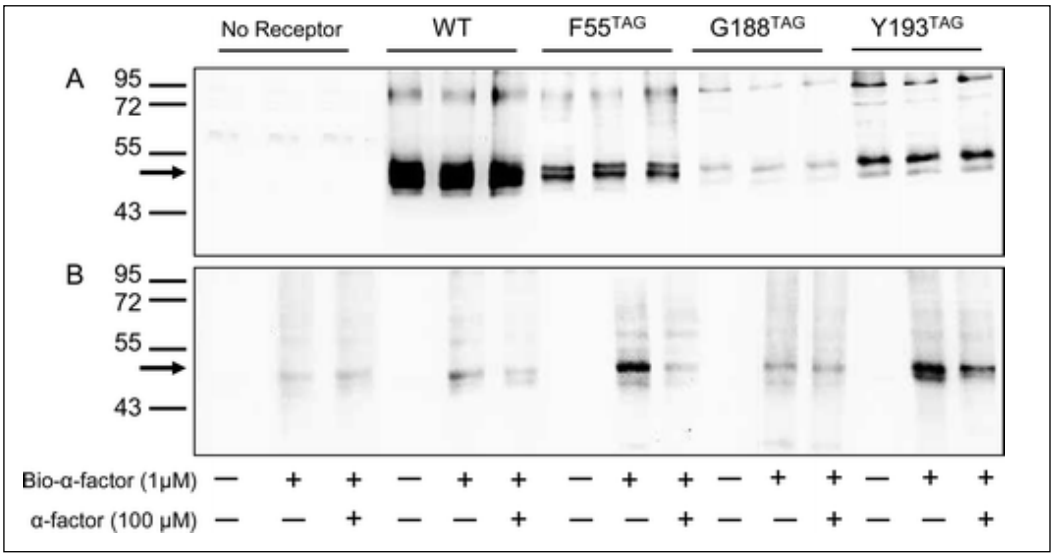

Figure 2.8 Cross-linking of biotinylated α factor into Bpa-containing receptors.

Membranes prepared from cells expressing the WT, F55^{TAG}, G188^{TAG}, and Y193^{TAG} receptors grown in the presence of Bpa were incubated with [K^{7}(biotinylamidocaproate), Nle^{12}]α factor (1 μM) in the presence (+) or absence (−) of nonbiotinylated α factor (100 μM). Membranes were also prepared from cells lacking the receptor as a negative control. (A) After photoactivation, membranes (2 μg for WT and 25 μg for mutants and the negative control) were immublotted and probed with FLAG antibody to detect Ste2p. (B) Membranes (25 μg for each lane) were immunoblotted and probed with

Neutravidin−HRP to detect biotinylated ligand. The arrow in both panels indicates the expected size for Ste2p.

Chapter 4

Discussion

Many experiments have been performed with a variety of methodologies to provide a wealth of knowledge concerning GPCR structure and function. However, an understanding of the mechanism of activation is still in its infancy. The gold standard would be to obtain crystal structures of the GPCR in both the resting and active state. Thus far, bovine rhodopsin and the human β-adrenergic receptor are the only GPCRs to have had their crystal structure solved (*41-43*). For rhodopsin, the receptor was crystallized in the inactive state, although recent reports of an active-state crystal at moderate to low resolution (2.7−5.5 Å) have been published (*44*). Crystallization of the β-adrenergic receptor required expression as a fusion protein (*43*) or interaction with an inverse agonist (*42*) to stabilize receptor conformation. The use of unnatural amino acid replacement provides an alternate method for examining the receptor structure as well as exploring the changes that occur in GPCRs upon receptor activation.

In an earlier study, a fluorescent amino acid was incorporated into a GPCR, the neurokinin-2 receptor, using heterologous expression in Xenopus oocytes (*12*). In this paper, we report the first evidence that an unnatural amino acid can be incorporated into the GPCR Ste2p expressed in its native environment in the yeast cell and still retain function. The incorporation was verified by mass spectrometry, and our studies indicate that, once incorporated, the photoactivatable Bpa in Ste2p can be used to covalently link the α-factor ligand to the receptor. Although there are many examples in the literature of photoactivated cross-linking of ligand to receptor, in all of those cases, the ligand

contained the photoactivatable moiety. To our knowledge, our study represents the first example of cross-linking of ligand to a GPCR in which the receptor contained the photoactivatable group used to "capture" the ligand.

We demonstrated that incorporation of Bpa into both the F55 (located in TM1) and Y193 (located in EL2) receptors resulted in capture of biotinylated pheromone. Photochemical capture of the ligand could be largely inhibited by the presence of excess nonbiotinylated pheromone. While F55 is positioned in the binding pocket of the receptor and was expected to interact with the pheromone (*27*), the ability of Y193 to capture the ligand suggests a possible role for EL2 in ligand binding. Previous studies using domain swapping indicated that EL2 was not a determinant of ligand specificity of the *S. cerevisiae* and S. kluyveri α-factor receptors (*45*). Thus, our observation of a putative contact between the EL2 region of Ste2p and α factor indicates the need for further study of EL2−α-factor interactions. Because of the low level of protein expression, it was unclear whether the G188 receptor was functional with respect to ligand capture, despite the fact that this receptor was determined to contain Bpa by mass spectrometry analysis (Figure 2.7). Saturation binding analysis (Figure 2.6) indicated that the $G188^{TAG}$ receptor was expressed on the cell surface at levels comparable to that of the $F55^{TAG}$ receptor, in which we were able to detect cross-linking of the receptor to the pheromone. In this light, despite the low level of total protein expression observed on the immunoblot, it is likely that there is enough of the $G188^{TAG}$ receptor on the cell surface to allow for cross-linking if the pheromone has access to the Bpa residue. Previously published data using cysteine scanning of Ste2p indicated that G188 is between 25 and 50% exposed on the basis of the

reaction with sulfhydryl reagents (*46*); thus, it is accessible to the solvent. If the pheromone was interacting nonspecifically with the receptor or if residue G188 was involved in ligand binding, then Bpa at this position should have been able to capture ligand.

In addition to ligand capture experiments, we can envision other applications of this mutagenesis methodology, such as studying changes in domain−domain interactions upon ligand binding, which will shed light on the receptor activation mechanism. An advantage of using the orthologous tRNA/aminoacyl-tRNA synthetase pair to incorporate Bpa into Ste2p in the yeast cell is that the GPCR remains in its native environment and is thus able to interact with downstream effector molecules, such as the heterotrimeric G-proteins, thus making assessment of both ligand binding and signal transduction possible.

Although the use of unnatural amino acids has the potential to answer very important questions in GPCR biology, there are still obstacles to overcome. In the experiments presented in this paper, eight mutant STE2 constructs ($F55^{TAG}$, $S107^{TAG}$, $G115^{TAG}$, $V127^{TAG}$, $G188^{TAG}$, $Y193^{TAG}$, $F204^{TAG}$, and $Y266^{TAG}$) were created with the amber TAG stop codon engineered at different sites within the open-reading frame. Theoretically, when the cells expressing these mutant receptors were grown in the presence of Bpa, the unnatural amino acid would be incorporated into the protein by the cognate tRNA/aminoacyl-tRNA synthetase also expressed in the cell. In the absence of Bpa, it was expected that the TAG codon would result in termination of protein synthesis, resulting in a truncated protein. For the mutants $G188^{TAG}$ and $Y193^{TAG}$, this was the case; in the presence of Bpa, cells responded to pheromone (Figure 2.2) and full-length

receptor was detected by immunoblot analysis (Figure 2.3, 2.4) and both bound ligand (Figure 2.6) with near WT affinity. However, mutants with TAG amber stops at positions F55, S107, G115, V127, and F204 exhibited variable amounts of inefficient stop codon recognition or read-through expression, as evidence by the halo assay, which in the context of the present experiments results in the production of full-length protein even in the absence of Bpa.

The efficiency with which nonsense codons, such as the UAG amber stop in mRNA, are suppressed can be affected by the context of the adjacent codons and poses a challenge (*47*). In *S. cerevisiae*, nucleotides within six bases flanking the stop codon can influence the efficiency of termination (*48*) and it has been determined that "backup" or tandem stop codons can be found three codons downstream of the authentic stop for some genes (*49*). In the case of read-through expression, noncognate tRNA species can misread the stop codon and insert an inappropriate amino acid. In the case of the UAG codon in yeast mRNA, the $tRNA^{Gln}$ can insert glutamine at the stop codon when it is present in a context unfavorable for release-factor recognition (*50*). In another tRNA/aminoacyl-tRNA synthetase system evolved to incorporate the fluorescent amino acid dansyl-alanine in response to the amber stop codon, read-through expression in the absence of dansyl-alanine was eliminated by mutation of the aminoacyl-tRNA synthetase to increase selectivity of the enzyme for dansyl-alanine (*18*). Thus, to optimize the system for insertion of Bpa into Ste2p, genetic manipulations in protein translation machinery (i.e., ribosomes, tRNAs, etc.) might be warranted.

Interestingly, for the mutants $F55^{TAG}$ and $F204^{TAG}$, protein function but not expression was eliminated when the cells were grown in the presence of Bpa (Figures 2.2, 2.3, 2.4). This indicates that the unnatural amino acid was incorporated into the protein but did not result in a signal-transducing receptor at the cell surface. The presence of mutant Ste2p or other GPCRs that are expressed and bind ligand but do not signal has been extensively reported (*3*). Indeed, binding without signaling is characteristic of antagonists, and mutation of GPCRs to preferentially recognize antagonists has been documented (*32, 33*).

Incorporation of Bpa into the various TAG mutant receptors was not 100% efficient, as can be seen by the presence of truncated receptors on immunoblots (Figure 2.3B), which could potentially interfere with the function of a full-length receptor. However, previous studies showed that overexpression of 14 different truncated Ste2p receptors failed to produce any significant alteration in Ste2p function (*51*). Thus, the loss of signaling function ($F55^{TAG}$ and $F204^{TAG}$) in the halo assays that we observed likely results from intolerance of Bpa at the positions into which it was inserted rather than to the interference by truncated receptors.

Using the orthologous tRNA/aminoacyl-tRNA synthetase pairs to incorporate Bpa at the engineered amber stop codon requires the presence of Bpa in the cytoplasm at sufficient concentrations to allow for effective charging of the tRNA. We have used a novel means to supply Bpa to yeast cells via the di/tripeptide transport system that is common to many eukaryotes (*52, 53*). In yeast, di/tripeptides as well as oligopeptides (tetra/pentapeptides) are not cleaved outside the cell but are transported intact across the

plasma membrane (*54*). Expression of the $Y193^{TAG}$ receptor as well as the $F55^{TAG}$ and $G188^{TAG}$ receptors was noticeably greater when the cells were grown in the presence of Met−Bpa at 0.1 mM when compared to Bpa (Figure 2.5). Because peptide transporters are ubiquitous in living cells (*53*), this method might be used to enhance the delivery of unnatural amino acids and extend this approach to amino acids that cannot enter cells through amino acid permeases.

In summary, in this paper, we provide evidence that the unnatural photoactivatable amino acid p-benzoyl-l-phenylalanine can be incorporated into a GPCR in its native cell. The $Y193^{TAG}$ mutant receptor responded to α factor and bound this ligand with nanomolar affinity. Other mutant receptors examined were expressed at the membrane at levels from 5 to 10% of the WT receptor under identical conditions. Mass spectrometry proved that Bpa was incorporated at the expected position for the $G188^{TAG}$ receptor. Expression could be increased when the unnatural amino acid was delivered as a dipeptide via the peptide transport system of *S. cerevisiae*. The enhancement of Bpa delivery as a dipeptide was most effective at low (0.1−0.5 mM) concentrations; at 2 mM, both dipeptide and Bpa were equally effective. Two Bpa-containing receptors were able to capture ligand after photoactivation, providing evidence for the utility of such labeled GPCRs to determine ligand−receptor interactions. These results set the stage for the use of unnatural amino acids technology in exploring the structure and function of integral membrane proteins in their native environment.

References for Part II

1. Eilers, M., Hornak, V., Smith, S. O., and Konopka, J. B. (2005) Comparison of class A and D G protein-coupled receptors: common features in structure and activation, *Biochemistry 44*, 8959-8975.
2. Karnik, S. S., Gogonea, C., Patil, S., Saad, Y., and Takezako, T. (2003) Activation of G-protein-coupled receptors: a common molecular mechanism, *Trends in endocrinology and metabolism: TEM 14*, 431-437.
3. Kristiansen, K. (2004) Molecular mechanisms of ligand binding, signaling, and regulation within the superfamily of G-protein-coupled receptors: molecular modeling and mutagenesis approaches to receptor structure and function, *Pharmacology & therapeutics 103*, 21-80.
4. Chin, J. W., Cropp, T. A., Anderson, J. C., Mukherji, M., Zhang, Z., and Schultz, P. G. (2003) An expanded eukaryotic genetic code, *Science 301*, 964-967.
5. Wang, L., Xie, J., and Schultz, P. G. (2006) Expanding the genetic code, *Annual review of biophysics and biomolecular structure 35*, 225-249.
6. Liu, W., Brock, A., Chen, S., and Schultz, P. G. (2007) Genetic incorporation of unnatural amino acids into proteins in mammalian cells, *Nature methods 4*, 239-244.
7. Chen, S., Schultz, P. G., and Brock, A. (2007) An improved system for the generation and analysis of mutant proteins containing unnatural amino acids in *Saccharomyces cerevisiae*, *Journal of molecular biology 371*, 112-122.

8. Xie, J., and Schultz, P. G. (2005) Adding amino acids to the genetic repertoire, *Current opinion in chemical biology 9*, 548-554.

9. Monahan, S. L., Lester, H. A., and Dougherty, D. A. (2003) Site-specific incorporation of unnatural amino acids into receptors expressed in Mammalian cells, *Chemistry & biology 10*, 573-580.

10. Sakamoto, K., Hayashi, A., Sakamoto, A., Kiga, D., Nakayama, H., Soma, A., Kobayashi, T., Kitabatake, M., Takio, K., Saito, K., Shirouzu, M., Hirao, I., and Yokoyama, S. (2002) Site-specific incorporation of an unnatural amino acid into proteins in mammalian cells, *Nucleic acids research 30*, 4692-4699.

11. Rodriguez, E. A., Lester, H. A., and Dougherty, D. A. (2006) In vivo incorporation of multiple unnatural amino acids through nonsense and frameshift suppression, *Proceedings of the National Academy of Sciences of the United States of America 103*, 8650-8655.

12. Turcatti, G., Nemeth, K., Edgerton, M. D., Meseth, U., Talabot, F., Peitsch, M., Knowles, J., Vogel, H., and Chollet, A. (1996) Probing the structure and function of the tachykinin neurokinin-2 receptor through biosynthetic incorporation of fluorescent amino acids at specific sites, *The Journal of biological chemistry 271*, 19991-19998.

13. Padgett, C. L., Hanek, A. P., Lester, H. A., Dougherty, D. A., and Lummis, S. C. (2007) Unnatural amino acid mutagenesis of the GABA(A) receptor binding site residues reveals a novel cation-pi interaction between GABA and beta 2Tyr97,

The Journal of neuroscience : the official journal of the Society for Neuroscience 27, 886-892.

14. McMenimen, K. A., Dougherty, D. A., Lester, H. A., and Petersson, E. J. (2006) Probing the Mg2+ blockade site of an N-methyl-D-aspartate (NMDA) receptor with unnatural amino acid mutagenesis, *ACS chemical biology 1*, 227-234.
15. Beene, D. L., Brandt, G. S., Zhong, W., Zacharias, N. M., Lester, H. A., and Dougherty, D. A. (2002) Cation-pi interactions in ligand recognition by serotonergic (5-HT3A) and nicotinic acetylcholine receptors: the anomalous binding properties of nicotine, *Biochemistry 41*, 10262-10269.
16. Tong, Y., Brandt, G. S., Li, M., Shapovalov, G., Slimko, E., Karschin, A., Dougherty, D. A., and Lester, H. A. (2001) Tyrosine decaging leads to substantial membrane trafficking during modulation of an inward rectifier potassium channel, *The Journal of general physiology 117*, 103-118.
17. Santarelli, V. P., Eastwood, A. L., Dougherty, D. A., Horn, R., and Ahern, C. A. (2007) A cation-pi interaction discriminates among sodium channels that are either sensitive or resistant to tetrodotoxin block, *The Journal of biological chemistry 282*, 8044-8051.
18. Summerer, D., Chen, S., Wu, N., Deiters, A., Chin, J. W., and Schultz, P. G. (2006) A genetically encoded fluorescent amino acid, *Proceedings of the National Academy of Sciences of the United States of America 103*, 9785-9789.
19. Deiters, A., Cropp, T. A., Mukherji, M., Chin, J. W., Anderson, J. C., and Schultz, P. G. (2003) Adding amino acids with novel reactivity to the genetic code of

Saccharomyces cerevisiae, *Journal of the American Chemical Society 125*, 11782-11783.

20. David, N. E., Gee, M., Andersen, B., Naider, F., Thorner, J., and Stevens, R. C. (1997) Expression and purification of the *Saccharomyces cerevisiae* alpha-factor receptor (Ste2p), a 7-transmembrane-segment G protein-coupled receptor, *The Journal of biological chemistry 272*, 15553-15561.
21. Mumberg, D., Muller, R., and Funk, M. (1995) Yeast vectors for the controlled expression of heterologous proteins in different genetic backgrounds, *Gene 156*, 119-122.
22. Gietz, D., St Jean, A., Woods, R. A., and Schiestl, R. H. (1992) Improved method for high efficiency transformation of intact yeast cells, *Nucleic acids research 20*, 1425.
23. Sherman, F. (2002) Getting started with yeast, *Methods in enzymology 350*, 3-41.
24. Naider, F., Becker, J. M., and Katzir-Katchalski, E. (1974) Utilization of methionine-containing peptides and their derivatives by a methionine-requiring auxotroph of *Saccharomyces cerevisiae*, *The Journal of biological chemistry 249*, 9-20.
25. Raths, S. K., Naider, F., and Becker, J. M. (1988) Peptide analogues compete with the binding of alpha-factor to its receptor in *Saccharomyces cerevisiae*, *The Journal of biological chemistry 263*, 17333-17341.

26. Konopka, J. B., Jenness, D. D., and Hartwell, L. H. (1988) The C-terminus of the *S. cerevisiae* alpha-pheromone receptor mediates an adaptive response to pheromone, *Cell 54*, 609-620.

27. Son, C. D., Sargsyan, H., Naider, F., and Becker, J. M. (2004) Identification of ligand binding regions of the *Saccharomyces cerevisiae* alpha-factor pheromone receptor by photoaffinity cross-linking, *Biochemistry 43*, 13193-13203.

28. Lin, J. C., Parrish, W., Eilers, M., Smith, S. O., and Konopka, J. B. (2003) Aromatic residues at the extracellular ends of transmembrane domains 5 and 6 promote ligand activation of the G protein-coupled alpha-factor receptor, *Biochemistry 42*, 293-301.

29. Lin, J. C., Duell, K., and Konopka, J. B. (2004) A microdomain formed by the extracellular ends of the transmembrane domains promotes activation of the G protein-coupled alpha-factor receptor, *Molecular and cellular biology 24*, 2041-2051.

30. Hauser, M., Kauffman, S., Lee, B. K., Naider, F., and Becker, J. M. (2007) The first extracellular loop of the *Saccharomyces cerevisiae* G protein-coupled receptor Ste2p undergoes a conformational change upon ligand binding, *The Journal of biological chemistry 282*, 10387-10397.

31. Akal-Strader, A., Khare, S., Xu, D., Naider, F., and Becker, J. M. (2002) Residues in the first extracellular loop of a G protein-coupled receptor play a role in signal transduction, *The Journal of biological chemistry 277*, 30581-30590.

32. Lee, B. K., Lee, Y. H., Hauser, M., Son, C. D., Khare, S., Naider, F., and Becker, J. M. (2002) Tyr266 in the sixth transmembrane domain of the yeast alpha-factor receptor plays key roles in receptor activation and ligand specificity, *Biochemistry 41*, 13681-13689.

33. Lee, Y. H., Naider, F., and Becker, J. M. (2006) Interacting residues in an activated state of a G protein-coupled receptor, *The Journal of biological chemistry 281*, 2263-2272.

34. Grishin, A. V., Weiner, J. L., and Blumer, K. J. (1994) Control of adaptation to mating pheromone by G protein beta subunits of *Saccharomyces cerevisiae*, *Genetics 138*, 1081-1092.

35. Weiner, J. L., Guttierez-Steil, C., and Blumer, K. J. (1993) Disruption of receptor-G protein coupling in yeast promotes the function of an SST2-dependent adaptation pathway, *The Journal of biological chemistry 268*, 8070-8077.

36. Shah, A., and Marsh, L. (1996) Role of Sst2 in modulating G protein-coupled receptor signaling, *Biochemical and biophysical research communications 226*, 242-246.

37. Mentesana, P. E., and Konopka, J. B. (2001) Mutational analysis of the role of N-glycosylation in alpha-factor receptor function, *Biochemistry 40*, 9685-9694.

38. Island, M. D., Perry, J. R., Naider, F., and Becker, J. M. (1991) Isolation and characterization of *S. cerevisiae* mutants deficient in amino acid-inducible peptide transport, *Current genetics 20*, 457-463.

39. Perry, J. R., Basrai, M. A., Steiner, H. Y., Naider, F., and Becker, J. M. (1994) Isolation and characterization of a Saccharomyces cerevisiae peptide transport gene, *Molecular and cellular biology 14*, 104-115.

40. Hauser, M., Kauffman, S., Naider, F., and Becker, J. M. (2005) Substrate preference is altered by mutations in the fifth transmembrane domain of Ptr2p, the di/tri-peptide transporter of *Saccharomyces cerevisiae*, *Molecular membrane biology 22*, 215-227.

41. Palczewski, K., Kumasaka, T., Hori, T., Behnke, C. A., Motoshima, H., Fox, B. A., Le Trong, I., Teller, D. C., Okada, T., Stenkamp, R. E., Yamamoto, M., and Miyano, M. (2000) Crystal structure of rhodopsin: A G protein-coupled receptor, *Science 289*, 739-745.

42. Rasmussen, S. G., Choi, H. J., Rosenbaum, D. M., Kobilka, T. S., Thian, F. S., Edwards, P. C., Burghammer, M., Ratnala, V. R., Sanishvili, R., Fischetti, R. F., Schertler, G. F., Weis, W. I., and Kobilka, B. K. (2007) Crystal structure of the human beta2 adrenergic G-protein-coupled receptor, *Nature 450*, 383-387.

43. Rosenbaum, D. M., Cherezov, V., Hanson, M. A., Rasmussen, S. G., Thian, F. S., Kobilka, T. S., Choi, H. J., Yao, X. J., Weis, W. I., Stevens, R. C., and Kobilka, B. K. (2007) GPCR engineering yields high-resolution structural insights into beta2-adrenergic receptor function, *Science 318*, 1266-1273.

44. Ridge, K. D., and Palczewski, K. (2007) Visual rhodopsin sees the light: structure and mechanism of G protein signaling, *The Journal of biological chemistry 282*, 9297-9301.

45. Sen, M., and Marsh, L. (1994) Noncontiguous domains of the alpha-factor receptor of yeasts confer ligand specificity, *The Journal of biological chemistry 269*, 968-973.

46. Choi, Y., and Konopka, J. B. (2006) Accessibility of cysteine residues substituted into the cytoplasmic regions of the alpha-factor receptor identifies the intracellular residues that are available for G protein interaction, *Biochemistry 45*, 15310-15317.

47. Xie, J., and Schultz, P. G. (2006) A chemical toolkit for proteins--an expanded genetic code, *Nature reviews. Molecular cell biology 7*, 775-782.

48. Williams, I., Richardson, J., Starkey, A., and Stansfield, I. (2004) Genome-wide prediction of stop codon readthrough during translation in the yeast *Saccharomyces cerevisiae*, *Nucleic acids research 32*, 6605-6616.

49. Liang, H., Cavalcanti, A. R., and Landweber, L. F. (2005) Conservation of tandem stop codons in yeasts, *Genome biology 6*, R31.

50. Edelman, I., and Culbertson, M. R. (1991) Exceptional codon recognition by the glutamine tRNAs in *Saccharomyces cerevisiae*, *The EMBO journal 10*, 1481-1491.

51. Martin, N. P., Leavitt, L. M., Sommers, C. M., and Dumont, M. E. (1999) Assembly of G protein-coupled receptors from fragments: identification of functional receptors with discontinuities in each of the loops connecting transmembrane segments, *Biochemistry 38*, 682-695.

52. Daniel, H., Spanier, B., Kottra, G., and Weitz, D. (2006) From bacteria to man: archaic proton-dependent peptide transporters at work, *Physiology (Bethesda) 21*, 93-102.

53. Saier, M. H., Jr. (2000) A functional-phylogenetic classification system for transmembrane solute transporters, *Microbiology and molecular biology reviews : MMBR 64*, 354-411.

54. Hauser, M., Donhardt, A. M., Barnes, D., Naider, F., and Becker, J. M. (2000) Enkephalins are transported by a novel eukaryotic peptide uptake system, *The Journal of biological chemistry 275*, 3037-3041.

PART III

Changes in Conformation at the Cytoplasmic Ends of the Fifth and Sixth Transmembrane Helices of a Yeast G Protein-Coupled Receptor in Response to Ligand Binding

Part III was published in its entirety as: Umanah GK, Huang LY, Maccarone JM, Naider F, and Becker JM. (2011) *Biochemistry* **50**(32):6841-54. Li-Yin Huang and George K. Umanah performed most of the work, Julie Maccarone determined the phenotypes of the Ste2p mutants and the peptides used were obtained from Dr. Naider's laboratory.

Abstract for Part III

The third intracellular loop (IL3) of G protein-coupled receptors (GPCRs) is an important contact domain between GPCRs and their G proteins. Previously, the IL3 of Ste2p, a *Saccharomyces cerevisiae* GPCR, was suggested to undergo a conformational change upon activation as detected by differential protease susceptibility in the presence and absence of ligand. In this study using disulfide cross-linking experiments we show that the Ste2p cytoplasmic ends of helix 5 (TM5) and helix 6 (TM6) that flank the amino and carboxyl sides of IL3 undergo conformational changes upon ligand binding, whereas the center of the IL3 loop does not. Single Cys substitution of residues in the middle of IL3 led to receptors that formed high levels of cross-linked Ste2p, whereas Cys substitution at the interface of IL3 and the contiguous cytoplasmic ends of TM5 and TM6 resulted in minimal disulfide-mediated cross-linked receptor. The alternating pattern of residues involved in cross-linking suggested the presence of a 3_{10} helix in the middle of IL3. Agonist (WHWLQLKPGQPNleY) induced Ste2p activation reduced cross-linking mediated by Cys substitutions at the cytoplasmic ends of TM5 and TM6 but not by residues in the middle of IL3. Thus, the cytoplasmic ends of TM5 and TM6 undergo conformational change upon ligand binding. An α-factor antagonist (des-Trp, des-His-α-factor) did not influence disulfide-mediated Ste2p cross-linking, suggesting that the interaction of the N-terminus of α-factor with Ste2p is critical for inducing conformational changes at TM5 and TM6. We propose that the changes in conformation revealed for residues at the ends of TM5 and TM6 are affected by the presence of G protein but not G protein activation. This study provides new information about role of

specific residues of a GPCR in signal transduction and how peptide ligand binding activates the receptor.

Chapter 1

Introduction

G protein-coupled receptors (GPCRs) are integral membrane proteins that are known to play important roles in cell communication by activating intracellular events through both G protein-dependent and -independent processes (*1-3*). These receptors are encoded by the largest gene family in mammals, constitute the main target of prescribed drugs, and represent promising targets for new drug development (*1, 3-6*). They are composed of seven transmembrane (TM) helical segments connected by intracellular and extracellular loops. The core region of the receptor containing the seven TMs has been found to be generally responsible for binding of small ligands, whereas peptide ligands often bind to the extracellular portions as well as the core of GPCRs (*7, 8*). In the classical model of ligand activation of a GPCR signal transduction pathway, the binding of an agonist to the receptor induces conformational changes in the TMs propagated to the cytoplasmic ends of a GPCR for G protein activation and transduction to various intracellular metabolic events (*1, 9*).

The cytoplasmic surfaces of GPCRs contain multiple contact regions responsible for receptor coupling to signal transduction complexes. The most prominent domains in GPCRs for coupling are the second and third (IL3) intracellular loops as well as the C-terminal tail and TM boundaries (*1-3*). Comparing the crystal structure of opsin and rhodopsin shows that the cytoplasmic end of TM6 is shifted outward from the center of the bundle relative to its position in the inactive state (rhodopsin) and is closer to TM5 in the active state (opsin) (*10*). Such movements have also been observed in other receptor

such as M3 and adrenergic receptors using disulfide cross-linking of Cys mutant receptors. In the M3 receptor, agonist binding increased the proximity between the cytoplasmic ends of TM5 and TM6. Possible TM6 rotational movements were also observed in the M3 receptor (*11*).

Several studies have shown that peptide ligands bind GPCRs and occupy a pocket defined by side chains from extracellular loops and helices. The binding of the ligand induces changes at the extracellular surface of the receptor resulting in conformational changes at the cytoplasmic surfaces. These phenomena are believed to be critical for GPCR activation (*2*). An explosion of recent crystal structures of ligand-bound (activated) β_1-adrenergic (*12*), β_2-adrenergic (*13*), and A_{2a} (*14*) receptors indicated major changes in the cytoplasmic ends of TM5 and TM6 as a result of receptor activation.

Ste2p, the yeast *Saccharomyces cerevisiae* receptor for the pheromone α-factor, is believed to have a structure similar to that of mammalian GPCRs. The third intracellular loop of Ste2p has been shown to play an important role in signal transduction and is involved in Gpa1p (the *S. cerevisiae* Gα protein) activation (*15-18*). Analysis of the Ste2p IL3 demonstrated that IL3 becomes hypersensitive to proteolytic digestion with trypsin in response to ligand binding, indicating that IL3 undergoes a conformational change that is likely to be important for G protein activation(*19*), although specific residues that are involved in these conformational changes were not identified. The TM5 and TM6 that flank the IL3 have also been shown to interact with each other and have been suggested to play a critical role in signaling (*20*). It is important to note that the Gα protein of the

heteromeric G protein complex need not dissociate from Ste2p during receptor activation as indicated by the full activity of a Ste2p-Gpa1p fusion chimera (*21*).

In this study, we have investigated IL3 and flanking TM5 and TM6 conformational changes by determining the propensity for disulfide cross-linking between receptors carrying Cys substitutions. The IL3-Cys mutant receptors were observed to form dimers with the pattern of dimer formation, suggesting the presence of a 3_{10} helix in the middle of the IL3 loop. Addition of α-factor affected the levels of disulfide formation in Cys-substituted receptors in portions of TM5 and TM6 contiguous with IL3, implying that activation of Ste2p involved ligand-induced conformational changes in the cytoplasmic ends of TM5 and TM6. In contrast, disulfide formation involving residues in the middle of IL3 was not sensitive to ligand addition, indicating that residues in the IL3 loop do not change conformation or availability during receptor activation. The presence of an α-factor antagonist or a non-hydrolyzable GTP analogue did not influence the levels of disulfide-mediated dimerization, suggesting that receptor activation but not Gα activation was necessary for the observed conformational changes.

Chapter 2

Material and Methods

Media, Reagents, and Strains and Transformation

Saccharomyces cerevisiae strain LM102 [*MATa, bar1, leu2, trp1, ura3, FUS1-lacZ::URA3, ste2Δ (22)*] was used for Ste2p growth arrest and FUS1-lacZ assays. The protease-deficient strain BJS21 [*MATa, prc1-407 prb1-1122 pep4-3 leu2 trp1 ura3-52 ste2::Kan*^{R} (*23*)] and TM5117 [*MATa, bar1, leu2, his3, ura3, FUS1-lacZ::URA3, ste2Δ, gpa1Δ* (*22*)] were used for protein isolation and immunoblot analysis and disulfide cross-linking. Plasmids coding for the STE2 mutants and GPA1 mutants were transformed by the method previously described (*22*) into LM102, TM5117, and BJS21 cells. Transformants were selected by growth on minimal medium (*24*) lacking tryptophan (designated as MLT) or lacking both tryptophan and uracil (designated as MLTU) to maintain selection for the plasmids. All media components were obtained from Becton-Dickinson (Franklin Lakes, NJ).

Cysteine Scanning Mutagenesis

C-terminal FLAG and His-tagged STE2 with the two native cysteine residues (Cys59 and Cys252) substituted with serine and cloned into the plasmid p424-GPD (high copy plasmid) to yield plasmid pBEC2 (*22*) was used as the backbone for mutagenesis of Ste2p. The plasmid pBEC2 was engineered by site-directed mutagenesis to individually replace 30 residues in Ste2p (V224-Q253, see Figure 3.1) with cysteine as previously described (*22*).

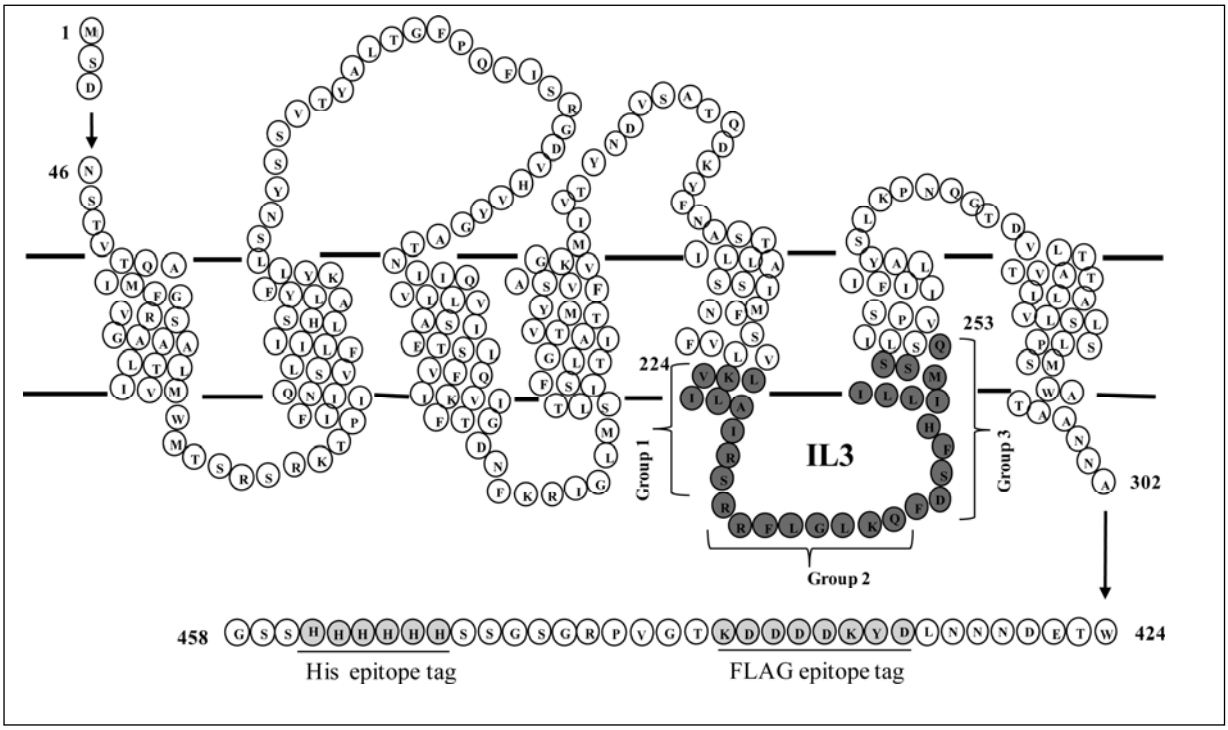

Figure 3.1 Schematic diagram of Ste2p. Single cysteine at positions 224 to 253 (solid circles) were introduced into the IL3 region of the *STE2* gene. The FLAG and His tags are underlined in the C-terminal tail.

Membrane Extraction and Immunoblots

BJS21 cells expressing STE2 and GPA1 constructs grown in their selective media were used to prepare total cell membranes isolated as previously described (*25*). Cells were harvested and lysed by agitation with glass beads in 700 μL of HEPES buffer (50 mM HEPES, 150 mM NaCl, pH 7.5) and the following concentrations of protease inhibitors: 1.0 mM leupeptin,10 μM pepstatin A, and 5.0 mM phenylmethanesulfonyl fluoride. The lysate was cleared by centrifugation at 3000g for 2 min. The membrane fraction was harvested by centrifugation at 15000g for 30 min and was then resuspended

in the HEPES buffer with 20% glycerol. Protein concentration was determined by BioRad (BioRad, Hercules, CA) protein assay as previously described (*22*). For immunoblot analyses the membrane extract was solubilized in SDS sample buffer (BioRad, Hercules, CA), and 5 μg was fractioned by 10% SDS-PAGE. Blots were probed with FLAG antibody (Sigma/Aldrich Chemical, St. Louis, MO) to detect Ste2p. The signals generated were analyzed using Quantity One software (Version 4.5.1) on a Chemi-Doc XRS photodocumentation system (BioRad, Hercules, CA). The student's t test was used to analyze differences in dimer formation (cross-linking) between pheromone treated and nontreated receptors. A probability of $p \leq 0.01$ was regarded as statistically significant. Statistical analyses were performed with Prism (GraphPad Software, San Diego, CA).

Growth Arrest Assays

LM102 cells expressing C-terminal FLAG and His tagged Ste2p were grown at 30°C in MLT, harvested by centrifugation, washed three times with water, and resuspended at a final concentration of 5×10^6 cells/mL according to previously described procedures (*23*). Cells (1 mL) were combined with 3.5 mL of agar noble (1.1%) and poured as a top agar lawn onto MLT medium agar plates. Filter disks (Whatman #1 paper) impregnated with α-factor pheromone (0.125–2.0 μg) were placed on the top agar. The plates were incubated at 30°C for 18 h and then observed for clear halos around the discs. The diameter of halos around the discs were measured, plotted as diameter versus pheromone amount, and analyzed by linear regression analysis using

Prism software (GraphPad Software, San Diego, CA) to determine the amount of pheromone that yielded a 15 mm halo. The experiment was repeated at least three times, and reported values represent the mean of these tests.

Fus1-lacZ Assays

LM102 cells expressing C-terminal FLAG and His tagged Ste2p Cys mutants were grown at 30°C in selective media, harvested, washed three times with fresh media, and resuspended at a final concentration of 5×10^7 cells/mL. Cells (0.5 mL) were combined with α-factor pheromone (final concentration of 1 μM) and incubated at 30°C for 90 min. The cells were transferred to a 96-well flat-bottom plate in triplicates and permeabilized with 0.5% Triton X-100 in 25 mM PIPES buffer, and then β-galactosidase assays were carried out using fluorescein di-β-galactopyranoside (Molecular Probes, OR) as a substrate (*26*). The reaction mixtures were incubated at 37°C for 60 min, and 1.0 M Na_2CO_3 was added to stop the reaction. The fluorescence of the samples (excitation of 485 nm and emission of 530 nM) was determined using a 96-well plate reader Synergy2 (BioTek Instruments, Inc., Winooski, VT). The data were analyzed using Prism software (GraphPad Software, San Diego, CA). The experiments were repeated at least three times, and reported values represent the mean of these tests.

Saturation Binding Assay

Tritiated α-factor (9.3 Ci/mmol) was used in saturation binding assays on whole cells. LM102 cells expressing Ste2p Cys-less as the wild-type and mutants with the Cys

substitutions in IL3 (L228C, A229C, R233C, R234C, L248C, and I249C) were harvested, washed three times with YM1 [yeast minimum medium with 0.5 M potassium phosphate (pH 6.24) containing 10 mM TAME, 10 mM sodium azide, 10 mM potassium fluoride, and 1% BSA], and adjusted to a final concentration of 4×10^7 cells/mL in binding medium YM1i (YM1 plus protease inhibitors). Cells (630 μL) were combined with 70 μL of 10X YM1i supplemented with [^{3}H]α-factor and incubated at room temperature for 30 min. The final concentration of [^{3}H]α-factor ranged from 0.4×10^{-9} to 50×10^{-9} M. Upon completion of the incubation interval, 200 μL aliquots of the cell–pheromone mixture were collected in triplicate and washed over glass fiber filter mats using the Standard Cell Harvester (Skatron Instruments, Sterling, VA). Retained radioactivity on the filter was counted by liquid scintillation spectroscopy. LM102 cells lacking Ste2p were used as a nonspecific binding control for the assays. Specific binding for each mutant receptor was calculated by subtracting the nonspecific values from those obtained for total binding. Specific binding data were analyzed by nonlinear regression analysis for single-site binding using Prism software (GraphPad Software, San Diego, CA) to determine the K_d (nM), and B_{max} values (receptors/cell) for each mutant receptor were calculated. The final values represent the binding constants from at least three independent experiments.

Binding Competition Assays

This assay was performed using LM102 cells expressing C-terminal FLAG and His-tagged Ste2p. Tritiated [^{3}H]-α-factor (10.2 Ci/mmol, 12 μM) prepared as previously

described (*23, 27*) was used in competition binding assays on whole cells. The cells were grown at 30°C in MLT, harvested, washed three times with YM1 [0.5 M potassium phosphate (pH 6.24) containing 10 mM TAME, 10 mM sodium azide, 10 mM potassium fluoride, and 1% BSA], and adjusted to a final concentration of 2×10^7 cells/mL in YM1 plus protease inhibitors [YM1i (*25*)]. For the competition binding studies, cells (600 μL) were combined with 150 μL of ice-cold 5X YM1i supplemented with 6nM [^{3}H]α-factor in the presence or absence α-factor or α-factor antagonist and incubated at room temperature for 30 min. The final concentrations of α-factor and α-factor antagonist varied from 0.5×10^{-10} to 1×10^{-6} M. After incubation, triplicate samples of 200 μL aliquots were filtered and washed over glass fiber filter mats using the Standard Cell Harvester (Skatron Instruments, Sterling, VA) and placed in scintillation vials. The radioactivity [^{3}H] on the filter was counted by liquid scintillation spectroscopy. The binding data were analyzed by nonlinear regression analysis for one-site competition binding using Prism software (GraphPad Software, San Diego, CA) (*28*). The final values represent the binding constants from at least three independent experiments.

Disulfide Cross-Linking

Membrane proteins (in HEPES buffer, 20% glycerol) extracted from BJS21 cells expressing Ste2p mutants coexpressed with wild-type Gpa1p were treated with CuP (1.0 μM Cu and 3.0 μM 1,10-phenanthroline) and incubated at room temperature for 30 min. The reaction was quenched by addition of EDTA (ethylenediaminetetraacetic acid) and NEM (N-ethylmaleimide) to final concentration of 10 mM. The cross-linked samples

were resuspended in nonreducing SDS sample buffer (BioRad, Hercules, CA) and resolved on 10% SDS-PAGE as described above. The disulfide reaction was reversed by reducing with 4% 2-mercaptoethanol (β-ME) in the SDS sample buffer before resolving it on SDS-PAGE. To investigate the effects of ligand or GTP-γ-S on cross-linking, membrane fractions were incubated in HEPES buffer containing 5 μM α-factor (WHWLQLKPGQPNleY) or 5 μM α-factor antagonist (desW,desH-α-factor = WLQLKPGQPNleY) in the presence or absence of 0.1 mM GTP-γ-S[1] before CuP treatment.

For *in vivo* (whole cell) cross-linking, cells were grown to mid-log phase, harvested, and washed with water by centrifugation (4000g for 5 min). The cells were resuspended in 100 mM LiAc and incubated at 30°C for 30 min with mixing. After centrifugation, the cells were resuspended in 25% PEG with 250 mM LiAc and incubated for 60 min to make them permeable to CuP. Cells were washed with HEPES buffer three times after LiAc treatment and then resuspended in YM1i buffer containing 5 μM α-factor or α-factor-antagonist and incubated at room temperature for 30 min. Disulfide cross-linking was induced by adding CuP to final concentrations of 0.5 mM Cu and 1.5 mM 1,10-phenanthroline as previously described for yeast whole cell cross-linking (*29*). The mixture was incubated at room temperature for 60 min with end-over-end mixing. EDTA and NEM to final concentrations of 10 mM were added to stop the reaction. The cells were washed three times with HEPES buffer containing EDTA (10 mM) and NEM (10 mM). Membrane extraction was carried as described above with HEPES buffer containing 10 mM EDTA/NEM. Reducing conditions of disulfide bond were carried out

by resuspending membrane samples in SDS-PAGE sample buffer containing 4% β-ME and incubating at room temperature for at least 15 min. To investigate the role of Gpa1p in the TM5-IL3-TM6 conformational changes, disulfide cross-linking of Cysless, L228C (TM5), L236 (IL3), and I249C (TM6) was carried out in a Gpa1p deleted strain, TM5117 as described above. For the time course experiments, the CuP-mediated disulfide cross-linking in BJS21 was terminated at the indicated time points by addition of EDTA and NEM to final concentrations of 10 mM.

Prediction and Modeling

All models of 3-D structures were generated by the Phyre Structural Bioinformatics Group prediction tools (*30*). The structures were viewed and labeled with the PyMOL pdb viewer software (DeLano Scientific LLC, Palo Alto, CA).

Chapter 3

Results

Phenotypes of Ste2p IL3 Cys Substitution Mutants

The signaling activities of the cysteine mutants were examined by α-factor-induced growth arrest and FUS1-lacZ induction assays. The growth arrest assay is a sensitive test that measures the ability of cells expressing Ste2p to maintain pheromone-induced cell division arrest at the G1 phase over a 24–36 h time frame, whereas the FUS1-lacZ induction assay measures an early response of the yeast cell to pheromone. The strains used in this study contain a reporter gene construct consisting of a fusion between FUS1 promoter and the lacZ gene encoding the enzyme β-galactosidase (*26*). This allows for rapid, sensitive detection of mating pathway activation by assessing β-galactosidase activity in response to mating pheromone.

The Cys-less Ste2p engineered as the background for the specific cysteine mutations has been shown to have biological activities identical to the wild-type receptor (*22*). In this study we grouped the IL3 residues into three categories based on their position as follows: group 1 (TM5-IL3 boundary) residues, V224–S232; group 2 (middle IL3) residues, R233–Q240; and group 3 (IL3-TM6 boundary) residues, F241–Q253 (Figure 3.1). Substitution of single cysteine residues in intracellular loop 3 (IL3) of Cys-less Ste2p resulted in constructs that were expressed and had biological activities identical or similar to that of the Cys-less receptor, except for K225C which was biologically inactive (see Table 3.1). The decreased sensitivity in biological assays caused by the K225C mutation has been observed in previous studies (*31*).

Table 3.1 Summary of Phenotypes of Ste2p IL3 Cys Substitution Mutants[a]

mutation	protein expression (%)	growth arrest activities (%)	*Fus1-LacZ* induction (%)
Cys-less	100	100	100
V224C	100	95	90
K225C	100	NA	NA
L226C	98	90	80
I227C	100	100	105
L228C	100	90	110
A229C	100	90	75
I230C	100	85	100
R231C	100	90	100
S232C	100	100	90
R233C	65	70	60
R234C	75	100	80
F235C	75	100	80
L236C	75	75	65
G237C	75	100	75
L238C	75	100	75
K239C	75	75	65
Q240C	75	100	80
F241C	100	100	80
D242C	85	85	85
S243C	100	95	100
F244C	100	90	95
H245C	90	90	70
I246C	100	90	70
L247C	100	90	75
L248C	100	85	95
I249C	100	85	100
M250C	100	95	80
S251C	100	100	110
S252C	100	95	90
Q253C	100	90	65

[a]The expression levels as measured by Western blots (Figures 3.3 and 3.6) and biological activities all had standard deviations between ±2 and ±5%. All assays were done at least three times independently.

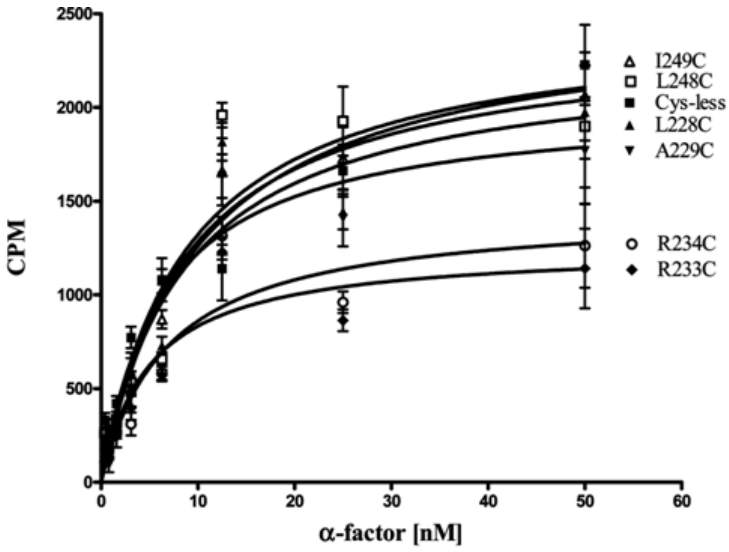

Mutants:	Cys-less	L228C	A229C	R233C	R234C	L248C	I249C
K_d (nM)	8.39	8.62	7.54	6.98	7.27	8.78	9.93
B-Max (CPM)	2292	2282	2021	1253	1450	2475	2488
Receptors/Cell	36,512	36,352	32,194	19,960	23,098	39,426	39,633
Expression (% of Cys-less)	100	99.6	88.2	54.7	63.2	107.9	108.5

Figure 3.2 Whole cell saturation binding assay of [^{3}H]α-factor to Cysless and IL3 Cys mutant receptors. A graph of CPM (count per minute of radioactivity of cells) versus the concentration of the [^{3}H]α-factor is shown. The data represents specific binding to cells as determined by subtracting the binding to cells lacking the receptor from binding to cells containing the Ste2p Cys mutant receptors. Below the graph is a table containing a summary of the binding affinities (K_d) and surface expression of the receptors.

Receptor expression was measured by Western blot signals that were quantitated using Quantity One software (Version 4.5.1) on a Chemi-Doc XRS photodocumentation system (BioRad, Hercules, CA). The Cys-less receptor signal was used as the measure of 100% expression. In addition to quantitation of the Western blot signals, saturation binding assays were carried out on selected mutants (L228C and A229C) from the TM5–IL3 boundary, (R233C and R234C) from the middle of IL3, and (L248C and I249C) from the IL3–TM6 boundary (Figure 3.2). The receptors showed almost equal K_d values for ligand binding, and receptors L228C, A229C, L248C, and I249C were expressed at levels within 12% of the Cys-less control, whereas R233C and R234C were expressed to about 55–63% of control, as judged by B_{max} values.

IL3 Cys Mutants Form Dimers

One of the most commonly used strategies to investigate GPCR agonist-induced conformational change is disulfide cross-linking involving cysteine-substituted mutant GPCRs. This approach involves determination of differences in disulfide formation between two receptor monomers containing Cys residues in the presence and absence of ligand (*29, 32, 33*). Ste2p predominates in SDS-PAGE as a monomer of about 50 kDa as noncovalent interactions between receptors are disrupted by the conditions of the SDS-PAGE. As observed in many studies (*8, 22*), some SDS-resistant dimers persist in all lanes including that of the Cys-less receptor (Figure 3.3). We observed strong dimer formation in some of the IL3 Cys mutant receptors when treated with CuP. Compared to the Cys-less receptor, which showed little or no increase in the dimer band at 100 kDa

upon incubation of membranes with CuP, both the R233C and R234C receptors showed marked increases in the dimer band. This increase was completely (R234C) or almost completely (R233C) reversed by addition of β-ME, indicating the involvement of disulfide bonds in stabilization of the dimer.

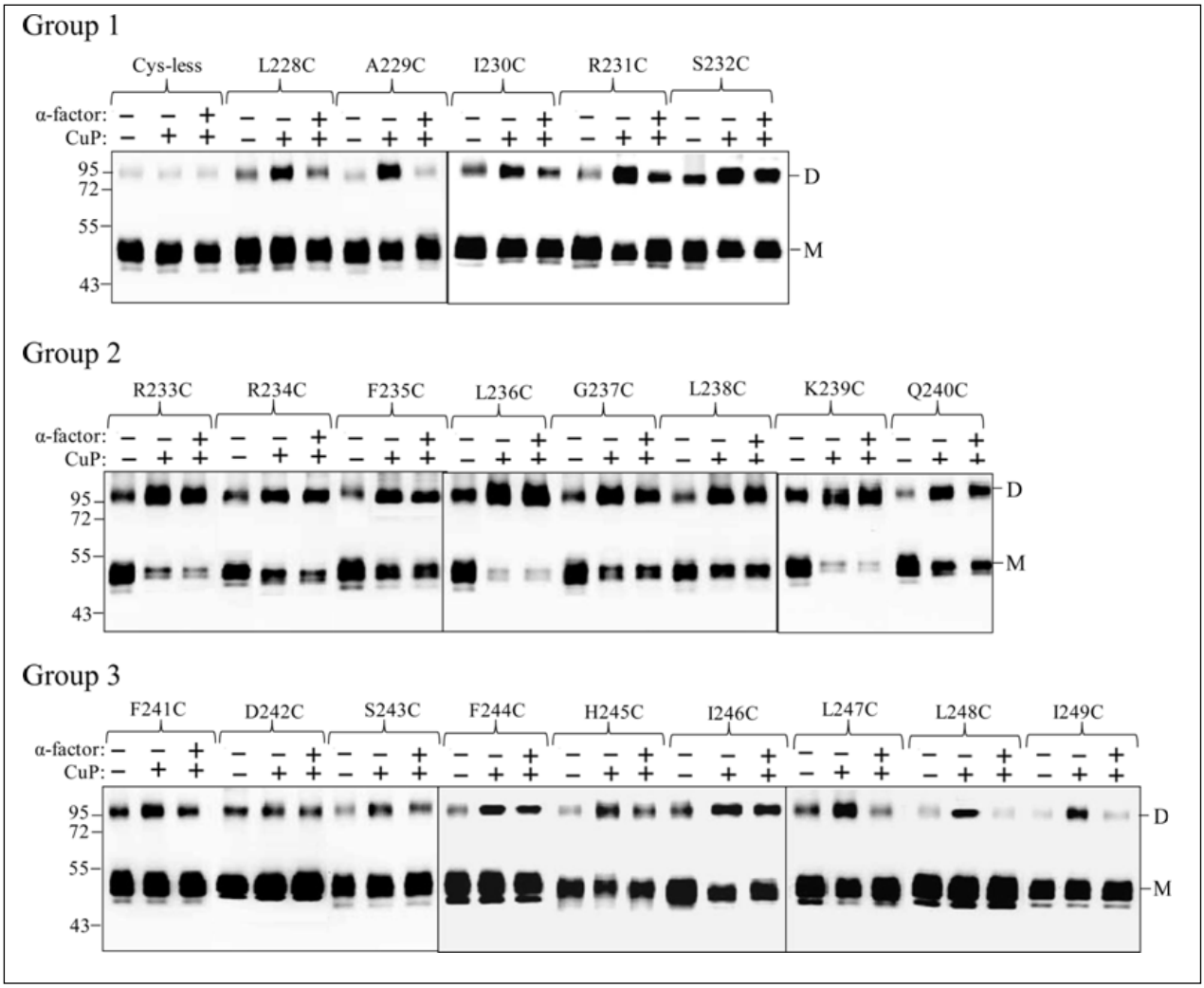

Figure 3.3 Ste2p IL3 Cys mutants form dimers. Membranes from various mutants were incubated with or without CuP in the presence or absence of α-factor as described in the Material and Methods. The membrane extracts were run on SDS-PAGE gels; the gels

were blotted and probed with anti-FLAG antibody to detect the presence of Ste2p at either the monomer (M) or dimer (D) positions. Each preparation was untreated (lanes −, −) or treated with CuP (lanes −, +) or with α-factor and CuP (lanes +, +).

Given that the disulfide cross-linking was observed with Ste2p(R233C) and Ste2p(R234C), a comprehensive examination of the cross-linking of Cys mutants in the IL3 region of the receptor was conducted. These experiments were done in the presence and absence of ligand in order to determine whether cross-linking changed during activation of the receptor (Figure 3.3). Examination of the ratio of dimer to monomer in the gels of all the IL3 Cys mutants showed that some mutants exhibited high levels of disulfide formation [e.g., Ste2p(L236C), group 2; Figure 3.3)], whereas others exhibited only a small increase in dimer content with the monomer remaining the predominant species (e.g., L228C, group 1; Figure 3.3). When treated with CuP in the absence of ligand, disulfide cross-linked receptor formation for the 22 single Cys mutants studied varied from 10% to 96% of the total Ste2p related bands (monomer plus dimer) (Figure 3.3, compare lanes "−−"and "−+"). Group 1 (L228C–S232C) and group 3 (F241C–I249C) residues displayed about 10–45% increase in disulfide formation upon incubation with CuP in the absence of ligand compared to the untreated receptor. In contrast, upon treatment with CuP in the absence of ligand group 2 (R233C–Q240C) mutants showed a greater increase (54–96%) in percent of cross-linked receptor.

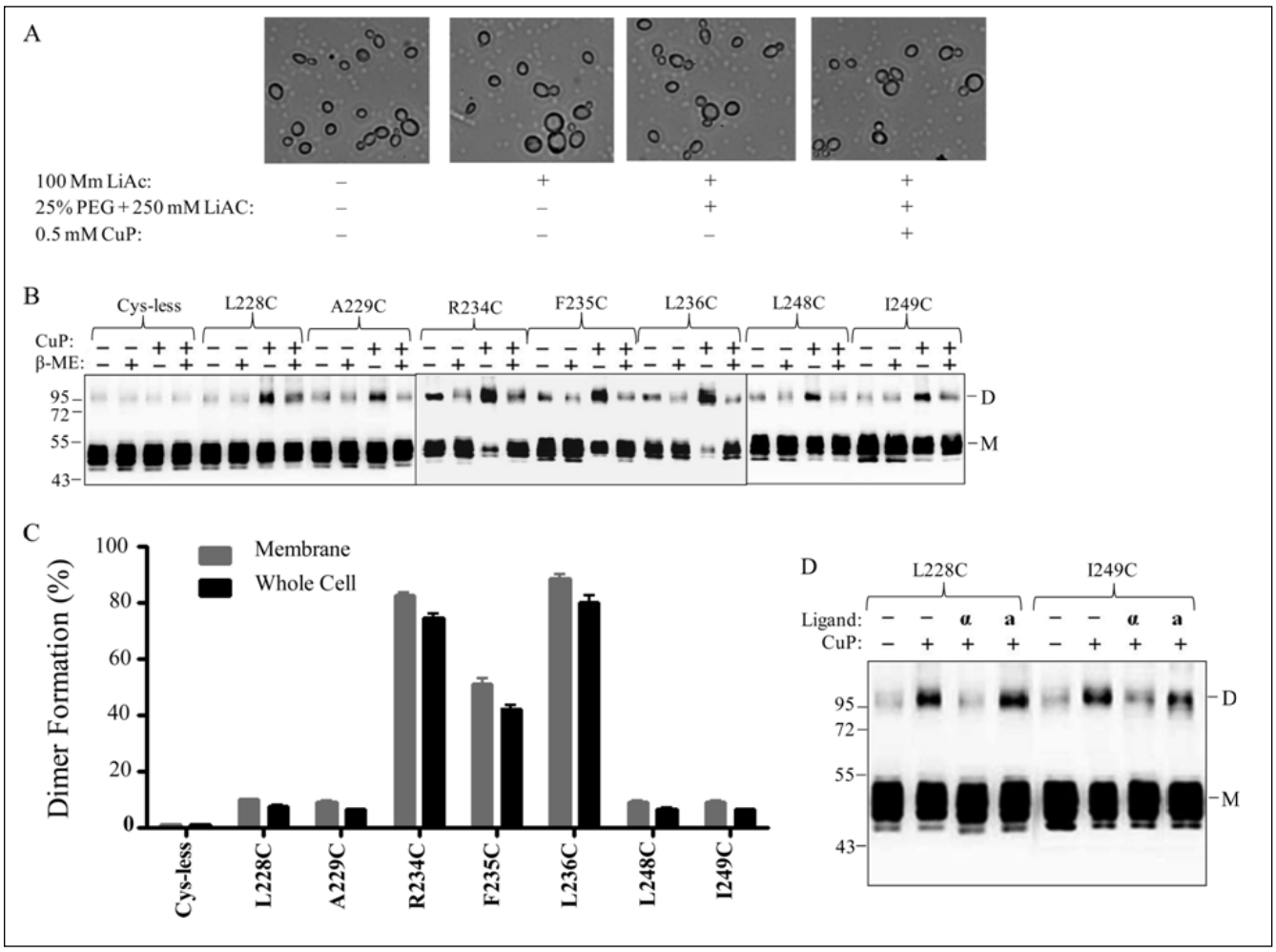

Figure 3.4 Analyses of Ste2p dimerization in whole yeast cells. Cells expressing various Ste2p IL3 cysteine mutants were permeabilized and exposed to CuP. (A) Images of cells treated with various reagents used during the whole cell disulfide cross-linking CuP treatment. (B) Blots of seven IL3 Cys mutants selected for whole cell cross-linking evaluation. The samples were probed with anti-FLAG antibody to detect the presence of Ste2p at either the monomer (M) or dimer (D) positions. Each preparation was untreated (lanes −, −) or treated with β-ME (lanes −, +) or CuP (lanes +, −) or with CuP and β-ME (lanes +, +). (C) A graph comparing the percentage of the Ste2p mutant receptors that

formed cross-linked dimers in membrane preparations and whole cells. (D) Whole cells expressing receptors L228C and I249C were untreated or incubated with ligand prior to Cu–P treatments. The blots were probed with anti-FLAG antibody to detect the presence of Ste2p at either the monomer or dimer positions, respectively. Each preparation was untreated (lanes −, −) or treated with Cu–P (lanes −, +) or with α-factor and Cu–P (lanes α, +) or with α-factor antagonist and Cu–P (lanes a, +).

The high degree of disulfide cross-linking found in some of the IL3 Cys mutants suggested that IL3 loops in two receptor subunits were within close proximity. However, we were concerned that some of these protein–protein interactions may have been artifacts related to the use of membranes. To determine whether disulfide formation was the same or different in whole cells in comparison to membrane preparations, an *in vivo* CuP treatment assay was performed. For this experiment we chose seven IL3 Cys mutants representing each group in IL3 and treated these receptors with CuP in live permeabilized cells (Figure 3.4). Microscopic observation (Figure 3.4A) showed that the cells were not morphologically affected by CuP treatment, and these treated cells were fully viable upon plating on growth media (data not shown). As was true with membranes, the disulfide formation catalyzed by CuP was reversed to various extents in the presence of β-ME (Figure 3.4B, +/+ lane). Comparison of the percent cross-linking in membranes and whole cells (Figure 3.4B, immunoblots, and Figure 3.4C, bar graph dimer/monomer ratio) showed that the trend for dimer formation in different IL3 mutants was similar in both preparations. Dimerization of some mutants was reduced or

disappeared upon α-factor addition; this together with the variations in the amount of dimerization among the Ste2p-IL3 Cys mutants observed in at least three independent experiments allows us to conclude that the dimer formation was reproducible and specific.

Conformational Changes in TM5 and TM6 upon α-Factor Binding

In previous studies it has been shown that binding of α-factor affected Ste2p dimer formation mediated through the TM regions, suggesting that these regions undergo conformational changes(*29, 34, 35*). We investigated whether incubation with α-factor would have any effect on CuP-mediated cross-linking of the IL3 mutants. While ligand binding had only a minor effect on disulfide formation in receptors carrying mutations in group 2 residues (Figure 3.3, R233C to Q240C, compare lanes "–+"and "++"), a reduction in cross-linking was observed for mutation near TM5 (I230C and R231C) and TM6 (F241C, S243C and H245C). Dimer formation was almost completely inhibited at boundaries between IL3 and TM5 (L228C and A229C) and TM6 (L247C, L248C, and I249C). The results suggest that α-factor binding induces conformational changes at the TM5 and TM6 cytoplasmic ends of Ste2p that change the availability of the Cys residues for chemical cross-linking, whereas in most of the IL3 loop the reactivity of these residues is not affected by ligand binding. We observed similar inhibition of cross-linking by α-factor in experiments using intact whole cells (Figure 3.4D).

A graphical representation showing the pattern of cross-link formation of IL3 Cys mutants of Ste2p in the inactive (ligand unbound) and active (ligand bound) states is

presented in Figure 3.5A. Analysis of the time course of disulfide (dimer) formation (Figure 3.5B) showed that the TM5 (e.g., A228C) and TM6 (e.g., L248C) Ste2p mutants formed dimers with a half-maximal time of about 3 min, whereas residues in the middle of IL3 loop (e.g., F235C) exhibited half-maximal time of about 1.5 min. The slower dimer formation at the TM5 and TM6 extracellular ends may suggest that these residues are farther from each other compared to residues in the IL3 loop. It is clear from these time course studies that formation of dimer is complete by 30 min under these experimental conditions.

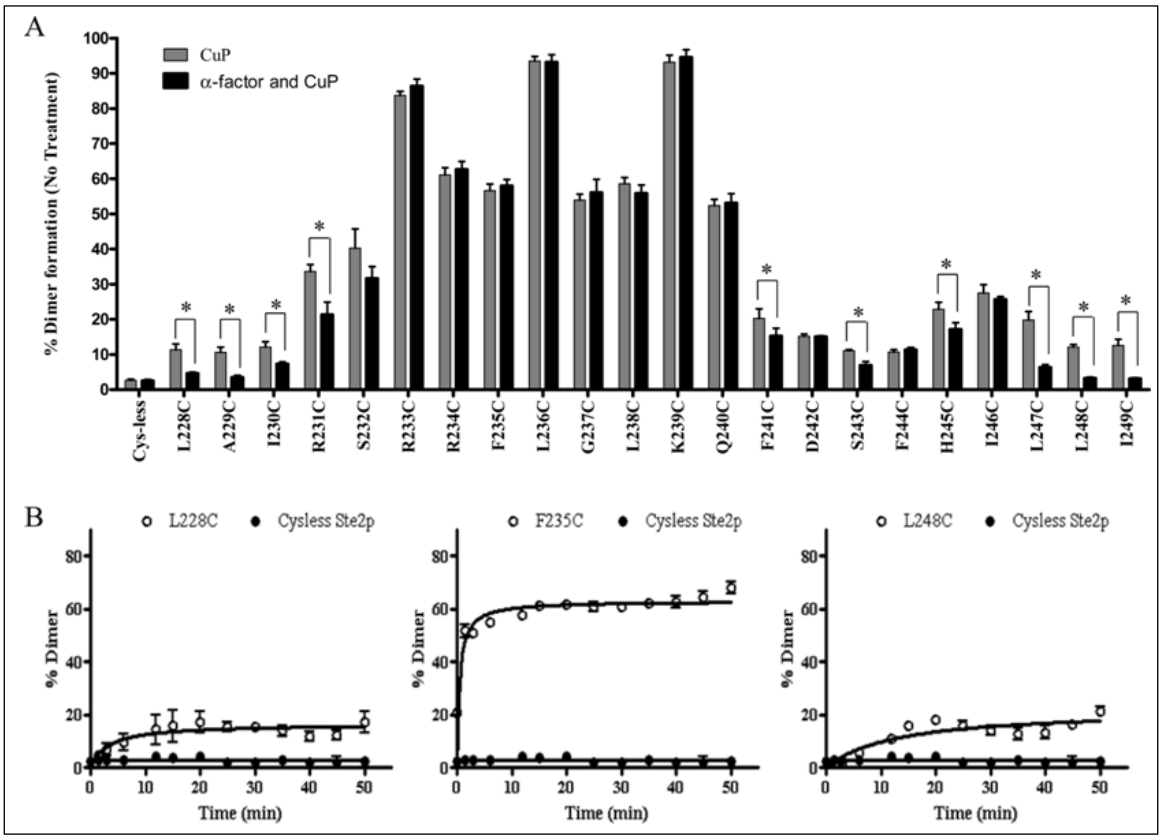

Figure 3.5 Dimer formation in Ste2p IL3. (A) Relative amount (%) of IL3-mediated dimer formation in the presence and absence of pheromone. The graph was plotted from

three independent experimental values. (*) The differences between the mean values were statistically significant ($P < 0.01$). (B) Time course of dimer formation after CuP treatment of Ste2p mutants L228C (TM5), F235C (IL3), and L248C (TM6). Preparations were treated for the indicated time and then analyzed on Western blots for dimer formation. Results represent the average of four to five independent experiments. Error bars indicate the standard deviation.

α-Factor Antagonist Did Not Induce Conformational Changes in TM5 and TM6

Biochemical and cross-linking studies in our lab have shown that the N-terminus of α-factor is necessary for activation but not binding to Ste2p (*36-38*). Recently, we showed that Trp1 of α-factor interacts with Lys^{269} (TM6) of Ste2p (*8*). The question of whether receptor activation involving the N-terminus of α-factor is important for the changes in conformation at the cytoplasmic ends of TM5 and TM6 was investigated. Membrane samples containing TM5 (L228C, A229C, I230C) and TM6 (I246C, L247C, L248C, I249C) receptors were incubated with α-factor (WHWLQLKPGQPNle^{12}Y) or an α-factor antagonist (desW1,desH2-WLQLKPGQPNle^{12}Y) prior to Cu–P treatment. The results (Figure 3.6A, compare lanes label "α" and "a") showed that, in contrast to the native α-factor, treatment with antagonist did not significantly change the percent of cross-linked product relative to that found in the unliganded receptor. Specifically for the L228, A229, I230 L247, L248, and I249 Cys mutant receptors the cross-link percentages for the unliganded and antagonist bound receptors were nearly identical, whereas minimal cross-linking was found in the presence of α-factor. We also examined

conformational changes in residues at positions 224–227 and 250–253 at the ends of the TM5 and TM6 helices, respectively. Dimer (disulfide bond) formation was observed in some residues (K225C, I227C, M250C, S251C, and Q253C) as shown in Figure 3.6B that were also affected by the presence of α-factor, suggesting that the cytoplasmic ends of the TM5/TM5 and TM6/TM6 helices in a dimeric receptor are indeed in very close proximity and that they participate in the conformational change associated with ligand binding.

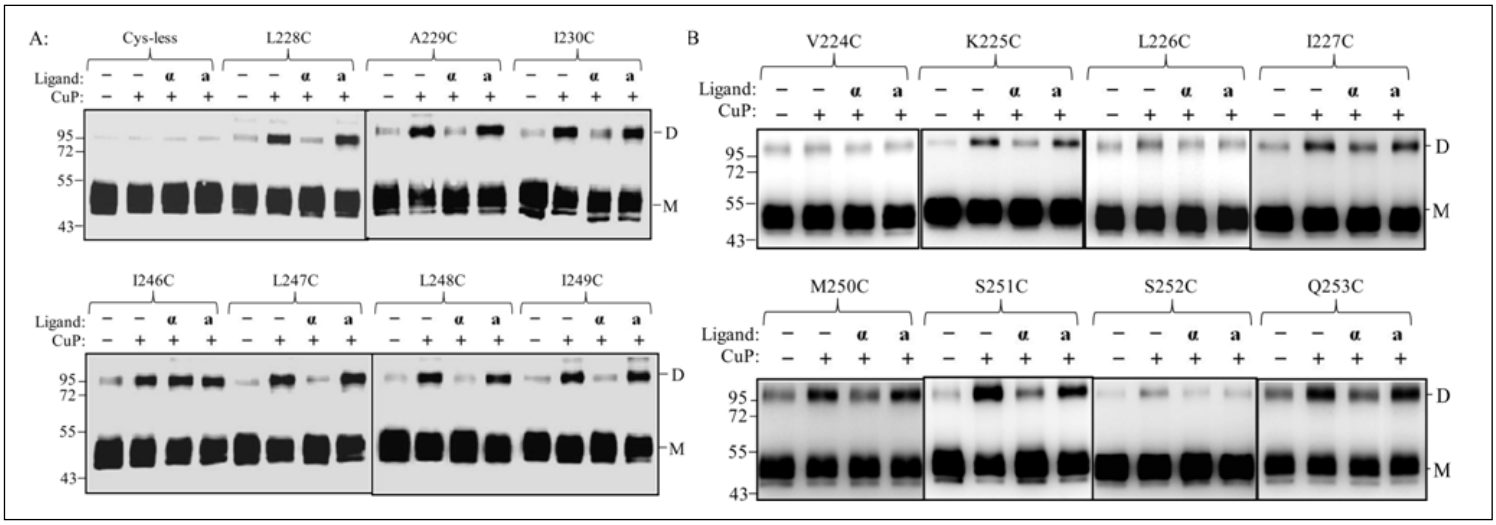

Figure 3.6 Effects α-factor antagonist on dimerization of TM5 and TM6 Cys mutants: (A) membranes from cells expressing Ste2p cysteine mutants at cytoplasmic ends of the helices and (B) membranes from cells expressing Ste2p cysteine mutants in helices that are suggested to be buried in the membrane were treated were incubated with CuP in the presence or absence of α-factor or α-factor antagonist as described in the Material and Methods. The membrane extracts were run on SDS-PAGE gels. The blots were probed with anti-FLAG antibody to detect the presence of Ste2p at either the

monomer (M, 53–55 kDa) or dimer (D, 106–110 kDa) positions. Each preparation was untreated (lanes −, −) or treated with Cu–P (lanes −, +) or with α-factor and Cu–P (lanes α, +) or with α-factor antagonist and Cu–P (lanes a, +).

GTP Did Not Affect Dimer Formation and Conformational Changes

The recent crystal structure of opsin with the 11 C-terminal residues of the Gα protein led the authors to conclude that the active conformation of this GPCR was stabilized by its interaction with Gα (*10*). Another study also reported GTP may affect the interaction of receptor with Gα (*39*). We therefore determined whether the presence or the absence of GTP would affect disulfide formation observed in this study. We coexpressed the IL3 Cys mutants A228C and I249C with wild-type Gpa1p under the control of the same promoter in order to maintain equal level of the receptor and its Gα protein and repeated the Cu–P treatment in the presence of GTP-γ-S. The results (Figure 3.7A) suggest that GTP-γ-S addition had no effect on the level of disulfide formation, indicating that Gα protein activation is not required for the observed conformational changes. In contrast, when cross-linking was carried out in a Gpa1p deleted strain (Figure 3.7B), the level of disulfide formation in the presence of ligand was not significantly reduced at the TM5 and TM6 ends in comparison to that observed in the Gpa1p background (Figures 3.7A, 3.3, and 3.6A).

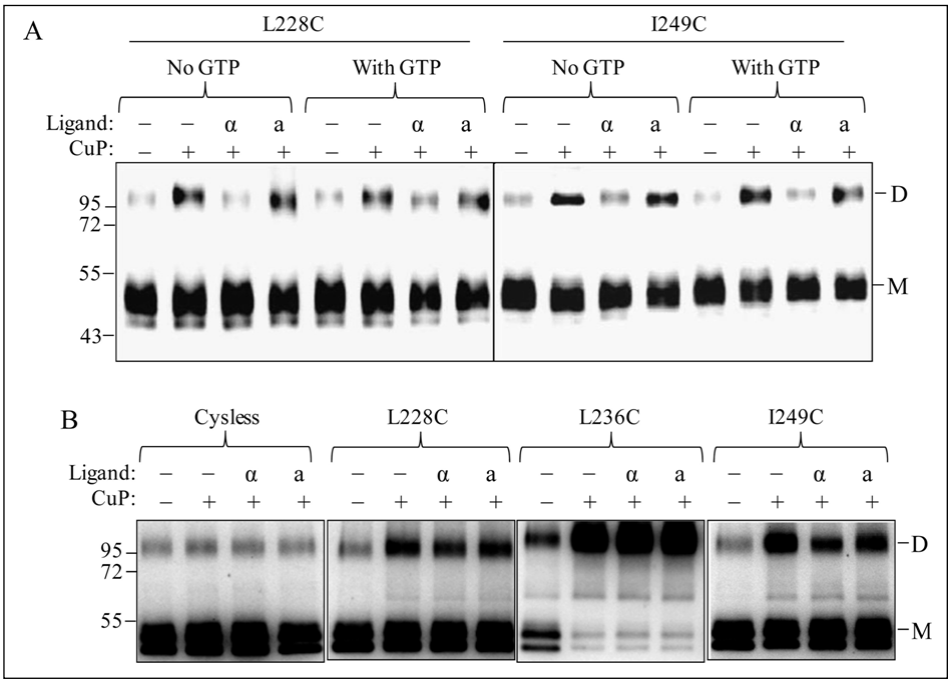

Figure 3.7 Effects of G protein expression and activation on TM5 and TM6 ligand induced conformational changes. (A) Whole cell membranes containing receptors A228C and I249C were treated with or without ligand in the presence or absence of 0.1 mM GTP-γ-S prior to Cu–P treatments. The blots were probed with anti-FLAG antibody to detect the presence of Ste2p at either the monomer (M, 53–55 kDa) or dimer (D, 106–110 kDa) positions. Each preparation was untreated (lanes −, −) or treated with Cu–P (lanes −, +) or with α-factor and Cu–P (lanes α, +) or with α-factor antagonist and Cu–P (lanes a, +). (B) Analyses of Ste2p dimerization in yeast cells (TM5117) devoid of Gα protein. Whole cell membranes containing Cysless, A228C, L236C, and I249C Ste2p, from cells lacking Gα were treated with or without ligand prior to Cu–P treatments. The blots were probed with anti-FLAG antibody to detect the presence of Ste2p at either the monomer or dimer positions.

Chapter 4

Discussion

We have used disulfide cross-linking analysis to probe conformational changes of residues in the third intracellular loop (IL3) and the ends of the contiguous fifth (TM5) and sixth (TM6) transmembrane domains of Ste2p during ligand-induced activation. An assumption of this approach is that the cysteine mutations may act as surrogates of the native residues in Ste2p. Therefore, it is critical that the mutations not affect the activity of the receptor, its conformation, or its spatial relationships to other receptor molecules or interacting proteins. Several studies have reported that individual residue mutations in Ste2p IL3 did not significantly affect receptor activity (*15-17*). Consistent with previous studies (*31*), Ste2p with mutations in IL3 was observed to tolerate Cys substitutions in our experiments except for the K225C receptor. The tolerance for substitutions in IL3 suggests that the contact points revealed in the cross-linking analysis likely exist in the native receptor and that activation of G protein by Ste2p involves multiple intermolecular interactions as observed for mammalian GPCRs (*40, 41*).

Given that IL3 has been suggested to be involved in receptor-Gα protein (Ste2p–Gpa1p) interactions (*15-17*), it is interesting that strong dimer formation occurred in the IL3 Cys mutants. This is consistent with the conclusion that IL3 in rhodopsin has been identified to play a role in receptor oligomerization (*42-44*). In addition, molecular dynamics simulations, correlated-mutation analysis, and evolutionary-trace analysis all predict the involvement of IL3 in GPCR dimerization (*32*). The dimer formations observed in our study were also detected in intact cells, indicating that the disulfide bond

formation between the two monomers of Ste2p occurs in the native environment of the receptor. Substitution cysteine accessibility studies on Ste2p-IL3 residues suggested all the residues, L228–I249, were accessible, and even though residues I246C and L247C were about 2-fold more accessible than most IL3 (R233–Q240) residues (*31*), in our study when treated with CuP these residues (I246C, L247C) exhibited only 22–30% dimer formation compared to the 54–96% dimer formation found for residues R233C–Q240C. In addition, though K225C, I227C, M250C, S251C, and Q253C at the cytoplasmic ends of the TM5 and TM6 helices have been shown to be buried in the membrane and not solvent accessible (*31*), we observed disulfide formation involving these residues that was reduced by the presence of α-factor, suggesting that the cytoplasmic ends of the TM5/TM5 and TM6/TM6 helices in the inactive state of Ste2p are in closer proximity than when activated by ligand. The differences in the results of the cysteine accessibility and disulfide cross-linking studies of Ste2p IL3 cysteine mutants suggest that the cross-linking (dimer formation) that we observed is not due to the fact that these residues are accessible and randomly cross-linking. Rather, we suggest that these results indicate that specific residues in the IL3 region are in positions and orientations that permit disulfide bond formation while others are not, irrespective of their accessibility.

The IL3 of Ste2p has been suggested to have the potential to form an α-helix with a distinct amphipathic character (*45*). The pattern of disulfide formation in our study, with R233C, L236C, and K239C mutant receptors having the highest percent of disulfide formation (Figures 3.3 and 3.5), suggests that the group 2 residues in IL3 (R233–Q240)

may form a 3_{10} helix as shown in Figure 3.8A. The Phyre structural bioinformatics group tools (*30*) also predicted a 3_{10} helix in the 3-D structure of IL3 (Figure 3.8B) consistent with our cross-linking studies. The IL3 3_{10} helix (RRFLGLKQ) is highly positively charged. It might be expected that in the wild-type Ste2p dimer there should be charge repulsion between IL3 loop residues in the two Ste2p monomers. However, in the mutants studied herein the data strongly suggest that the substituted Cys residues are close enough to effectively form disulfide bonds. One might suggest that the Cys substitution alone changes the physical chemical characteristics of the loop leading to non-native interactions. However, the L236C mutant still contains all three positive residues (R233, R234, and K239) yet is capable of forming about 95% dimer, indicating that the IL3 residues in the dimeric receptor are indeed in very close proximity. We conclude that in native dimers of Ste2p the IL3 residues are close enough to make contacts that can be captured in disulfide cross-linking experiments. As pointed out by others, the interpretation of such dimers in terms of receptor function must be tempered by the possible changes in the monomer–dimer equilibrium that are effected by chemical cross-linking (*29, 35*).

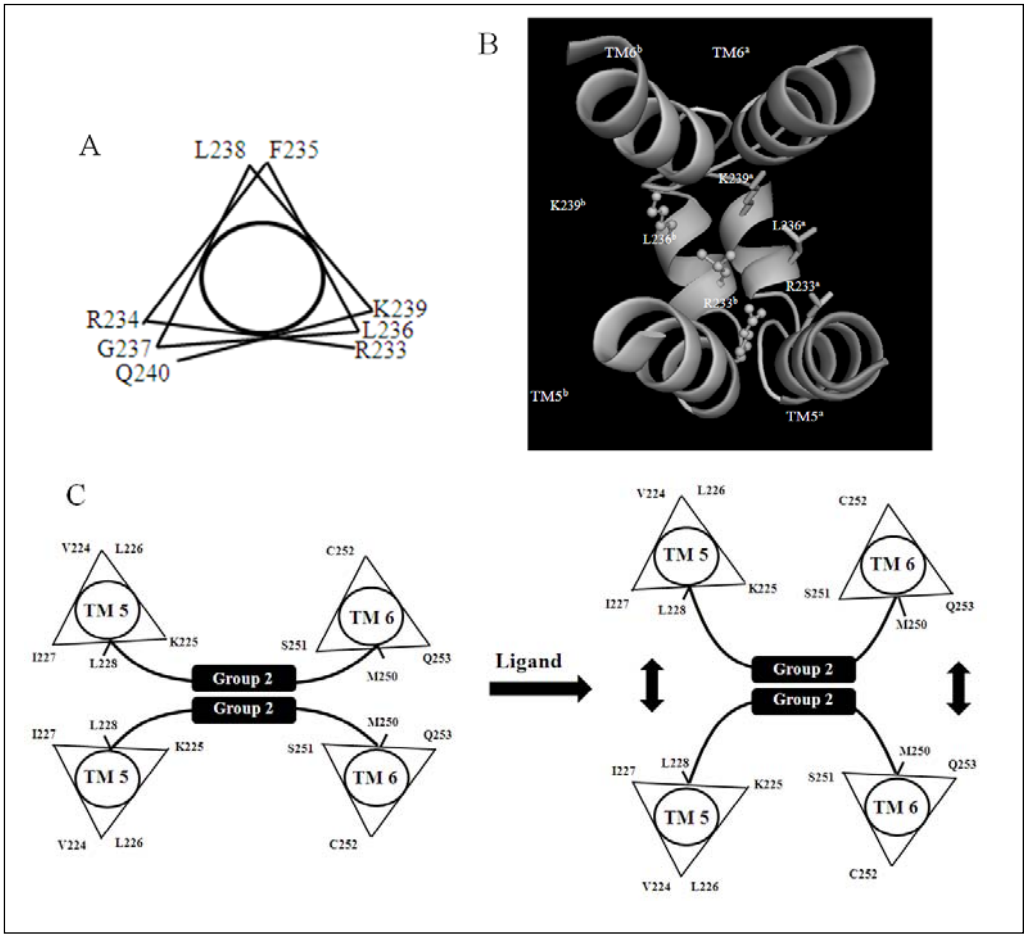

Figure 3.8 Helical wheel projections and 3D model of IL3 residues involved in Ste2p–Ste2p interactions. (A) The IL3 residues R233 to Q240 are suggested to form a 3_{10} helix structure with a periodicity of 3.2 residues per turn in the helical wheel (*46*). (B) The 3D structure of two Ste2p molecules showing regions TM5, TM6, and IL3 with a 310 helix in IL3 as predicted by the Phyre Structural Bioinformatics Group prediction tools (*30*). The IL3 310 helixes of two Ste2p subunits are suggested to be in close proximity that permit disulfide cross-linking. (C) A schematic diagram showing possible shifts at the cytoplasmic ends of TM5 and TM6 upon ligand binding. The vertical arrows indicate a shift of the TMs away from each other.

A previous study used limited trypsin digestion of Ste2p to identify conformational changes induced by the binding of α-factor. The presence of α-factor caused the third intracellular loop of the receptor to become more accessible to trypsin, suggesting that α-factor binding to Ste2p-induced conformational changes of IL3 (*19*). However, specific residues or regions of the IL3 involved in such changes were not identified. As judged by their availability to form disulfide cross-links, our data suggest that the residues in the middle of IL3 do not undergo conformational change, whereas the residues at the TM5–IL3 and IL3–TM6 boundaries do, leading to a change in their availability for disulfide formation.

The recent crystal structure of chemokine receptor, CXCR4, in the dimer form suggests that the monomers interact only at the extracellular side of helices TM5 and TM6 to play an important role in stabilizing the dimeric receptor (*7*). Our results suggest that Ste2p TM5/TM5 and TM6/TM6 interact at the cytoplasmic ends. We propose that the Ste2p residues in TM5 (K225, I227, L228, A229, I230) and in TM6 (L247, L248, I249, S251, and Q253) at the cytoplasmic ends may be involved in Ste2p–Ste2p interactions. Such interactions are disrupted upon ligand binding as shown by the disappearance or reduction of disulfide-mediated dimerization of the various Cys mutants in the presence of α-factor. The α-factor induced similar changes in the cross-linking of the various receptors in intact whole cells (Figure 3.4D). Since in this latter experiment α-factor should only bind to the receptors at the cell surface (at the plasma membrane), the results suggest that the changes at the TM5 and TM6 cytoplasmic ends found in disulfide

cross-linking experiments reflect the native state of these receptors. Disulfide cross-linking efficiencies reflect both the spatial proximity of the sulfhydryl groups and their mobility. Thus, changes in conformation at the ends of TM5 and TM6 upon α-factor induced Ste2p activation can be inferred from the data. Another possibility is that α-factor activation changes the flexibility of these regions of Ste2p. A model consistent with our experimental data would have the TM5 and TM6 ends of a Ste2p dimer shift away from each other so that it is not possible to form a disulfide bond as shown in Figure 3.8C. A similar reorientation of TM5 and TM6 has been proposed for activated forms of mammalian GPCRs (*11, 47-49*) and shown recently in a series of X-ray crystallographic studies (*12-14, 50*). Antagonist-bond dopamine receptor also showed reorientation of TM regions (*50*).

It is possible that the 100 kDa band observed in the gels represents interaction of Ste2p with some protein other than itself. The fact that all Ste2p Cys mutants we examined form this band makes this possibility highly unlikely. In addition, a number of papers (*8, 22, 23, 29, 35, 51-54*) showed that Ste2p labeled by a variety of epitopes (FLAG, MYC, RHO) react with antibodies to these epitopes at positions in the gels that correspond to the molecular weight of a dimer of Ste2p. The antibodies react with no other bands except proteins at the Ste2p dimer or monomer position in these SDS-PAGE immunoblots. Similar results are obtained with an antibody generated against the N-terminus of Ste2p. Furthermore, purified Ste2p confirmed by MALDI-TOF and nanospray MS exhibits a 100 kDa at the same position we have attributed to the Ste2p dimer (*55*). Most importantly, the major conclusion of this paper is that the results

indicate that the cytoplasmic ends of TM5 and TM6 undergo conformational change upon ligand binding. This conclusion would remain even if there were a second partner. At the TM6 cytoplasmic end, residues L247, L248 I249, M250, S251, and Q253 all formed about 10–20% Ste2p-Ste2p dimers; however, in the presence of ligand the percent of Ste2p–Ste2p dimer is greatly reduced, and residues L247C and I249C interact with Gpa1p (Umanah, unpublished). The switch of L247C and I249C from involvement in Ste2p–Ste2p interaction in the inactive state to Ste2p–Gpa1p heterodimer interactions in the active state would be consistent with a clockwise rotation of this region of the receptor as observed in other mammalian GPCRs (*11, 47-49*). In the inactive state the TM5 cytoplasmic ends residues K225, I227, L228, A229, and I230 also formed about 10–15% Ste2p–Ste2p homodimers, and in the presence of ligand, these residues displayed reduced Ste2p–Ste2p homodimer formation and L228C formed a Ste2p–Gpa1p heterodimer (Umanah, unpublished). We therefore propose that the TM5 cytoplasmic end undergoes a counterclockwise rotation as observed in other GPCRs (*56*).

Previously, we showed that Ste2p Tyr266 (on the extracellular end of TM6) interacted with Asn205 (on the extracellular end of TM5) only in the active conformation of the receptor (*57*), suggesting that these extracellular regions of the Ste2p TM5 and TM6 undergo conformational changes upon α-factor binding. Thus, our cross-linking results would support a model where binding of α-factor to Ste2p leads to conformational changes at the extracellular regions of TM5 and TM6 which are propagated to the cytoplasmic ends of these helices and result in exposure of L247C, L248, and I249C for activation of Gα.

The N-terminus of α-factor pheromone has been suggested to interact with Ste2p residues, S251–M294 which comprises part of TM6, the third extracellular loop, and part of TM7 (*36-38*). Recently, we show that Trp1 of α-factor interacts with K269 located at the extracellular boundary of TM6 (*8*). Previous studies showed that the α-factor antagonist was capable of competing out α-factor binding to Ste2p but did not exhibit measurable biological activities, suggesting that the interactions of the first two amino acids of α-factor with residues at extracellular regions of Ste2p TM5/TM6 are critical for receptor activation. The experiments presented in this study suggest that the antagonist was not able to block or reduce disulfide formation compared to the native α-factor, implying that antagonist binding to Ste2p does not induce the conformational changes or changes in flexibility at the TM5 and TM6 cytoplasmic ends.

It has been shown that the exchange of GDP for GTP in Gα proteins during receptor activation is induced by interactions of Gα with the receptor during activation and also that GTP binding to Gα may affect ligand affinity for its GPCR (*1*). The addition of GTP-γ-S to membrane fractions prior to CuP treatment to induce disulfide cross-linking did not have any observable effects on dimer formation though Ste2p and Gpa1p were expressed under the same promoter. Cross-linking carried out in a Gpa1p deleted strain was not affected by a large excess of agonist, suggesting that Gpa1p–Ste2p interactions may influence conformational changes or changes in side chain flexibility at the cytoplasmic ends of TM5 and TM6. We conclude that the putative conformational changes at the cytoplasmic ends of TM5 and TM6 in Ste2p require interactions of the N-

terminal amino residues of α-factor and are affected by the interactions with Gα, but not by Gα activation.

In conclusion, we show for the first time changes in receptor conformation or flexibility that influence the availability for disulfide formation of residues in the region of IL3 of Ste2p close to the contiguous TM5 and TM6 helices. The hydrophilic residues located in the middle of the IL3 loop (R231–Q240) do not change conformation/availability during receptor activation, whereas many hydrophobic residues at the TM5 and TM6 cytoplasmic junctions do. These conformational changes require ligand-induced activation of Ste2p and appear to depend on Ste2p–Gα protein interactions. The pattern of disulfide formation observed is consistent with a 3_{10} helical structure in the center of IL3 and suggests that the IL3 loop of two Ste2p subunits remain in close proximity both in the active and inactive states of the receptors. Since Ste2p has been shown to have structure–function relationships similar to the physiologically and pharmacologically important rhodopsin-like GPCR family (*58*), the role of IL3 observed in this study has implications not only for Ste2p but also other GPCR systems.

References for Part III

1. Ratnala, V. R., and Kobilka, B. (2009) Understanding the ligand-receptor-G protein ternary complex for GPCR drug discovery, *Methods Mol Biol 552*, 67-77.
2. Rosenbaum, D. M., Rasmussen, S. G., and Kobilka, B. K. (2009) The structure and function of G-protein-coupled receptors, *Nature 459*, 356-363.
3. Williams, C., and Hill, S. J. (2009) GPCR signaling: understanding the pathway to successful drug discovery, *Methods Mol Biol 552*, 39-50.
4. Panetta, R., and Greenwood, M. T. (2008) Physiological relevance of GPCR oligomerization and its impact on drug discovery, *Drug discovery today 13*, 1059-1066.
5. De Amici, M., Dallanoce, C., Holzgrabe, U., Trankle, C., and Mohr, K. (2010) Allosteric ligands for G protein-coupled receptors: a novel strategy with attractive therapeutic opportunities, *Medicinal research reviews 30*, 463-549.
6. Lundstrom, K. (2009) An overview on GPCRs and drug discovery: structure-based drug design and structural biology on GPCRs, *Methods Mol Biol 552*, 51-66.
7. Wu, B., Chien, E. Y., Mol, C. D., Fenalti, G., Liu, W., Katritch, V., Abagyan, R., Brooun, A., Wells, P., Bi, F. C., Hamel, D. J., Kuhn, P., Handel, T. M., Cherezov, V., and Stevens, R. C. (2010) Structures of the CXCR4 chemokine GPCR with small-molecule and cyclic peptide antagonists, *Science 330*, 1066-1071.
8. Umanah, G. K., Huang, L., Ding, F. X., Arshava, B., Farley, A. R., Link, A. J., Naider, F., and Becker, J. M. (2010) Identification of residue-to-residue contact

between a peptide ligand and its G protein-coupled receptor using periodate-mediated dihydroxyphenylalanine cross-linking and mass spectrometry, *The Journal of biological chemistry 285*, 39425-39436.

9. Cabrera-Vera, T. M., Vanhauwe, J., Thomas, T. O., Medkova, M., Preininger, A., Mazzoni, M. R., and Hamm, H. E. (2003) Insights into G protein structure, function, and regulation, *Endocrine reviews 24*, 765-781.

10. Scheerer, P., Park, J. H., Hildebrand, P. W., Kim, Y. J., Krauss, N., Choe, H. W., Hofmann, K. P., and Ernst, O. P. (2008) Crystal structure of opsin in its G-protein-interacting conformation, *Nature 455*, 497-502.

11. Wess, J., Han, S. J., Kim, S. K., Jacobson, K. A., and Li, J. H. (2008) Conformational changes involved in G-protein-coupled-receptor activation, *Trends in pharmacological sciences 29*, 616-625.

12. Warne, T., Moukhametzianov, R., Baker, J. G., Nehme, R., Edwards, P. C., Leslie, A. G., Schertler, G. F., and Tate, C. G. (2011) The structural basis for agonist and partial agonist action on a beta(1)-adrenergic receptor, *Nature 469*, 241-244.

13. Rosenbaum, D. M., Zhang, C., Lyons, J. A., Holl, R., Aragao, D., Arlow, D. H., Rasmussen, S. G., Choi, H. J., Devree, B. T., Sunahara, R. K., Chae, P. S., Gellman, S. H., Dror, R. O., Shaw, D. E., Weis, W. I., Caffrey, M., Gmeiner, P., and Kobilka, B. K. (2011) Structure and function of an irreversible agonist-beta(2) adrenoceptor complex, *Nature 469*, 236-240.

14. Xu, F., Wu, H., Katritch, V., Han, G. W., Jacobson, K. A., Gao, Z. G., Cherezov, V., and Stevens, R. C. (2011) Structure of an agonist-bound human A2A adenosine receptor, *Science 332*, 322-327.

15. Clark, C. D., Palzkill, T., and Botstein, D. (1994) Systematic mutagenesis of the yeast mating pheromone receptor third intracellular loop, *The Journal of biological chemistry 269*, 8831-8841.

16. Stefan, C. J., and Blumer, K. J. (1994) The third cytoplasmic loop of a yeast G-protein-coupled receptor controls pathway activation, ligand discrimination, and receptor internalization, *Molecular and cellular biology 14*, 3339-3349.

17. Celic, A., Martin, N. P., Son, C. D., Becker, J. M., Naider, F., and Dumont, M. E. (2003) Sequences in the intracellular loops of the yeast pheromone receptor Ste2p required for G protein activation, *Biochemistry 42*, 3004-3017.

18. Gladue, D. P., and Konopka, J. B. (2008) Scanning mutagenesis of regions in the Galpha protein Gpa1 that are predicted to interact with yeast mating pheromone receptors, *FEMS yeast research 8*, 71-80.

19. Bukusoglu, G., and Jenness, D. D. (1996) Agonist-specific conformational changes in the yeast alpha-factor pheromone receptor, *Molecular and cellular biology 16*, 4818-4823.

20. Dube, P., DeCostanzo, A., and Konopka, J. B. (2000) Interaction between transmembrane domains five and six of the alpha -factor receptor, *The Journal of biological chemistry 275*, 26492-26499.

21. Medici, R., Bianchi, E., Di Segni, G., and Tocchini-Valentini, G. P. (1997) Efficient signal transduction by a chimeric yeast-mammalian G protein alpha subunit Gpa1-Gsalpha covalently fused to the yeast receptor Ste2, *The EMBO journal 16*, 7241-7249.

22. Hauser, M., Kauffman, S., Lee, B. K., Naider, F., and Becker, J. M. (2007) The first extracellular loop of the *Saccharomyces cerevisiae* G protein-coupled receptor Ste2p undergoes a conformational change upon ligand binding, *The Journal of biological chemistry 282*, 10387-10397.

23. Huang, L. Y., Umanah, G., Hauser, M., Son, C., Arshava, B., Naider, F., and Becker, J. M. (2008) Unnatural amino acid replacement in a yeast G protein-coupled receptor in its native environment, *Biochemistry 47*, 5638-5648.

24. Tsevat, J., Sherman, S. N., McElwee, J. A., Mandell, K. L., Simbartl, L. A., Sonnenberg, F. A., and Fowler, F. J., Jr. (1999) The will to live among HIV-infected patients, *Annals of internal medicine 131*, 194-198.

25. David, N. E., Gee, M., Andersen, B., Naider, F., Thorner, J., and Stevens, R. C. (1997) Expression and purification of the *Saccharomyces cerevisiae* alpha-factor receptor (Ste2p), a 7-transmembrane-segment G protein-coupled receptor, *The Journal of biological chemistry 272*, 15553-15561.

26. Trueheart, J., Boeke, J. D., and Fink, G. R. (1987) Two genes required for cell fusion during yeast conjugation: evidence for a pheromone-induced surface protein, *Molecular and cellular biology 7*, 2316-2328.

27. Raths, S. K., Naider, F., and Becker, J. M. (1988) Peptide analogues compete with the binding of alpha-factor to its receptor in *Saccharomyces cerevisiae*, *The Journal of biological chemistry 263*, 17333-17341.

28. Lee, B. K., Khare, S., Naider, F., and Becker, J. M. (2001) Identification of residues of the *Saccharomyces cerevisiae* G protein-coupled receptor contributing to alpha-factor pheromone binding, *The Journal of biological chemistry 276*, 37950-37961.

29. Wang, H. X., and Konopka, J. B. (2009) Identification of amino acids at two dimer interface regions of the alpha-factor receptor (Ste2), *Biochemistry 48*, 7132-7139.

30. Kelley, L. A., and Sternberg, M. J. (2009) Protein structure prediction on the Web: a case study using the Phyre server, *Nature protocols 4*, 363-371.

31. Choi, Y., and Konopka, J. B. (2006) Accessibility of cysteine residues substituted into the cytoplasmic regions of the alpha-factor receptor identifies the intracellular residues that are available for G protein interaction, *Biochemistry 45*, 15310-15317.

32. Bouvier, M. (2001) Oligomerization of G-protein-coupled transmitter receptors, *Nature reviews. Neuroscience 2*, 274-286.

33. Park, P. S., Filipek, S., Wells, J. W., and Palczewski, K. (2004) Oligomerization of G protein-coupled receptors: past, present, and future, *Biochemistry 43*, 15643-15656.

34. Overton, M. C., and Blumer, K. J. (2002) The extracellular N-terminal domain and transmembrane domains 1 and 2 mediate oligomerization of a yeast G protein-coupled receptor, *The Journal of biological chemistry 277*, 41463-41472.

35. Kim, H., Lee, B. K., Naider, F., and Becker, J. M. (2009) Identification of specific transmembrane residues and ligand-induced interface changes involved in homo-dimer formation of a yeast G protein-coupled receptor, *Biochemistry 48*, 10976-10987.

36. Eriotou-Bargiota, E., Xue, C. B., Naider, F., and Becker, J. M. (1992) Antagonistic and synergistic peptide analogues of the tridecapeptide mating pheromone of *Saccharomyces cerevisiae*, *Biochemistry 31*, 551-557.

37. Henry, L. K., Khare, S., Son, C., Babu, V. V., Naider, F., and Becker, J. M. (2002) Identification of a contact region between the tridecapeptide alpha-factor mating pheromone of *Saccharomyces cerevisiae* and its G protein-coupled receptor by photoaffinity labeling, *Biochemistry 41*, 6128-6139.

38. Son, C. D., Sargsyan, H., Hurst, G. B., Naider, F., and Becker, J. M. (2005) Analysis of ligand-receptor cross-linked fragments by mass spectrometry, *The journal of peptide research : official journal of the American Peptide Society 65*, 418-426.

39. Smith, B., Hill, C., Godfrey, E. L., Rand, D., van den Berg, H., Thornton, S., Hodgkin, M., Davey, J., and Ladds, G. (2009) Dual positive and negative regulation of GPCR signaling by GTP hydrolysis, *Cellular signalling 21*, 1151-1160.

40. Slessareva, J. E., Ma, H., Depree, K. M., Flood, L. A., Bae, H., Cabrera-Vera, T. M., Hamm, H. E., and Graber, S. G. (2003) Closely related G-protein-coupled receptors use multiple and distinct domains on G-protein alpha-subunits for selective coupling, *The Journal of biological chemistry 278*, 50530-50536.

41. Kristiansen, K. (2004) Molecular mechanisms of ligand binding, signaling, and regulation within the superfamily of G-protein-coupled receptors: molecular modeling and mutagenesis approaches to receptor structure and function, *Pharmacology & therapeutics 103*, 21-80.

42. Fotiadis, D., Liang, Y., Filipek, S., Saperstein, D. A., Engel, A., and Palczewski, K. (2003) Atomic-force microscopy: Rhodopsin dimers in native disc membranes, *Nature 421*, 127-128.

43. Liang, Y., Fotiadis, D., Filipek, S., Saperstein, D. A., Palczewski, K., and Engel, A. (2003) Organization of the G protein-coupled receptors rhodopsin and opsin in native membranes, *The Journal of biological chemistry 278*, 21655-21662.

44. Filizola, M., Wang, S. X., and Weinstein, H. (2006) Dynamic models of G-protein coupled receptor dimers: indications of asymmetry in the rhodopsin dimer from molecular dynamics simulations in a POPC bilayer, *Journal of computer-aided molecular design 20*, 405-416.

45. Blumer, K. J., and Thorner, J. (1991) Receptor-G protein signaling in yeast, *Annual review of physiology 53*, 37-57.

46. Kim, S., and Cross, T. A. (2004) 2D solid state NMR spectral simulation of 3(10), alpha, and pi-helices, *J Magn Reson 168*, 187-193.

47. Bhattacharya, S., Hall, S. E., and Vaidehi, N. (2008) Agonist-induced conformational changes in bovine rhodopsin: insight into activation of G-protein-coupled receptors, *Journal of molecular biology 382*, 539-555.

48. Jaakola, V. P., Griffith, M. T., Hanson, M. A., Cherezov, V., Chien, E. Y., Lane, J. R., Ijzerman, A. P., and Stevens, R. C. (2008) The 2.6 angstrom crystal structure of a human A2A adenosine receptor bound to an antagonist, *Science 322*, 1211-1217.

49. Ludeke, S., Mahalingam, M., and Vogel, R. (2009) Rhodopsin activation switches in a native membrane environment, *Photochemistry and photobiology 85*, 437-441.

50. Chien, E. Y., Liu, W., Zhao, Q., Katritch, V., Han, G. W., Hanson, M. A., Shi, L., Newman, A. H., Javitch, J. A., Cherezov, V., and Stevens, R. C. (2010) Structure of the human dopamine D3 receptor in complex with a D2/D3 selective antagonist, *Science 330*, 1091-1095.

51. Blumer, K. J., Reneke, J. E., and Thorner, J. (1988) The STE2 gene product is the ligand-binding component of the alpha-factor receptor of *Saccharomyces cerevisiae*, *The Journal of biological chemistry 263*, 10836-10842.

52. Konopka, J. B., Jenness, D. D., and Hartwell, L. H. (1988) The C-terminus of the *S. cerevisiae* alpha-pheromone receptor mediates an adaptive response to pheromone, *Cell 54*, 609-620.

53. Yesilaltay, A., and Jenness, D. D. (2000) Homo-oligomeric complexes of the yeast alpha-factor pheromone receptor are functional units of endocytosis, *Molecular biology of the cell 11*, 2873-2884.

54. Shi, C., Shin, Y. O., Hanson, J., Cass, B., Loewen, M. C., and Durocher, Y. (2005) Purification and characterization of a recombinant G-protein-coupled receptor, *Saccharomyces cerevisiae* Ste2p, transiently expressed in HEK293 EBNA1 cells, *Biochemistry 44*, 15705-15714.

55. Lee, B. K., Jung, K. S., Son, C., Kim, H., VerBerkmoes, N. C., Arshava, B., Naider, F., and Becker, J. M. (2007) Affinity purification and characterization of a G-protein coupled receptor, *Saccharomyces cerevisiae* Ste2p, *Protein expression and purification 56*, 62-71.

56. Domazet, I., Martin, S. S., Holleran, B. J., Morin, M. E., Lacasse, P., Lavigne, P., Escher, E., Leduc, R., and Guillemette, G. (2009) The fifth transmembrane domain of angiotensin II Type 1 receptor participates in the formation of the ligand-binding pocket and undergoes a counterclockwise rotation upon receptor activation, *The Journal of biological chemistry 284*, 31953-31961.

57. Lee, Y. H., Naider, F., and Becker, J. M. (2006) Interacting residues in an activated state of a G protein-coupled receptor, *The Journal of biological chemistry 281*, 2263-2272.

58. Eilers, M., Hornak, V., Smith, S. O., and Konopka, J. B. (2005) Comparison of class A and D G protein-coupled receptors: common features in structure and activation, *Biochemistry 44*, 8959-8975.

PART IV

Residue-to-Residue Interactions Between a G Protein-Coupled Receptor (GPCR) and its Gα Protein in the *Saccharomyces cerevisiae* Model System

Part IV presents collaborative work with Dr. Fred Naider's laboratory at the City University of New York, Staten Island. Li-Yin Huang and George K. E. Umanah performed most the work, Julie Maccarone assisted with the phenotypes of the Gpa1p mutants and the peptides used were obtained from Dr. Naider's laboratory.

Abstract for Part IV

Understanding the interactions between G protein-coupled receptors (GPCRs) and their cognate Gα proteins is an important goal for drug discovery as interference or enhancement of this interaction will directly modify signal transduction. Ste2p, the GPCR for the tridecapeptide pheromone α-factor of *Saccharomyces cerevisiae*, has been used extensively as a model for investigating GPCR structure and function as Ste2p has structure-function relationships similar to mammalian GPCRs. Using cysteine disulfide cross-linking we have identified specific residue-to-residue interactions between Ste2p and Gpa1p, its Gα protein. Using combinatorial expression and assay of 242 Ste2p and Gpa1p cysteine mutants, five Ste2p residues located at the cytoplasmic ends of the fifth and sixth transmembrane domains were identified to interact with five residues of the C-terminus of Gpa1p. Different cross-linking reactions of the Ste2p residues with Gpa1p residues in the absence and presence of the α-factor pheromone suggested that during activation both transmembrane 5 and 6 of Ste2p and the α5-helix (C-terminus) of Gpa1p undergo conformational changes that results in withdrawal of the α5-helix from the receptor. This study is the first to identify specific residue-to-residue interactions between a GPCR and its cognate Gα protein in its active and inactive states.

Chapter 1

Introduction

G protein-coupled receptors (GPCRs) are medically important receptors that are comprised of seven transmembrane domains (TMs) and function by activating heterotrimeric G proteins. These receptors are the most diverse group of membrane-bound receptors and are the targets of a multitude of current prescription drugs (*1-3*). Despite the availability of crystal structures for GPCRs (*4*) and G proteins (*5, 6*), the molecular mechanisms leading to activation of G proteins upon ligand binding to GPCRs remain unclear. GPCR–G protein interactions have implications with regards to drug discovery: If drugs can be identified that interfere or promote GPCR-G protein interaction, change the pattern of GPCR–G protein associations, or cause a GPCR to preferentially associate with one G protein and not others, then it would be possible to regulate the activities and functions of a specific receptor (*1, 7-9*).

The mating pathway of *Saccharomyces cerevisiae* has been a valuable tool for studying GPCR signal transduction mechanisms for many reasons including the fact that the yeast mating pheromone receptors activate only one Gα (Gpa1p) making the yeast system highly amenable to identification of specific interactions between the receptor and a Gα (*10-12*). Ste2p, the α-factor pheromone receptor of *S. cerevisiae*, shows an overall similar structural architecture to mammalian GPCRs and Gpa1p shows about 45% sequence similarity with various mammalian Gα proteins (*13*). Comparison of Ste2p with the rhodopsin (class A) subfamily of GPCRs suggests that there are underlying similarities in the mechanism of signal transduction between Ste2p and the Class A

GPCRs (*11*). These characteristics of Ste2p make it a good model for peptide-responsive GPCRs.

Studies on the interactions between Ste2p and Gpa1p indicate that the Ste2p third intracellular loop (IL3) is involved in Gpa1p activation (*14-17*). Like the mammalian Gα proteins, the region of Gpa1p that has been most commonly predicted to interact with Ste2p is the C-terminus (*18, 19*). Despite the intense studies carried out on the interactions of Ste2p with Gpa1p, the specific residue-to-residue interactions between Ste2p and Gpa1p have not been determined.

Several models have been proposed for signal transfer from the activated receptor to the Gα protein. The "gear shift", "lever arm" and "sequential fit" models have in common that the α5 helix (C-terminus) of Gα is the key transmission domain for the receptor-G protein signal transfer (*20*). The binding of Gα to the activated receptor is suggested to cause movement of the α5 helix that affects GDP binding at the β6-α5 loop (*21*). Recently, using structural and kinetic modeling of the C-terminus of transducin, Gα was proposed to undergo rotational and translational movements during activation (*20*). It has also been suggested that the receptor must induce conformational changes in the G protein that result in the exchange of GDP for GTP (*22*). Evidence for this complex series of interactions and for structural transitions in the G protein have also been experimentally determined using spin-labeled, reconstituted Gαi and rhodopsin (*21*).

This study identifies specific residue-to-residue interactions between Ste2p and Gpa1p in both the activated and inactive state using biochemical analysis by disulfide cross-linking. The patterns of Gpa1p interaction with the inactive and active forms of

Ste2p suggest possible rotational and "withdrawal" movements at the C-terminus of Gpa1p that are required for proper Ste2p coupling and Gpa1p activation. These experimental conclusions are used to develop a proposed mechanism for Ste2p-Gpa1p signal transfer. The approaches and information from this study will be valuable for future studies on mammalian GPCRs signaling pathways.

Chapter 2

Material and Methods

Media, Reagents, and Strains and Transformation

Saccharomyces cerevisiae strains LM102 [*MATa, bar1, leu2, trp1, ura3, FUS1-lacZ::URA3, ste2*Δ (*23*)] and TM5117 [*MATa, bar1, leu2, his3, ura3, FUS1-lacZ::URA3, ste2*Δ*, gpa1*Δ (*23*)] were used for biological activity assays and the protease-deficient strain BJS21 [*MATa, prc1-407 prb1-1122 pep4-3 leu2 trp1 ura3-52 ste2::Kan*^{R} (*24*)] was used for protein isolation and immunoblot analysis. The STE2 and GPA1 mutant plasmids were transformed by the method of Geitz (*25*) into the *S. cerevisiae* strains.

Cysteine Scanning Mutagenesis

C-terminal FLAG™ and His tagged STE2 with the two cysteine residues (Cys^{59} and Cys^{252}) substituted with serine and cloned into the plasmid p424-GPD to yield plasmid pBEC2 (*23, 26*) was used for expressing Ste2p. The plasmid pBEC2 was engineered by site-directed PCR mutagenesis to replace 22 residues, one at a time, in Ste2p (Ala^{228}-Ile^{249}) with cysteine. The open reading frame of GPA1 was PCR amplified from the plasmid YepGαβγ (*27*) and cloned into the plasmids p426 and p423-GPD (*28*) to yield plasmids pBUG6 and pBUG3 for expression in the BJS21 and TM5117 strains, respectively. The pBUG6 and pBUG3 were engineered by site-directed mutagenesis to replace 11 residues in Gpa1p (Ile^{461}-Ile^{471}) with cysteine. The sequence of all cysteine mutants was verified by DNA sequence analysis completed by the molecular biology

resource facility located on the campus of the University of Tennessee. Mutagenic and sequencing primers were purchased from Invitrogen (Carlsbad, CA).

Membrane Extraction and Immunoblots

BJS21 cells expressing STE2 and GPA1 mutant constructs grown in selective media were used to prepare total cell membranes isolated as previously described (*29*). Membrane extracts were resuspended in HEPES buffer (50 mM HEPES, 150 mM NaCl, pH 7.5, 20% glycerol). For immunoblotting blots were probed with FLAG™ antibody (Sigma/Aldrich Chemical, St. Louis, MO) to detect Ste2p or an antibody directed against Gpa1p (Santa Cruz Biotechnology, Inc., CA). The signals generated were quantitated using Quantity One software (Version 4.5.1) on a Chemi-Doc XRS photodocumentation system (BioRad, Hercules, CA) to determine expression levels.

Growth Arrest Assays

LM102 cells expressing C-terminal FLAG and His tagged Ste2p were grown at 30 ºC in MLT (minimal medium (*30*) lacking tryptophan), harvested, washed three times with water and resuspended at a final concentration of 5 x 10^6 cells/ml (*24*). Cells (1 ml) were combined with 3.5 ml agar noble (1.1 %) and poured as a top agar lawn onto MLT medium agar plates. Filter disks (BD, Franklin Lakes, NJ) impregnated with α-factor pheromone (0.125 – 2.0 μg) were placed on the top agar. The plates were incubated at 30ºC for 18 hours and then observed for clear halos around the discs. The diameter of halos around the discs were measured and analyzed by linear regression analysis using

Prism software (GraphPad Software, San Diego, CA). The experiment was repeated at least three times and reported values represent the mean of these tests.

Fus1-lacZ Assays

LM102 cells expressing C-terminal FLAG and His tagged Ste2p Cys mutants were grown at 30ºC in selective media, harvested, washed three times with fresh media and resuspended at a final concentration of 5 x 10^7 cells/ml. Cells (0.5 ml) were combined with α-factor pheromone (final concentration of 1 μM) and incubated at 30ºC for 90 minutes. The cells were transferred to a 96-well flatbottom plate in triplicates, permeabilized with 0.5% Triton X-100 in 25 mM PIPE buffer and then β-galactosidase assays were carried out using fluorescein di-β-galactopyranoside (Molecular Probes, OR) as a substrate (*31*). The reaction mixtures were incubated at 37ºC for 60 minutes and 1.0 M Na_2CO_3 was added to stop the reaction. The fluorescence of the samples (excitation of 485 nm and emission of 530 nM) was determined using a 96-well plate reader Synergy2 (BioTek Instruments, Inc., Winooski, VT). The data were analyzed using Prism software (GraphPad Software, San Diego, CA). The experiments were repeated at least three times and reported values represent the mean of these tests.

Saturation Binding Assay

Tritiated α-factor (9.3 Ci/mmol) was used in saturation binding assays on whole cells. LM102 cells expressing C-terminal FLAG and His tagged Ste2p Cys mutants were harvested, washed three times with YM1 [yeast minimum medium with 0.5 M potassium

phosphate (pH 6.24) containing 10 mM TAME, 10 mM sodium azide, 10 mM potassium fluoride, and 1% BSA], and adjusted to a final concentration of 4×10^7 cells/ml in binding medium YM1i (YM1 plus protease inhibitors). Cells (630 µl) were combined with 70 µl of 10X YM1i supplemented with [^{3}H]α-factor and incubated at room temperature for 30 min. The final concentration of [^{3}H]α-factor ranged from 0.4×10^{-9} to 50×10^{-9} M. Upon completion of the incubation interval, 200 µl aliquots of the cell–pheromone mixture were collected in triplicate and washed over glass fiber filter mats using the Standard Cell Harvester (Skatron Instruments, Sterling, VA). Retained radioactivity on the filter was counted by liquid scintillation spectroscopy. LM102 cells lacking Ste2p were used as a nonspecific binding control for the assays. Specific binding for each mutant receptor was calculated by subtracting the nonspecific values from those obtained for total binding. Specific binding data were analyzed by nonlinear regression analysis for single-site binding using Prism software (GraphPad Software, San Diego, CA) to determine the K_d (nM), and B_{max} values (receptors/cell) for each mutant receptor were calculated. The final values represent the binding constants from at least three independent experiments.

Disulfide Crosslinking

Membrane samples were incubated with or without Cu-P (1.0 µM Cu and 3.0 µM 1,10-phenanthroline) in the absence or presence of a saturating amount of α-factor (5 µM) at room temperature for 30 min and then quenched by addition of EDTA (10 mM). The membrane samples were resuspended in non-reducing SDS sample buffer (BioRad,

Hercules, CA), separated by 10% SDS-PAGE, and then analyzed by immunoblotting as previously described (29). The disulfide reaction was reversed by reducing with 4% 2-mercaptoethanol (β-ME) in the SDS sample buffer. For in vivo cross-linking, cells were grown to mid-log phase, harvested, and washed with water by centrifugation (4000g for 5 min). The cells were resuspended in 100 mM LiAc and incubated at 30ºC for 30 min with mixing. After centrifugation, the cells were resuspended in 25% PEG with 250 mM LiAc for another 60 min incubation. Cells were washed with HEPES buffer three times after LiAc treatment. To evaluate the effect of receptor activation on in vivo crosslinking, whole cells were first incubated with KF (10 mM) and NaN_3 (10mM) in HEPES buffer at room temperature for 15 min to inhibit receptor endocytosis (*32*) and then α-factor was added to a final concentration of 5 μM. Disulfide cross-linking was induced by adding Cu-P to final concentrations of 0.5 mM Cu and 1.5 mM 1,10-phenanthroline as previously described for whole cell experiments in yeast (*33*). Membrane extraction was carried as described above with HEPES buffer containing 10 mM EDTA/NEM.

Prediction and Modeling

All models of 3-D structures were generated by the Phyre Structural Bioinformatics Group prediction tools (*34*). The structures were viewed and labeled with the PyMOL pdb viewer software (DeLano Scientific LLC, Palo Alto, CA). Aligment of the last 11 amino acids of transducin (Gα of rhodopsin) with Gpa1p was carried out using European Bioinformatics Institute online sequence alignment tools (http://www.ebi.ac.uk/).

Chapter 3

Results

Phenotypes of Ste2p IL3 Cys Mutants

The Cys-less Ste2p (C59S and C252S), with FLAG™ and HIS-epitope tags in the C-terminus, engineered as the background for the specific cysteine mutations has been previously shown to have expression levels and biological activities identical to those of the wild type receptor as determined by several assays (*23, 26*). Substitution of single cysteine residues from L228C through I249C in intracellular loop 3 (IL3) of Cys-less Ste2p resulted in constructs that were expressed and had biological activities identical or similar to (within 25% of Cys-less, except for R233C, L236C, and K239C) that of the Cys-less receptor (see Table 4.1). In addition to quantitation of the Western blot signals, saturation binding assays were carried out on selected mutants (L228C and A229C from the TM5-IL3 boundary, R233C and R234C from the middle of IL3, and L248C and I249C from the IL3-TM6 boundary). The receptors showed almost equal K_d values for ligand binding and were expressed at levels within 12% difference (L228C, A229C, L248C, and I249C) to about 55-63% (R233C and R234C) of the Cys-less control respectively (Figure 4.1). Since the A229C mutant does not crosslink whereas the L228C, L248C and I249C do, we conclude that the expression levels are not the reason for the differences in crosslinking we noted.

Table 4.1 Summary of phenotypes of Ste2p IL3 Cys substitution mutants. The expression levels as measured by western blots and biological activities all had standard deviations between ±4 and ±7 percent. All assays were done three times independently.

Mutation	Protein Expression (%)	Growth arrest activities (%)	*Fus1-LacZ* induction (%)
Cys-less	100	100	100
L228C	100	90	110
A229C	100	90	75
I230C	100	85	100
R231C	100	90	100
S232C	100	100	90
R233C	65	70	60
R234C	75	100	80
F235C	75	100	80
L236C	75	75	65
G237C	75	100	75
L238C	75	100	75
K239C	75	75	65
Q240C	75	100	80
F241C	100	100	80
D242C	85	85	85
S243C	100	95	100
F244C	100	90	95
H245C	90	90	70
I246C	100	90	70
L247C	100	90	75
L248C	100	85	95
I249C	100	85	100

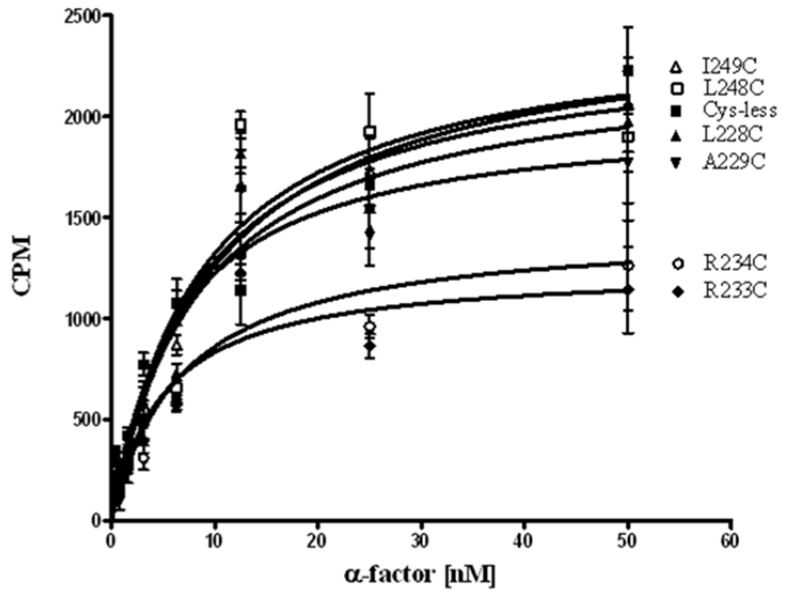

Mutants:	Cys-less	L228C	A229C	R233C	R234C	L248C	I249C
K_d (nM)	8.39	8.62	7.54	6.98	7.27	8.78	9.93
B-Max (CPM)	2292	2282	2021	1253	1450	2475	2488
Receptors/Cell	36,512	36,352	32,194	19,960	23,098	39,426	39,633
Expression (% of Cys-less)	100	99.6	88.2	54.7	63.2	107.9	108.5

Figure 4.1 Whole cell saturation binding assay of [^{3}H]α-factor to Cysless and IL3 Cys mutant receptors. A graph of CPM (count per minute of radioactivity of cells) versus the concentration of the [^{3}H]α-factor is shown. The data represents specific binding to cells as determined by subtracting the binding to cells lacking the receptor from binding to cells containing the containing Ste2p Cys mutant receptors. Below the graph is a table containing a summary of the binding affinities (K_d) and surface expression of the receptors.

Expression and Activities of Gpa1p Cys-Mutants

Most of the cysteine residues in Gpa1p are localized within highly conserved stretches of Gpa1p that share about 45% amino acid identity to transducin (*17*). In addition some of these cysteine residues, especially C3, are very important for biological activities such as thioacetylation, palmitoylation, signaling, and membrane localization (*35*). Thus, we did not mutate the endogenous Cys residues, because we were concerned that removing these cysteine residues would affect the localization and signaling of the Gpa1p. The Gpa1p Cys mutants generated in this study have expression levels similar to wild type Gpa1p (Figure 4.2A). A high molecular weight protein [denoted as a non-specific (NS) signal] that reacted with anti-Gpa1p was seen in all samples and also in extracts from TM5117 cells that were deleted for Gpa1p. The yeast strain TM5117 used to express the Gpa1p mutants has the endogenous GPA1 deleted resulting in high FUS1-lacZ activities in the absence of pheromone because the Gβγ subunits constitutively activate the signal transduction pathway (Figure 4.2B). Expression of the mutant Gα subunits with the various Cys-substituted mutations showed that all could interact with the endogenous Gβγ subunits leading to reduced FUS1-lacZ activities in the TM5117 yeast strain in the absence of pheromone (Figure 4.2B). In the presence of α-factor, the FUS1-lacZ activities increased, implying that all of the Gα mutants can couple productively with both the Ste2p receptor and the G protein βγ subunits. However, the mutants K468C, I469C and I471C exhibited about 60-70% capacity to activate signal transduction as measured by FUS1-lacZ activity in comparison to the other Cys-mutants.

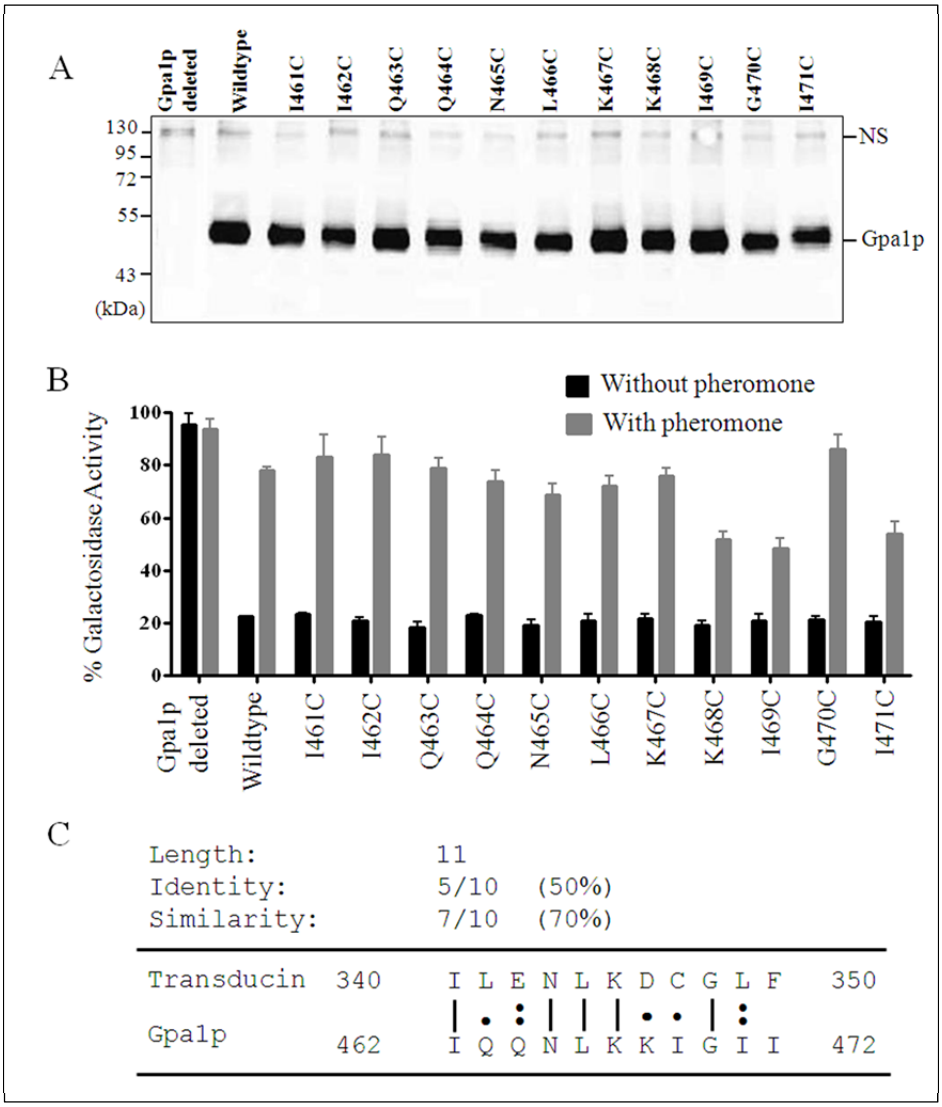

Figure 4.2 Expression and signaling activity of Gpa1p Cys-mutants. A: Immunoblot of Gpa1p Cys mutants probed with anti-Gpa1p. NS represents a non-specific reactive band. B: β-galactosidase activity from the induction of the reporter gene Fus1-LacZ by activation of Ste2p mediated signaling in strains containing Gpa1p Cys mutants with (gray bars) and without (black bars) added pheromone. The data is normalized to activity in the Gpa1p-deleted mutant. C: Sequence alignment of eleven amino acids of Gpa1p and transducin at C-terminal end.

Disulfide Crosslinking of Ste2p and Gpa1p

The molecular weight of the epitope tagged Cys-less Ste2p used to generate the IL3 Cys mutants is about 51 kDa. This receptor is normally observed as a monomer (51-55 kDa, appearing with three bands due to N-glycosylation at two sites on the N-terminus) and a dimer (106-110 kDa) on blots (*23*). The wild type Gpa1p used in this study is observed at 52-54 kDa (Figure 4.2A). The Ste2p-Gpa1p disulfide crosslinked product (~103-108 kDa) is therefore expected to be at a position similar to that of the Ste2p dimer (~102-110 kDa) on immunoblots. Since the IL3 Cys mutants have been shown to form homo-dimers we needed to differentiate a 103-108 kDa Ste2p homodimer band from a Ste2p-Gpa1p heterodimeric cross-linked product at a similar position on immunoblots. To detect the Ste2p-Gpa1p cross-linked product we used an antibody directed against Gpa1p. This antibody reacted with the 52-54 kDa (Gpa1p) band and detected a 103-108 kDa Ste2p-Gpa1p heterodimer since Gpa1p does not form a homodimer. As seen in Figure 4.2A the wildtype Gpa1p and its Cys analogs exhibit only one strong band at the molecular weight expected for the monomer (~52 kDa). All of the Gpa1p constructs and the Gpa1p deletion strain exhibit a very weak band at a high molecular weight (~130 kDa). These results clearly show that Gpa1p and the Cys analogs examined herein do not form homodimers.

To determine whether IL3 residues (L228-I249) in Ste2p interacted with the C-terminal (I461-I471) residues in Gpa1p as measured by disulfide crosslinking, the IL3 Cys-mutants were each co-expressed with all the Gpa1p Cys-mutants including wild type Gpa1p. Thus 23 different IL3 receptors (22 with one Cys residue in IL3 and the control Cys-less Ste2p) were co-expressed with 12 different Gpa1p proteins (11 with one Cys residue in the C-terminus and the control Gpa1p without Cys) to give 276 different combinations of Ste2p/Gpa1p. Membranes extracted from all of the different combinations were incubated with or without 5 μM α-factor to activate Ste2p and then treated with Cu-P to facilitate Cys-Cys disulfide formation (*36*). To illustrate the Ste2p-Gpa1p cross-linking results we compare Ste2p-I246C, Ste2p-L247C and a Cys-less Ste2p control interacting with various Gpa1p Cys mutants (Figure 4.3). Of the 36 expression combinations shown in Figure 4.3, only 2 (Ste2p-L247 C with either Gpa1pN465C or Gpa1pK467C) showed bands at the position expected for a Ste2p-Gpa1p crosslinked product. These are indicated by asterisks in the Figure. Interestingly, the L247C-N465C crosslink is formed only in the absence of α-factor whereas the L247C-K467C crosslink is formed only in the presence of the pheromone. To determine whether the endogenous cysteine residues in Gpa1p could cross-link to Ste2p, all the Ste2p Cys mutants that we generated were co-expressed with the wildtype Gpa1p (containing all endogenous cysteine residues) for cross-linking as shown in blots in Figure 4.3. We did not observe any cross-linking between the wildtype Gpa1p and any of the Ste2p Cys mutants. Thus the endogenous cysteine residues were not involved in Ste2p-Gpa1p crosslinking.

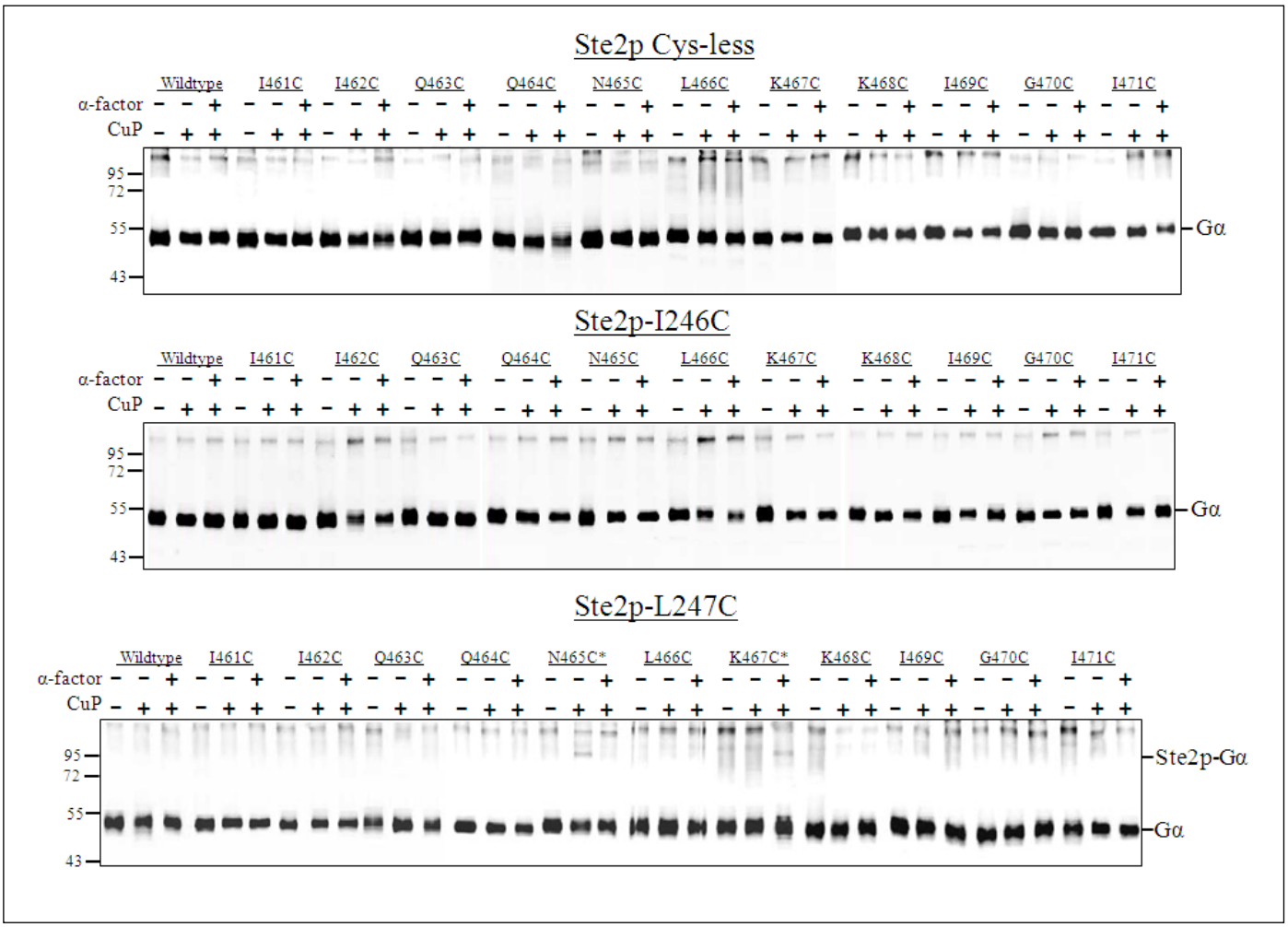

F**igure 4.3 Immunoblots of two cysteine mutants of the IL3 region of Ste2p co-expressed with eleven Gpa1p Cys-mutants probed with anti-Gpa1p.** Membrane preparations from transformants that were untreated (lanes -, -), treated with Cu-P in the absence of α-factor (lanes -, +) or treated with Cu-P in the presence of α-factor (lanes +, +) were probed with anti-Gpa1p antibody to detect the presence of Gpa1p (Gα) at either the 52-54 kDa or 103-108 kDa (Ste2p-Gα cross-linked) position. The samples were resolved on 10% SDS-PAGE. The blot images were spliced together from different gels to place the mutants in order according to the residue number of the Gpa1p cysteine

replacement. The top panel is data from a Ste2p Cys-less strain co-transformed with various Gpa1p Cys mutants. The middle and bottom panels present similar experiments from Ste2p-I246C and Ste2p-L247C, respectively. The combinations that showed crosslinks are designated with asterisks.

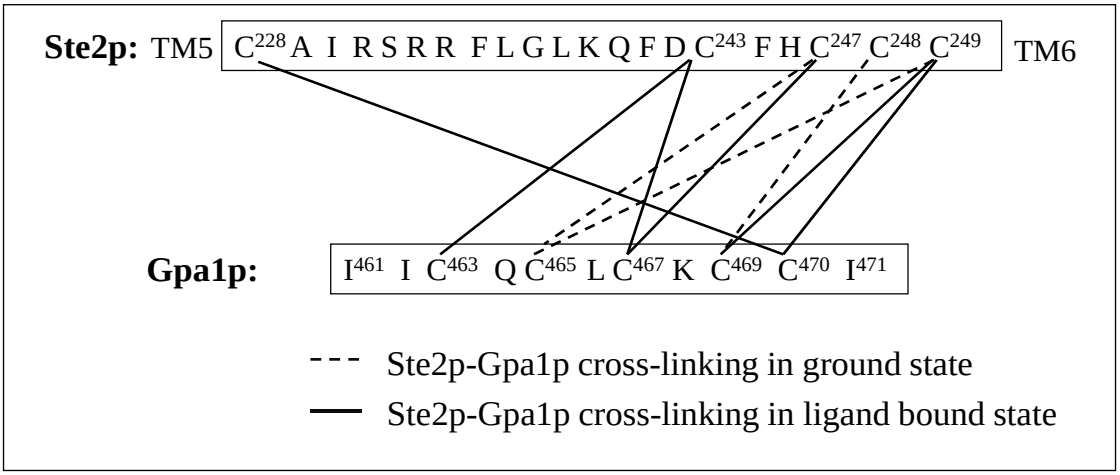

Figure 4.4 Diagrammatic representation of cross-links formed between Ste2p and Gpa1p Cys-substituted mutants in the active and inactive state. The cysteine residue is that which would be present in the individual mutated Ste2p or Gpa1p proteins.

Out of the 22 Ste2p Cys-mutants tested, 5 mutants (L228C, S243C, L247C, L248C and I249C) showed a cross-linked band with 5 out of the 11 Gpa1p Cys-mutants (Q463C, N465C, K467C, I469C and G470C) in either the ligand-unbound or ligand-bound state of Ste2p (schematically indicated in Figure 4.4). Examination of all the anti-Gpa1p blots quantitatively showed that the NS signal intensity varied and was independent of the Ste2p-Gpa1p signal. Furthermore, CuP catalyzed oxidation in the absence of alpha-factor or in the presence of alpha-factor resulted in a quantifiable

reduction in Gpa1p when the crosslinked heterodimer Ste2p-Gpa1p was formed, and the sum of the band intensities of Ste2p-Gpa1p and Gpa1p are in reasonable agreement with the intensity of Gpa1p in the untreated control. We conclude that the weak NS signal can not be related to the amount of Gpa1p or Ste2p-Gpa1p in the sample.

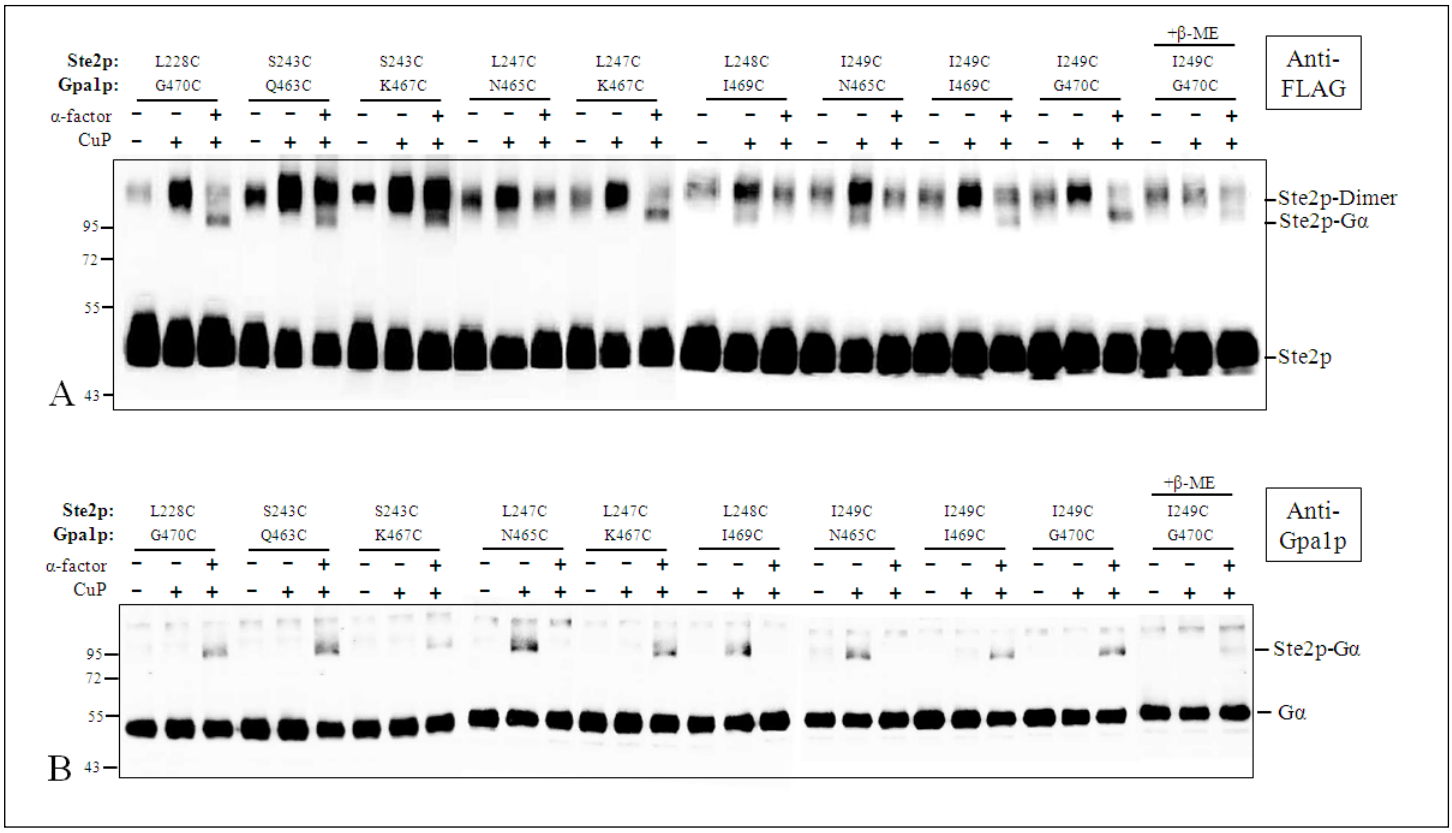

Figure 4.5 Immunoblots of various combinations of Ste2p and Gpa1p Cys mutants probed with anti-FLAG™ antibody (anti-Ste2p) and anti-Gpa1p. The samples were resolved on a 4-12 % gradient SDS-PAGE. A: The blots were probed with anti-FLAG to detect the presence of Ste2p at either ~51-55 kDa (Ste2p monomer) or ~108-110 kDa (Ste2p-dimer) or ~103-108 kDa (Ste2p-Gα cross-linked) position. B: The blots were also probed with anti-Gpa1p antibody to detect the presence of Gpa1p (Gα) at either the ~53-

54 kDa (monomer) or ~103-108 kDa (Ste2p-Gα cross-linked) position. The blot images were spliced together from different gels. The last two combinations Ste2p(I249C)/Gpa1p(470C) were run in the presence and absence of 4% β-mercaptoethanol.

The Gpa1 polyclonal antibody (Santa Cruz) was generated to a peptide comprising residues 183-472 (290 residues) of Gpa1p, so that this polyclonal antibody was expected to react with Gpa1p with single cysteine mutations within the small region (461-471) tested in our studies and also detect Gpa1p crosslinked through its extreme C-terminus to Ste2p. To confirm that the signal on the anti-Gpa1p blots are indeed Ste2p-Gpa1p cross-linked all the Cu-P treatments of mutants with detectable cross-linked products were probed using both anti-Gpa1p (Figure 4.5B) and anti-FLAG (Figure 4.5A) to detect Ste2p-monomer (53-55 kDa), Ste2p-dimer (106-110 kDa) and Ste2p-Gpa1p cross-linked product (103-108 kDa). This allowed us to distinguish between Ste2p homodimers and the crosslinked Ste2p-Gpa1p protein. Both antibodies revealed the same crosslinking patterns for Ste2p and Gpa1p. However, because the Ste2p probe also revealed homodimer and multiple-glycosylated proteins, these bands are much broader and it is more difficult to discern the Ste2p-Gpa1p crosslinked product which is often obscured by the Ste2p dimers (compare top and bottom gels). The Ste2p-Gpa1p cross-linked products were nearly completely reversed by treatment with 4% β-ME (see Figure 4.5, last three lanes for I249C-G470C), indicating that a disulfide bond connected the hetero-dimeric Ste2p-Gpa1p. The fact that probing with both anti-Ste2p and anti-Gpa1p

(Figure 4.5B) resulted in the same signal on the gels indicates that the Santa Cruz antibody can interact with the Ste2p-Gpa1p crosslinked product.

In the inactive state (without α-factor binding, Figure 4.4B α-factor "-" lanes) L248C in IL3 reacted with I469C in Gpa1p, whereas both L247C and I249C in IL3 reacted with N465C in Gpa1p (Figure 4.4, broken lines). Although previous studies showed that I246C is highly accessible to a sulfhdryl reagent (*37*) this residue did not react with the Gpa1p residues tested in this study. No detectable disulfide product was observed for residues located in the middle of the IL3 loop or at the TM5 boundary in the inactive conformation of Ste2p. In the ligand-bound, active conformation (Figure 4.5B α-factor "+" lanes) both L228C (TM5) and I249C (TM6) reacted with G470C of Gpa1p. S243C and L247C of the receptor reacted with K467C of Gpa1, whereas receptor I249C reacted with I469C of Gpa1 (Figure 4.4, solid lines; Figure 4.5B). The Ste2p IL3 Cys mutants (L228C, S243C, L247C, L248C and I249C) all displayed increased Ste2p-homodimer formation when treated with Cu-P in the absence of α-factor (ligand) binding to Ste2p (Figure 4.5A lanes labeled "– +"). In the presence of α-factor binding to Ste2p (Figure 4.5A lanes labeled "+ +") Ste2p-homodimer formation was reduced.

To test whether the IL3-Gpa1p interactions observed in the membrane samples existed in the whole cell before membrane preparation, in vivo Cu-P treatment was carried out on whole cells. For these experiments, cells co-expressing Ste2p-I249C and Gpa1p mutants, N465C, L466C, K467C, K468C, I469C, G470C and I471C in the presence or absence of α-factor were used. In this series of experiments N465, I469 and G470 (indicated by asterisks) formed the heterodimers whereas L466, K467, K468 and

I471 did not. These results (Figure 4.6) show that in vivo the interaction of receptor mutant I249C with Gpa1p was similar to what was observed in membrane preparations.

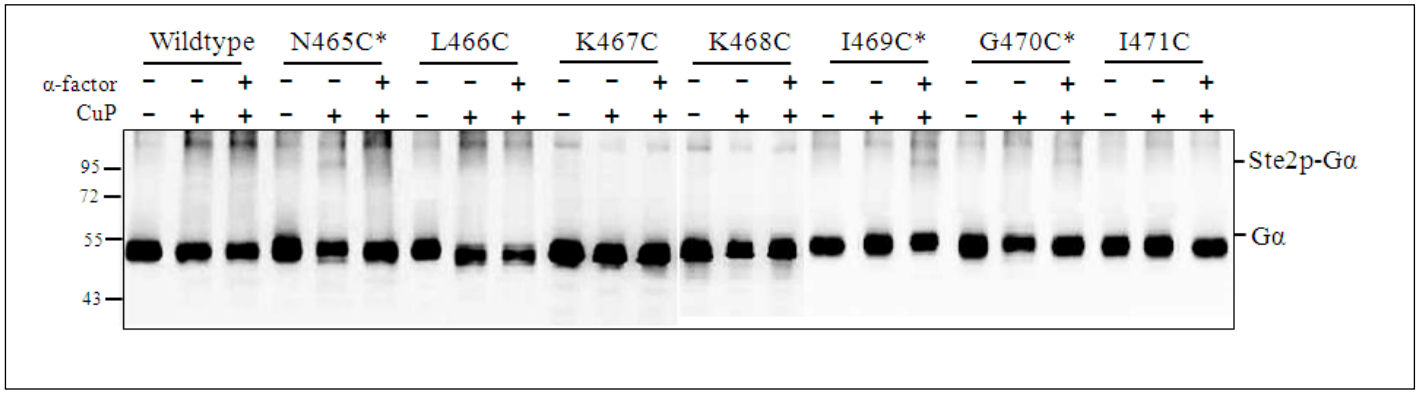

Figure 4.6 Immunoblots of membranes from whole cells expressing Ste2p-I249C together with various Gpa1p-Cys mutants (N465C-I471C) probed with anti-Gpa1p. Samples were untreated (lanes -,-) or treated with Cu-P in absence (lanes -, +) or the presence (lanes +, +) of α-factor. Membrane samples prepared from these cells were resolved on 10% SDS-PAGE. The combinations that showed crosslinks are designated with asterisks.

Chapter 4

Discussion

We have used disulfide cross-linking to determine specific residue-to-residue interactions between a yeast GPCR, Ste2p, in the active and inactive state and its cognate Gα, Gpa1p, allowing identification of conformational changes involved in signal transduction. Ste2p IL3 was observed to tolerate Cys substitutions well in our experiments (*37*). The alignment of the C-terminus of Gpa1p with the last 11 amino acids of transducin showed that in this region these two proteins are 50% identical and 70% similar (Figure 4.2C). This portion of transducin was suggested to directly interact with opsin and was used for co-crystallization with opsin to determine its binding to opsin (*38*). Cysteine substitution of the individual eleven residues (I461-I471) of Gpa1p tested in this study was well tolerated except for K468C, I469C and I471C which all resulted in a partial pheromone response (Figure 4.2B), consistent with previous studies (*17*). Signaling defects caused by mutation of the last five residues of Gpa1p have been observed in most studies (*14-16, 39*) suggesting that these residues are indeed critical for proper receptor coupling and Gpa1p activation. None of our mutations affected the coupling of Gpa1p with the Gβγ protein subunits, implying that the carboxyl tail of Gpa1p is essential for Ste2p coupling but not for interaction with Gβγ.

The crystal structure of opsin in its G protein-interacting conformation shows that cytoplasmic ends of TM5 and TM6 provide a surface for hydrophobic interactions with the C-terminus of transducin Gα (*38*). The disulfide cross-linking results from our study indicated that analogously to the transducin-opsin interaction the C-terminus of Gpa1p

interacts with TM5 and TM6 of Ste2p. In opsin, TM5 and TM6 are involved in van der Waals interactions with the C-terminus of transducin, and a hydrogen bonded network links the transducin and opsin residues (*38*). Cysteine disulfide cross-linking studies on Cys-mutant residues in Ste2p IL3 suggested that α-factor binding to Ste2p resulted in conformational changes involving the hydrophobic residues at the cytoplasmic ends of TM5 and TM6 (Figure 4.5A). The close proximity of these hydrophobic residues (L228, I247, L248, and L249) of Ste2p to the extreme C-terminus of Gpa1p indicates that these residues provide a hydrophobic environment that favors the Gpa1p C-terminus interaction. The crosslinking of S243C (Ste2p) with Q463C and K467C (Gpa1p) suggests that the three polar residues are involved in a hydrogen bond bridged network. These hydrogen-bonded bridges may be present during receptor activation, since these cross-links were only observed in the active form of the receptor. However, this may be just one of many networks, so the S243-Q463-K467 interaction may not be sufficient for full activation of the receptor and/or Gpa1p.

In the classical GPCR-G protein ternary complex model the binding of an agonist to the receptor induces the formation of a ternary complex consisting of a ligand, the receptor, and a G protein, followed by the exchange of GDP for GTP. The complex dissociates to Gα-GTP, Gβγ, and the receptor (*9, 19*). Although several models have been proposed to explain the coupling between GPCRs and G proteins, the coupling mode is still not well understood. The results from this study concur with the "precoupled" model which suggests that the receptor and G protein are precoupled and may form a stable complex regardless of the receptor activation state (*40*). The cross-linking of Ste2p Cys-

mutants to Gpa1p Cys-mutants in the presence and absence of ligand implies that the two proteins are in close proximity both in the active and inactive receptor conformation. These results provide physical evidence that the receptor-G protein complex exists prior to activation and that it is not formed by random collision where the Gα couples with the active receptor as suggested by the "collision coupling" model (*41*).

Activation of the Gα proteins by GPCRs has been observed to alter interactions of residues in the GDP binding domains that open the GDP-binding cleft, allowing GDP dissociation and the subsequent binding of GTP. Since the receptor binding domain of Gα is on the opposite face of this protein from the GDP-binding cleft, the interaction with the activated receptor must be transmitted to the GDP binding site by conformational changes (*18, 19, 21, 22, 41, 42*). Recently, it has been shown that the exchange of GDP for GTP in Gα proteins during receptor activation is induced by interactions of Gα with the receptor regardless of the presence or absence Gβγ. Thus, interactions of receptor with Gα proteins are the main requirements for the GDP/GTP exchange in Gα (*9*). Conformational changes at the C-terminus of transducin Gα involving a helix-switch were proposed based on structural and kinetic modeling. This helix-switch mechanism suggests that the α5-helix (C-terminus) of transducin Gα rotates counter-clockwise around its axis by 90° and tilts relative to the membrane by 42° (*20*) during activation.

Our disulfide crosslinking results suggest that two conformational changes affect the interactions of residues at the Gpa1 carboxyl terminus with residues at the cytoplasmic ends of TM5-TM6 of the receptor during Ste2p activation. The first conformational change, which is a rotational movement of the C-terminus of Gpa1p,

would be explained by the helix-switch mechanism model that is based on kinetic modeling (*20*). This movement is supported by the switch of the disulfide crosslinks from Gpa1p-N465C/Ste2p-L247C or Gpa1p-N465C/Ste2p-I249C in the inactive conformation to Gpa1p-K467C/Ste2p-L247C or Gpa1p-I469C/Ste2p-I249C in the active conformation (see Figure 4.7). Since the C-terminus of the Gpa1p is predicted to have a helical structure similar to that of transducin (*17*) a rotation of the helix of ~120° is required to switch a Gpa1p-N465C/Ste2p-L247C interaction to a Gpa1p-K467C/Ste2p-L247C interaction. Based on our Ste2p crosslinking studies we have postulated that TM6 undergoes ~30° clockwise rotation upon ligand binding (Fig 4.5A), similar to what has been suggested for TM6 of some mammalian GPCRs (*2*). Therefore, it is likely that Gpa1p may not have to undergo the full ~120° rotation to switch the residue interactions; an ~90° anti-clockwise rotation would suffice.

The second conformational change that would be consistent with our disulfide crosslinking results is what we call the "withdrawal" movement. This movement is necessary to explain the switch of the interactions between Gpa1p-N465/Ste2p-I249 in the inactive conformation to Gpa1p-I469/Ste2p-I249 in the active conformation. This switch requires the C-terminus (α5-helix) of Gpalp to move a distance that is approximately the height of the pitch of an α-helix (~5.4 Å) and undergo a simultaneous horizontal translation resulting in about 5 Å withdrawal from Ste2p. The concerted rotational and translational movements are proposed to result in a shift of the Gpa1p α5-helix from the TM6 cytoplasmic end towards the inner core of the receptor closer to TM5 and other TMs such as TM3 similar to the "translational" movement predicted by the

helix-switch mechanism derived from kinetic modeling (*20*). The "withdrawal" movement of Gpa1p α5-helix agrees with the α5-transmission rod concept of mammalian Gα proteins in which the α5-helix acts as a transmission "piston rod" to propagate the conformational changes from the receptor-G protein interface to the nucleotide binding pocket (*19, 20*). We propose that the Gpa1p α5-helix ("rod") rotates and moves away from Ste2p. These movements may cause distortion at the β6-α5 loop of Gpa1p that connects the C-terminus to the nucleotide-binding cleft, allowing GDP dissociation and the subsequent exchange of GDP for GTP.

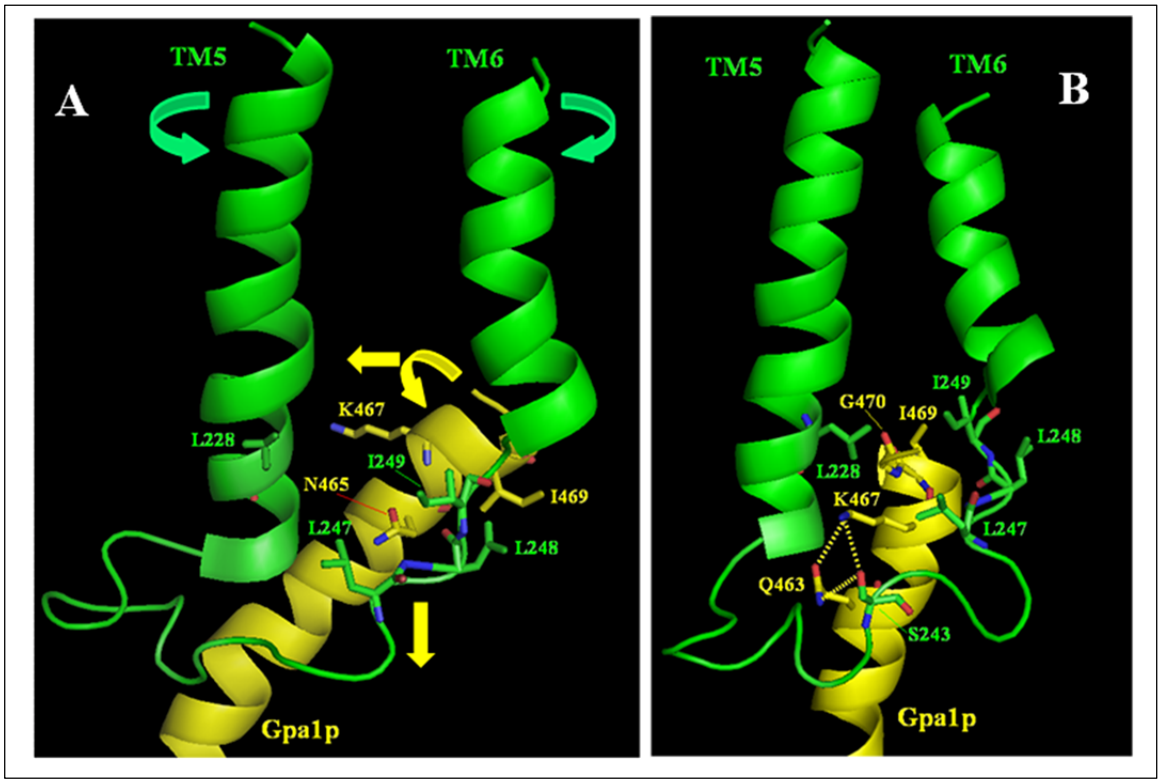

Figure 4.7 Proposed 3D model illustrating conformational changes in the cytoplasmic ends of TM5-TM6 from Ste2p and the C-terminus of Gpa1p during activation. Ste2p and Gpa1p residues are labeled green and blue, respectively. A

(inactive state): The C-terminus of Gpa1p is suggested to be closer to TM6 than TM5 in the inactive state. Upon α-factor binding changes occur at the cytoplasmic ends of TM5 and TM6. TM5 and TM6 are proposed to undergo rotation of ~30° in the anti-clockwise and clockwise directions, respectively (indicated by green arrows) The C-terminus of Gpa1p undergoes two possible changes (indicated by yellow arrows), an anti-clockwise rotation of ~90° and a withdrawal of ~5.0 Å (horizontal and vertical shifts) from the inner core of the receptor to the cytoplasmic end. B (active state): TM5 and TM6 are closer due to a shift in TM6 towards TM5 as observed in other GPCRs (*2, 43*). The C-terminus of Gpa1p is now closer to TM5 and withdrawn into the cytoplasmic surface of TM5-TM6. There are possible H-bond links between S243 of Step and Q463/K467 of Gpa1p.

Several studies have shown that GPCR activation results in conformational changes at the TM5-TM6 cytoplasmic ends that appear to be essential for G protein activation in all GPCRs (*2, 43-45*). In this study we propose that the conformational changes that occur at the TM5 and TM6 cytoplasmic ends induce rotational and translational movements at the C-terminus of the Gpa1p that results in withdrawal of the α5-helix of Gpa1p from Ste2p. The rotational and translational conformational changes are consistent with a proposed model for the transducin-opsin system (*20*). Although, further experimental work, such as identifying other residues in Ste2p and Gpa1p that are involved in these movements will be needed to refine the mechanism of activation, the information obtained in this study will serve as a platform for further understanding of GPCR-G protein interactions in other systems.

References for Part IV

1. Lundstrom, K. (2009) An overview on GPCRs and drug discovery: structure-based drug design and structural biology on GPCRs, *Methods Mol Biol 552*, 51-66.
2. Rosenbaum, D. M., Rasmussen, S. G., and Kobilka, B. K. (2009) The structure and function of G-protein-coupled receptors, *Nature 459*, 356-363.
3. Williams, C., and Hill, S. J. (2009) GPCR signaling: understanding the pathway to successful drug discovery, *Methods Mol Biol 552*, 39-50.
4. Worth, C. L., Kleinau, G., and Krause, G. (2009) Comparative sequence and structural analyses of G-protein-coupled receptor crystal structures and implications for molecular models, *PloS one 4*, e7011.
5. Wall, M. A., Coleman, D. E., Lee, E., Iniguez-Lluhi, J. A., Posner, B. A., Gilman, A. G., and Sprang, S. R. (1995) The structure of the G protein heterotrimer Gi alpha 1 beta 1 gamma 2, *Cell 83*, 1047-1058.
6. Lambright, D. G., Sondek, J., Bohm, A., Skiba, N. P., Hamm, H. E., and Sigler, P. B. (1996) The 2.0 A crystal structure of a heterotrimeric G protein, *Nature 379*, 311-319.
7. De Amici, M., Dallanoce, C., Holzgrabe, U., Trankle, C., and Mohr, K. (2010) Allosteric ligands for G protein-coupled receptors: a novel strategy with attractive therapeutic opportunities, *Medicinal research reviews 30*, 463-549.
8. Eglen, R. M., and Reisine, T. (2009) New insights into GPCR function: implications for HTS, *Methods Mol Biol 552*, 1-13.

9. Ratnala, V. R., and Kobilka, B. (2009) Understanding the ligand-receptor-G protein ternary complex for GPCR drug discovery, *Methods Mol Biol 552*, 67-77.

10. Naider, F., and Becker, J. M. (2004) The alpha-factor mating pheromone of Saccharomyces cerevisiae: a model for studying the interaction of peptide hormones and G protein-coupled receptors, *Peptides 25*, 1441-1463.

11. Eilers, M., Hornak, V., Smith, S. O., and Konopka, J. B. (2005) Comparison of class A and D G protein-coupled receptors: common features in structure and activation, *Biochemistry 44*, 8959-8975.

12. Minic, J., Sautel, M., Salesse, R., and Pajot-Augy, E. (2005) Yeast system as a screening tool for pharmacological assessment of g protein coupled receptors, *Current medicinal chemistry 12*, 961-969.

13. Dohlman, H. G. (2002) G proteins and pheromone signaling, *Annual review of physiology 64*, 129-152.

14. Clark, C. D., Palzkill, T., and Botstein, D. (1994) Systematic mutagenesis of the yeast mating pheromone receptor third intracellular loop, *The Journal of biological chemistry 269*, 8831-8841.

15. Stefan, C. J., and Blumer, K. J. (1994) The third cytoplasmic loop of a yeast G-protein-coupled receptor controls pathway activation, ligand discrimination, and receptor internalization, *Molecular and cellular biology 14*, 3339-3349.

16. Celic, A., Martin, N. P., Son, C. D., Becker, J. M., Naider, F., and Dumont, M. E. (2003) Sequences in the intracellular loops of the yeast pheromone receptor Ste2p required for G protein activation, *Biochemistry 42*, 3004-3017.

17. Gladue, D. P., and Konopka, J. B. (2008) Scanning mutagenesis of regions in the Galpha protein Gpa1 that are predicted to interact with yeast mating pheromone receptors, *FEMS yeast research 8*, 71-80.

18. Kallal, L., and Kurjan, J. (1997) Analysis of the receptor binding domain of Gpa1p, the G(alpha) subunit involved in the yeast pheromone response pathway, *Molecular and cellular biology 17*, 2897-2907.

19. Cabrera-Vera, T. M., Vanhauwe, J., Thomas, T. O., Medkova, M., Preininger, A., Mazzoni, M. R., and Hamm, H. E. (2003) Insights into G protein structure, function, and regulation, *Endocrine reviews 24*, 765-781.

20. Scheerer, P., Heck, M., Goede, A., Park, J. H., Choe, H. W., Ernst, O. P., Hofmann, K. P., and Hildebrand, P. W. (2009) Structural and kinetic modeling of an activating helix switch in the rhodopsin-transducin interface, *Proceedings of the National Academy of Sciences of the United States of America 106*, 10660-10665.

21. Oldham, W. M., Van Eps, N., Preininger, A. M., Hubbell, W. L., and Hamm, H. E. (2006) Mechanism of the receptor-catalyzed activation of heterotrimeric G proteins, *Nature structural & molecular biology 13*, 772-777.

22. Ramachandran, S., and Cerione, R. A. (2006) How GPCRs hit the switch, *Nature structural & molecular biology 13*, 756-757.

23. Hauser, M., Kauffman, S., Lee, B. K., Naider, F., and Becker, J. M. (2007) The first extracellular loop of the Saccharomyces cerevisiae G protein-coupled

receptor Ste2p undergoes a conformational change upon ligand binding, *The Journal of biological chemistry 282*, 10387-10397.

24. Huang, L. Y., Umanah, G., Hauser, M., Son, C., Arshava, B., Naider, F., and Becker, J. M. (2008) Unnatural amino acid replacement in a yeast G protein-coupled receptor in its native environment, *Biochemistry 47*, 5638-5648.

25. Gietz, D., St Jean, A., Woods, R. A., and Schiestl, R. H. (1992) Improved method for high efficiency transformation of intact yeast cells, *Nucleic acids research 20*, 1425.

26. Umanah, G. K., Son, C., Ding, F., Naider, F., and Becker, J. M. (2009) Cross-linking of a DOPA-containing peptide ligand into its G protein-coupled receptor, *Biochemistry 48*, 2033-2044.

27. Dosil, M., Giot, L., Davis, C., and Konopka, J. B. (1998) Dominant-negative mutations in the G-protein-coupled alpha-factor receptor map to the extracellular ends of the transmembrane segments, *Molecular and cellular biology 18*, 5981-5991.

28. Mumberg, D., Muller, R., and Funk, M. (1995) Yeast vectors for the controlled expression of heterologous proteins in different genetic backgrounds, *Gene 156*, 119-122.

29. David, N. E., Gee, M., Andersen, B., Naider, F., Thorner, J., and Stevens, R. C. (1997) Expression and purification of the Saccharomyces cerevisiae alpha-factor receptor (Ste2p), a 7-transmembrane-segment G protein-coupled receptor, *The Journal of biological chemistry 272*, 15553-15561.

30. Sherman, F. (2002) Getting started with yeast, *Methods in enzymology 350*, 3-41.

31. Slauch, J. M., Mahan, M. J., and Mekalanos, J. J. (1994) Measurement of transcriptional activity in pathogenic bacteria recovered directly from infected host tissue, *BioTechniques 16*, 641-644.

32. Jenness, D. D., and Spatrick, P. (1986) Down regulation of the alpha-factor pheromone receptor in S. cerevisiae, *Cell 46*, 345-353.

33. Wang, H. X., and Konopka, J. B. (2009) Identification of amino acids at two dimer interface regions of the alpha-factor receptor (Ste2), *Biochemistry 48*, 7132-7139.

34. Kelley, L. A., and Sternberg, M. J. (2009) Protein structure prediction on the Web: a case study using the Phyre server, *Nature protocols 4*, 363-371.

35. Song, J., and Dohlman, H. G. (1996) Partial constitutive activation of pheromone responses by a palmitoylation-site mutant of a G protein alpha subunit in yeast, *Biochemistry 35*, 14806-14817.

36. Kim, H., Lee, B. K., Naider, F., and Becker, J. M. (2009) Identification of specific transmembrane residues and ligand-induced interface changes involved in homo-dimer formation of a yeast G protein-coupled receptor, *Biochemistry 48*, 10976-10987.

37. Choi, Y., and Konopka, J. B. (2006) Accessibility of cysteine residues substituted into the cytoplasmic regions of the alpha-factor receptor identifies the intracellular residues that are available for G protein interaction, *Biochemistry 45*, 15310-15317.

38. Scheerer, P., Park, J. H., Hildebrand, P. W., Kim, Y. J., Krauss, N., Choe, H. W., Hofmann, K. P., and Ernst, O. P. (2008) Crystal structure of opsin in its G-protein-interacting conformation, *Nature 455*, 497-502.

39. Hirsch, J. P., Dietzel, C., and Kurjan, J. (1991) The carboxyl terminus of Scg1, the G alpha subunit involved in yeast mating, is implicated in interactions with the pheromone receptors, *Genes & development 5*, 467-474.

40. Hein, P., and Bunemann, M. (2009) Coupling mode of receptors and G proteins, *Naunyn-Schmiedeberg's archives of pharmacology 379*, 435-443.

41. Oldham, W. M., and Hamm, H. E. (2008) Heterotrimeric G protein activation by G-protein-coupled receptors, *Nature reviews. Molecular cell biology 9*, 60-71.

42. Herrmann, R., Heck, M., Henklein, P., Kleuss, C., Hofmann, K. P., and Ernst, O. P. (2004) Sequence of interactions in receptor-G protein coupling, *The Journal of biological chemistry 279*, 24283-24290.

43. Wess, J., Han, S. J., Kim, S. K., Jacobson, K. A., and Li, J. H. (2008) Conformational changes involved in G-protein-coupled-receptor activation, *Trends in pharmacological sciences 29*, 616-625.

44. Domazet, I., Martin, S. S., Holleran, B. J., Morin, M. E., Lacasse, P., Lavigne, P., Escher, E., Leduc, R., and Guillemette, G. (2009) The fifth transmembrane domain of angiotensin II Type 1 receptor participates in the formation of the ligand-binding pocket and undergoes a counterclockwise rotation upon receptor activation, *The Journal of biological chemistry 284*, 31953-31961.

45. Reynolds, K. A., Katritch, V., and Abagyan, R. (2009) Identifying conformational changes of the beta(2) adrenoceptor that enable accurate prediction of ligand/receptor interactions and screening for GPCR modulators, *Journal of computer-aided molecular design 23*, 273-288.

PART V

Crosslinking of an α-factor Analog [K^0(BioACA), K^7(DHPA), Nle^{12}]α-factor (Bio-$DHPA^7$ α-factor) into its G Protein-Coupled Receptor, Ste2p

Part V presents collaborative work with Dr. Fred Naider's laboratory at the City University of New York, Staten Island. Li-Yin Huang performed most of the work, George K. E. Umanah assisted with the biochemical studies, and the peptides used were obtained from Dr. Naider's laboratory.

Abstract for Part V

Fundamental knowledge about how G protein-coupled receptors and their ligands interact is important for understanding receptor-ligand binding and the development of new drug discovery strategies. We have used periodate-mediated crosslinking and matrix-assisted laser desorption/ionization (MALDI) spectrometric analyses to investigate the interaction of the center of the *Saccharomyces cerevisiae* tridecapeptide pheromone, α-factor (WHWLQLKPGQPMY), and Ste2p, its cognate G protein-coupled receptor. Chemically synthesized [Lys^0(BioACA),Lys^7(DHPA),Nle^{12}]α-factor with a 3,4-dihydroxyphenylacetyl (DHPA) attaching to lysine at position 7 (Bio-$DHPA^7$ α-factor) was used to bind with Ste2p. Even though bio-$DHPA^7$ α-factor exhibited about 40-fold decrease in binding affinity with Ste2p, it was able to activate growth arrest in yeast cell. Bio-$DHPA^7$ α- factor was crosslinked with Ste2p as demonstrated by Western blot analysis using NeutrAvidin-HRP conjugates to detect Bio-$DHPA^7$ α-factor and Ste2p crosslinked product. Ste2p-ligand crosslinked complex was purified with His affinity resin to pull down Ste2p that has a His tag at the C-terminus and with Avidin beads to capture Bio-$DHPA^7$ α- factor. After cyanogen bromide digestion, a crosslinked fragment at the size of ~13 kDa was detected in Western blot probed with NeutrAvidin-HRP and also in MALDI-TOF mass spectrum. The result of chemical crosslinking suggests that Bio-$DHPA^7$ α-factor interacts with transmembrane domain 2 to 3 flanking extracellular loop 1 (TM2-EL1-TM3) region. Site-directed mutagenesis at this region is currently being carried out to identify the exact crosslinked residue of Ste2p with DHPA7 α-factor.

This is the first study to investigate the interacting residues between Ste2p and position 7 of α-factor.

Chapter 1

Introduction

G protein-coupled receptors (GPCR) are composed of a superfamily of membrane proteins that have a common structure of seven transmembrane domains. The superfamily is divided into 6 groups (rhodopsin-like GPCRs, secretin receptor family GPCRs, metabotropic glutamate GPCRs, fungal mating pheromone receptors, cyclic AMP receptors, and Frizzled/Smoothened) based on the sequence homology and functional similarity (*1*). The human genome encodes about 800-1000 GPCRs which mediate a variety of signal transduction pathways (*2*), such as light, odorants, hormone, and small molecule neurotransmitters. About 50% of the current medicines and 25% of the top 100 best-selling drugs target GPCRs (*3*). Knowledge of GPCR structures, including how they interact with their ligands and how they are activated, is an important component aiding the development of novel drugs (*4*).

Understanding the interaction between ligands and their cognate GPCRs is necessary for designing analogues useful in therapy of many human disorders. Using Ste2p as a model to understand GPCR structure, the Konopka lab has shown by random mutagenesis that residues near the extracellular ends of the transmembrane domains are important for ligand binding and Ste2p activation (*5, 6*). According to the results of site-directed mutagenesis in the Becker lab, several residues (S47, T48, T50, L102, F204, N205, Y266, L276, and A280) at transmembrane domains of Ste2p have been identified to be important for ligand binding and receptor activation (*7, 8*). In order to determine direct contact points between α-factor and Ste2p, chemical (DOPA) and photoaffinity

(Bpa) crosslinkers were used to label the ligand and capture the receptor. During α-factor binding, a tryptophan at the N-terminus of α-factor is in close proximity to the Lys^{269} side chain near the extracellular surface of the TM6-TM7 bundle of Ste2p (*9, 10*). A tyrosine at the C-terminus of α-factor is likely to interact with Arg^{58} and Cys^{59} at transmembrane domain 1 of Ste2p (*11, 12*). A conclusion of these studies was that the chemical crosslinker 3,4-dihydroxyphenylalanine (DOPA) is apparently more specific in generating covalent linkage with specific residues of the receptor, which can be applied to indetify the exact contact residues between DOPA-labeled peptide and the receptor.

Here, to indentify binding sites between α-factor and Ste2p, we used 3,4-dihydroxyphenylacetyl (DHPA) as a crosslinker to label lysine residue in position 7 of α-factor to create [K^0(BioACA), K^7(DHPA), Nle^{12}]α-factor (Bio-$DHPA^7$-α-factor). DHPA is similar to DOPA in that both contain the dihydroxyphenyl moiety involved in chemical activation and crosslinking. DOPA was used as a replacement for an amino acid in α-factor in previous studies, wheareas DHPA was linked to the epsilon-amine of Lys^7 of α-factor in the present study. Bio-$DHPA^7$-α-factor was able to bind with Ste2p and activate downstream cellular responses. After His-tag (for purification of tagged Ste2p) purification and cyanogen bromide digestion, avidin (to capture any biotinylated peptide) purification was performed to capture crosslinked α-factor and Ste2p, and a 10-15 kDa crosslinked fragment containing biotin and DHPA was identified. MALDI-TOF mass spectrometric analysis confirmed the digested fragment, which suggests that Bio-$DHPA^7$-α-factor formed a covalent cross-linkage with the residue at the boundary of transmembrane 2 and 3 flanking extracellular loop 1 (TM2-EL1-TM3).

Chapter 2

Materials and Methods

Media, Reagents, Strains and Plasmids

Saccharomyces cerevisiae strain LM102 [*MATa, bar1, his4, leu2, trp1, met1, ura3, FUS1-lacZ::URA3, ste2Δ* (*13*)] was used for growth arrest and binding assays and protease deficient strain BJS21 [*MATa, prc1-407 prb1-1122 pep4-3 leu2 trp1 ura3-52 ste2::Kan*^{R} (*14*)] was used for protein isolation and immunoblot analysis. The plasmid pBEC1 containing C-terminal FLAG and His tagged *STE2* (*13*) was transformed by the method of Geitz (*15*) into LM102 and BJS21 cells. Transformants were selected by growth on yeast media (*16*) lacking tryptophan (designated as MLT) to maintain selection for the plasmid. The Cells were cultured in MLT and grown to mid-log phase at 30°C with shaking (200 rpm) for all assays. The tridecapeptide pheromone α-factor analog [(BioACA)-Lys^0 (3,4-dihydroxyphenylacetyl)-Lys^7, Nle^{12}] (designated Bio-DHPA^7 α-factor) was synthesized using automated solid-phase peptide synthesis and purified by reverse-phase high-performance liquid chromatography (HPLC) to greater than 99% homogeneity. All protected amino reagents were purchased from Advanced Chem Tech (Louisville, KY) and all solvents and reagents were of the highest purity available.

Mass Spectrometric Analysis of Peptides

For matrix-assisted laser-desorption ionization (MALDI) analysis the peptides were resuspended in 50:50 water-acetonitrile with 0.1% trifluoroacetic acid (TFA) at a final concentration of 0.1μg/μl. A 20mg/ml α-cyano-4-hydroxy-trans-cinnamic acid [(α-

ACHA), Sigma/Aldrich Chemical Company, St. Louis, MO] matrix was prepared by dissolving recrystallized α-ACHA in 50:50 water-acetonitrile with 0.1% TFA. An equal volume (0.5 µl) of peptide solution was mixed with matrix before spotting on the MALDI plate. The MADLI-TOF spectra were acquired on a Bruker Daltonics (Boston, MA) Microflex using the reflector methods.

Growth Arrest Assays

LM102 cells expressing C-terminal FLAG and His tagged Ste2p were grown at 30ºC in MLT, harvested, washed three times with water and resuspended at a final concentration of 5 x 10^6 cells/ml (*14*). Cells (1 ml) were combined with 3.5 ml agar noble (1.1%) and poured as a top agar lawn onto MLT medium agar plate. Filter disks (BD, Franklin Lakes, NJ) impregnated with α-factor or various α-factor analogs were placed on the top agar. The plates were incubated at 30ºC for 18 hours and then observed for clear halos around the discs. The experiment was repeated at least three times.

Binding Competition Assays

This assay was performed using LM102 cells expressing C-terminal FLAG and His tagged Ste2p. Tritiated [^{3}H]-α-factor (10.2 Ci/mmol, 12 µM) prepared as previously described (*14, 17*) was used in competition binding assays on whole cells. The cells were grown at 30ºC in MLT, harvested, washed three times with YM1 [0.5 M potassium phosphate (pH 6.24) containing 10 mM TAME, 10 mM sodium azide, 10 mM potassium fluoride, and 1% BSA] and adjusted to a final concentration of 2 x 10^7 cells per ml in

YM1 plus protease inhibitors [YM1i] (*18*). For competition binding studies, cells (600 µl) were combined with 150 µl of ice cold YM1i supplemented with 6 nM [^{3}H]α-factor in the presence or absence α-factor analogs and incubated at room temperature for 30 minutes. The final concentrations of α-factor analogs ranged from 0.5 x 10^{-10} to 1 x 10^{-6} M. After incubation, triplicate aliquots of 200 µl samples were filtered and washed over glass fiber filter mats using the Standard Cell Harvester (Skatron Instruments, Sterling, VA) and placed in scintillation vials. The radioactivity [^{3}H] on the filter was counted by liquid scintillation spectroscopy. The binding data were analyzed by non-linear regression analysis for one-site competition binding using Prism software (GraphPad Software, San Diego, CA) to determine the binding affinity (K_d) for each peptide. The *Ki* values were calculated by using the equation of Cheng and Prusoff, where $Ki = EC50 / (1 + [ligand] / K_d)$ (*7*).

DHPA Chemical Crosslinking

BJS21 cells expressing C-terminal FLAG and His tagged Ste2p were grown and total cell membranes were isolated as previously described (*14*). Protein concentration was determined by BioRad (BioRad, Hercules, CA) protein assay (*13*). The membranes were re-suspended in NEBuffer [20 mM HEPES, pH 7.9, 20% glycerol, 100 mM KCl, 12.5 mM EDTA, 0.5 mM DTT (*19*)] incubated with Bio-DHPA^7 α-factor analog (1 µM) in the presence or absence of 100 µM α-factor (WHWLQLKPGQPNle^{12}Y) for 120 minutes at 4°C. For periodate mediated crosslinking, a final concentration of 1.0 mM $NaIO_4$ was added to the mixture and incubated for 2 minutes. A final concentration of

100 mM DTT (1,4-Dithiothreitol) was used to quench the reaction (*19*). The cross-linked membranes were washed three times with CAPS buffer [Ncyclohexyl-3-aminopropanesulfonic acid (Sigma, St. Louis, MO.), 10 mM, pH 10] by centrifugation to remove non-bound Bio-DHPA^7 α-factor. The washed crosslinked samples were fractionated by SDS-PAGE and then transferred to immunoblots. The blots were probed with an antibody directed against the FLAG tag at C-terminal of Ste2p and with NeutrAvidin-HRP conjugate (Pierce, Rockford, IL) to detect biotin tag on Bio-DHPA^7 pheromone covalently linked to Ste2p. The signal generated were analyzed using Quantity One software (Version 4.5.1) on a Chemi-Doc XRS photodocumentation system (BioRad, Hercules, CA).

Purification of Intact Crosslinked Ste2p

Crosslinked Ste2p was enriched using His-Select^{TM} HC-Nickel affinity gel (Sigma/Aldrich Chemical Co., St. Louis, MO) following the manufacturer's directions. Approximately 10 mg cell membrane containing crosslinked Ste2p were resuspended in ice-cold solubilization buffer (50 mM Tris HCl, pH 7.4, 150 mM NaCl, 1% Triton X-100) with protease inhibitors (PMSF, pepstatin A and leupeptin) and incubated overnight at 4ºC with end-over-end mixing, then centrifuged at 15,000 x g for 30 minutes to remove non-soluble material. The solubilized proteins were then mixed with His-Nickel resin and incubated at 4ºC with end-over-end mixing for 1 hour. The resin was collected by centrifugation at low speed (500 x g, 1 minute) and resuspended and collected four times in wash buffer (50 mM sodium phosphate, pH 8.0, 0.3 M sodium chloride, and 5 mM

imidazole). Ste2p was eluted by resuspending the resin in 1 ml ice-cold elution buffer (50 mM sodium phosphate, pH 8.0, 0.3 M sodium chloride, and 250 mM imidazole) and incubated at 4ºC with end-over-end mixing for 10 minutes. The resin was pelleted by centrifugation (2000 x g, 1 minute) and the supernatant, containing eluted Ste2p, transferred to a fresh tube. The samples were analyzed by immunoblotting using an antibody directed against the FLAG tag at C-terminal of Ste2p and with Neutravidin-HRP conjugate to detect the biotin tag on the DHPA peptide covalently linked to Ste2p.

Digestion of Crosslinked Ste2p

Crosslinked Ste2p samples eluted from the His-Nickel resin were digested with cyanogen bromide (CNBr). The eluted samples containing Ste2p (~20 μg) were dried by vacuum centrifugation (Thermo Scientific, Waltham, MA) then dissolved in 100% trifluoroacetic acid (TFA) containing 10 mg/ml CNBr. Deionized distilled water (ddH2O) was then added to adjust the final TFA concentration to 80%, and the samples were incubated at 37°C in the dark for 18 hours (*14, 20*). The samples were dried by vacuum centrifugation and washed three times with ddH2O, and then 1 M Tris-HCl (pH 8.0) was added to neutralize the acidic mixture.

Purification of Crosslinked Ste2p Fragments

After CNBr digestion, crosslinked Ste2p fragments were resuspended in PBS buffer (0.1 M sodium phosphate, 0.15 M sodium chloride; pH 7.0), mixed with NeutrAvidin resin (Pierce Thermo Scientific, Rockford, IL,USA) and incubated for 6

hours at 4ºC with end-over-end mixing (*21*). The resin was collected by centrifugation at low speed (1000 x g, 1 minute) and washed four times in PBS buffer. Crosslinked Ste2p fragments were eluted by resuspending the resin in 200 µl ice cold elution buffer (0.1 M glycine, pH 2.5) and incubating at 4ºC with end-over-end mixing for 5 minutes. The resin was pelleted by centrifugation (2000 x g, 1 minute) and the supernatant, containing the eluted crosslinked Ste2p fragments, transferred to a fresh tube containing 20 µl of TBS (0.5 M Tris HCl, pH 7.4, 1.5 M NaCl).

MALDI-TOF Analysis of Crosslinked Peptides

The eluted samples from the avidin resin were further washed and concentrated using a pipette with C18 chromatographic media (ZipTipC18 pipette tips; Millipore Corporation, Billerica, MA) following the manufacturer's directions and resuspended in 60% acetonitrile 40% water (0.1% TFA). For MALDI-TOF analysis α-CHCA [20 mg/ml (in 50:50 acetoneisopropanol)] was used as the matrix. The samples (0.5 µl), were either mixed with 0.5 µL of matrix before spotting on the target or 1.0 µl of matrix was spotted and allowed to dry before applying 1.0 µL of samples (*14*). MALDI-TOF spectra were acquired on a Bruker Daltonics Microflex using the reflector method. Masses were calculated using PROWL peptide mass prediction tools (*22*) and also based on the chemistry of the DHPA cross-linking (*19*).

Chapter 3

Results

Synthesis and Characterization of Bio-DHPA^7 α-factor

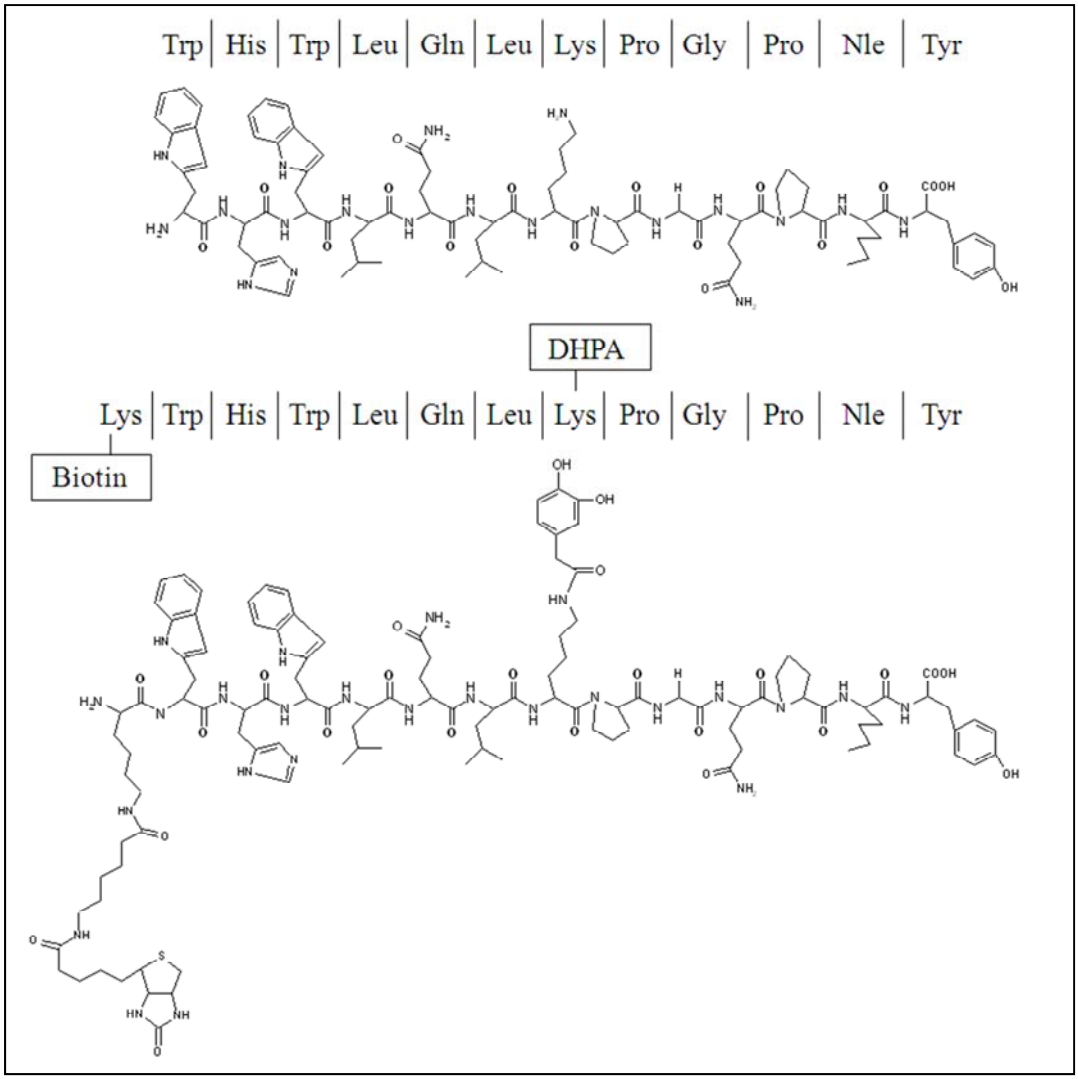

Figure 5.1 Structures of α-factor and Bio-DHPA^7 analogue. Biotin (Bio) is conjugated through its carboxyl group to the ε–amine of Lys^1 using aminocaproate as a linker and 3,4-dihydroxyphenylacetyl (DHPA) is attached to Lys^7 residue to form [K^0(BioACA), K^7(DHPA), Nle^{12}]α-factor (Bio-DHPA^7 α-factor) analogue of α-factor.

The synthesis of α-factor analogs containing 3,4-dihydroxyphenylacetyl (DHPA) was carried out by automated solid phase synthesis using standard coupling and deprotection protocols (*10*, *12*). Fmoc protected peptide was obtained in high yield and purity and was used in the hydroxysuccinimiude mediated addition of biotinylamido caproate (*9*). The final peptides used in bioassays and cross-linking studies were virtually homogeneous as judged by gradient HPLC and had the expected molecular weights. The structures of α-factor and Bio-DHPA[7] analogue are shown in Figure 5.1; MALDI-TOF analyses and MS/MS spectra are shown in Figure 5.2. Observed mass of the peptides as determined by MALDI-TOF were similar to masses predicted by the PROWL peptide mass prediction tools (*23*).

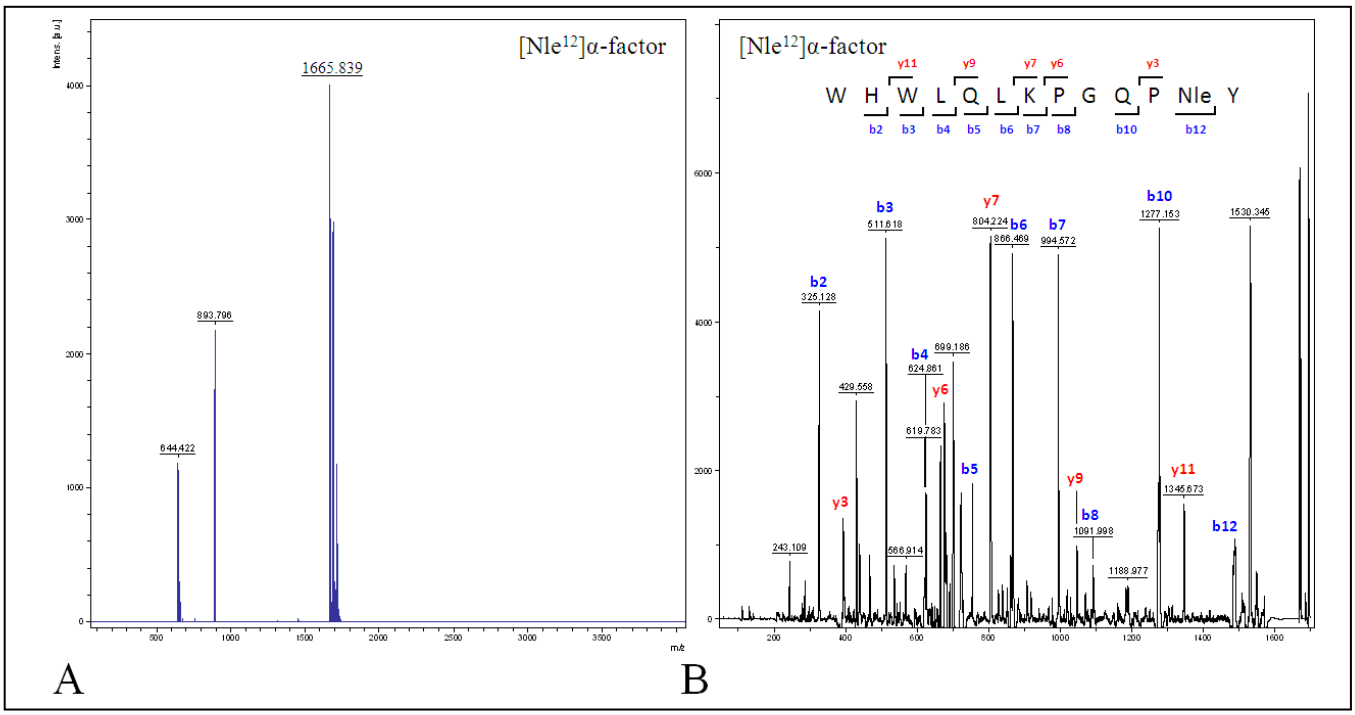

Figure 5.2 Mass spectrometric analysis and MALDI post-source decay spectra of α-factor and Bio-DHPA[7] analog. (Continued on next page)

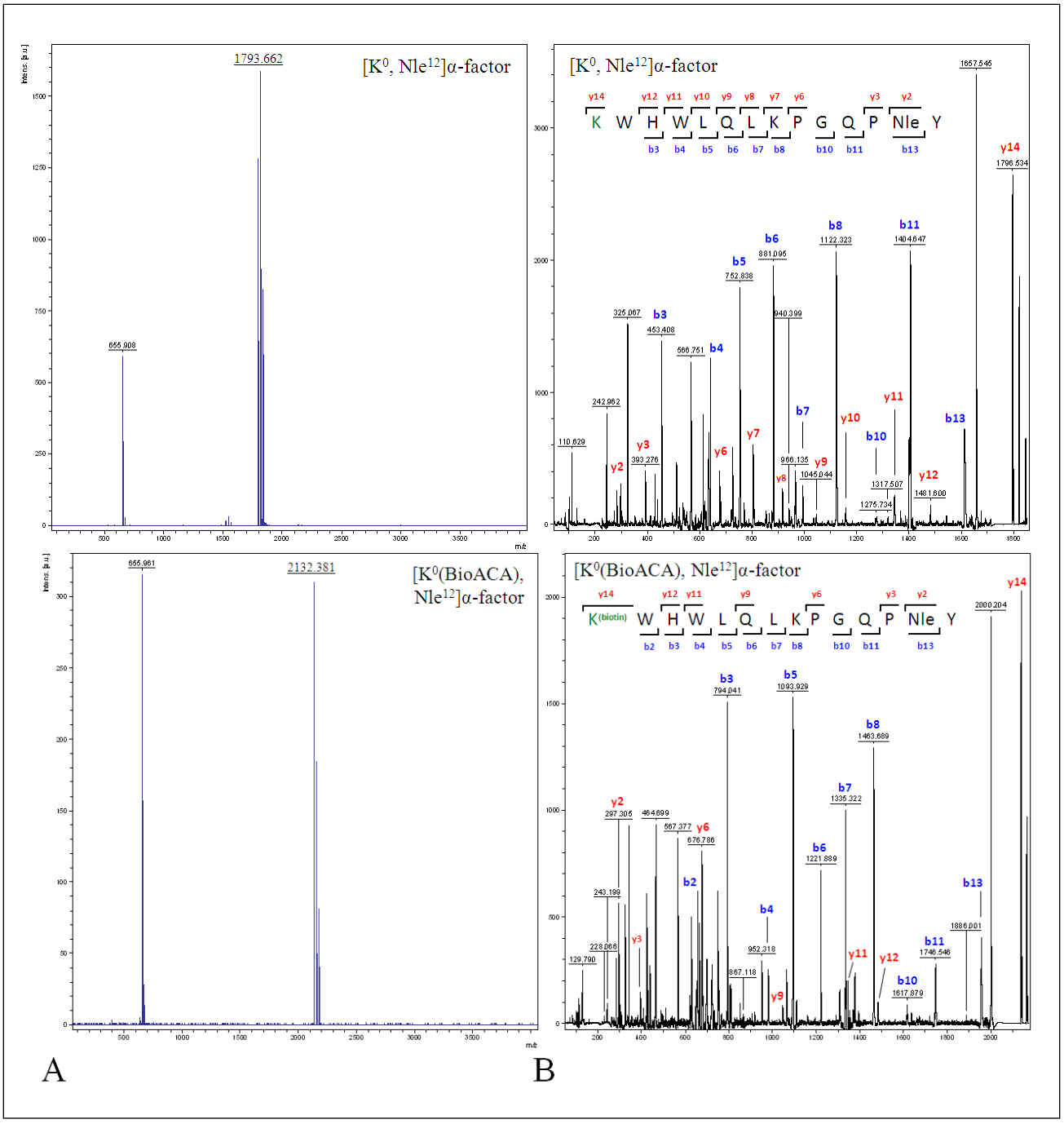

Figure 5.2 Mass spectrometric analysis and MALDI post-source decay spectra of α-factor and Bio-DHPA[7] analog. Panel A (left): Observed masses of the peptides determined by MALDI-TOF. Panel B (right): MALDI post-source decay spectra. (Continued on next page)

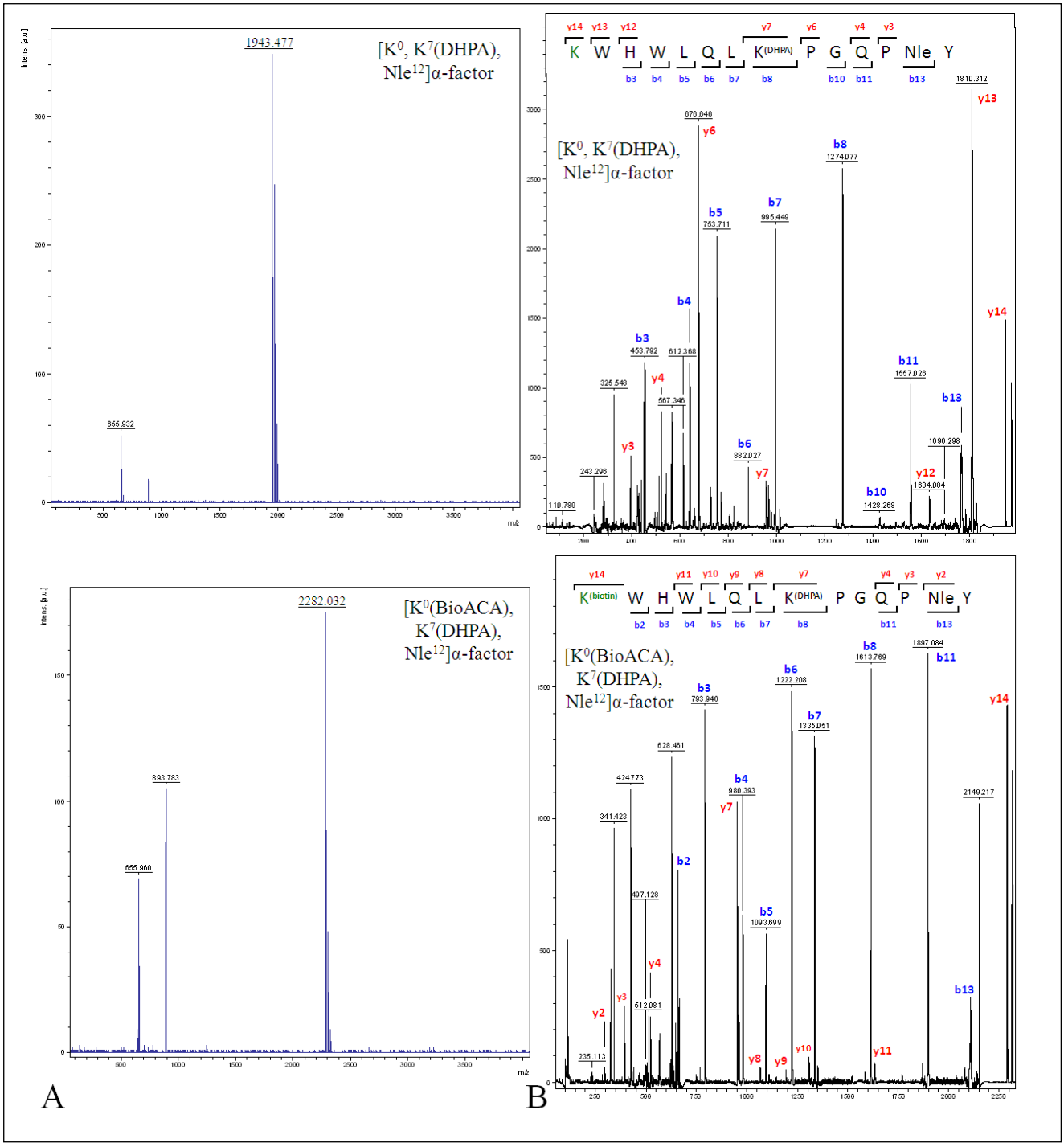

Figure 5.2 Mass spectrometric analysis and MALDI post-source decay spectra of α-factor and Bio-DHPA^7 analog. Panel A (left): Observed masses of the peptides as determined by MALDI-TOF were similar to masses predicted by PROWL peptide mass

prediction tools (*22*): [Nle^{12}]α-factor 1665.96 Da, [K^0, Nle^{12}]α-factor 1794.15 Da, [K^0(BioACA), Nle^{12}]α-factor 2133.61 Da, [K^0, K^7(DHPA), Nle^{12}]α-factor 1944.34 Da, and [K^0(BioACA), K^7(DHPA), Nle^{12}]α-factor 2283.74 Da. Panel B (right): One-letter inserts are abbreviations of amino acid residues. Peptides and spectra are labeled with identified *y* and *b* ion types.

A total of four α-factor analogues were synthesized: [K^0, Nle^{12}]α-factor has a lysine added at the N-terminus of α-factor (position 0), [K^0(BioACA), Nle^{12}]α-factor has a biotin added to the lysine at position 0, [K^0, K^7(DHPA), Nle^{12}]α-factor has lysine at position 0 and dihydroxyphenylacetyl (DHPA) attached to the lysine at position 7, and [K^0(BioACA), K^7(DHPA), Nle^{12}]α-factor (Bio-$DHPA^7$ α-factor) has biotin labeling on the lysine at position 0 and DHPA attached to the lysine at position 7. MALDI-TOF Mass spectrometry was used to determine molecular mass of α-factor analogues (Figure 5.2). According to mass spectra, [K^0, Nle^{12}]α-factor showed a monoisotopic peak at 1793.662 Da (predicted 1794.15 Da), [K^0(BioACA), Nle^{12}]α-factor showed a peak at 2132.381 Da (predicted 2133.61 Da), [K^0, K^7(DHPA), Nle^{12}]α-factor showed a peak at 1943.477 Da (predicted 1944.34 Da), and [K^0(BioACA), K^7(DHPA), Nle^{12}]α-factor showed a peak at 2282.032 Da (predicted 2283.74 Da). Some of the peptides showed more than one peak, which might be due to impurities in the samples. FAST program in MALDI-TOF was used for further fragmentation and detailed mapping of peptide sequence. Ionized fragments matched the sequence of α-factor analogues (Figure 5.2).

Binding and Bioactivity of Bio-DHPA^7 α-factor

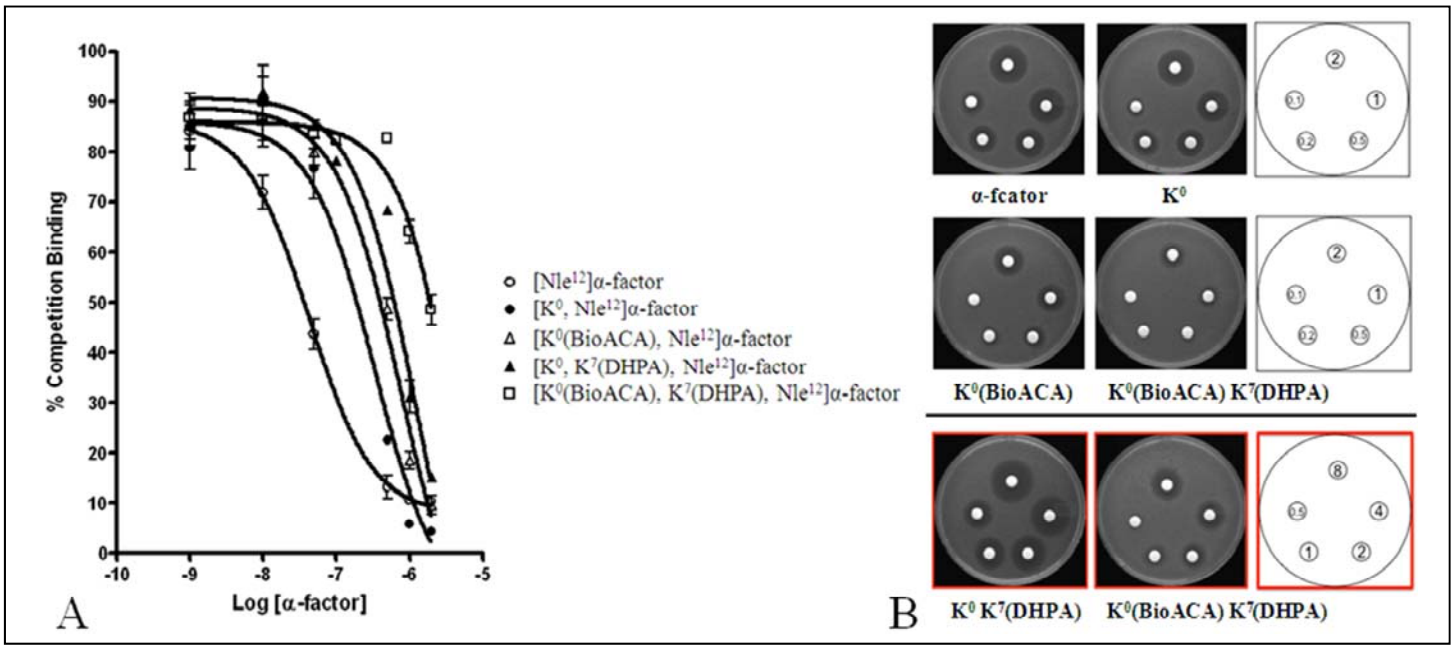

Figure 5.3 Binding and bioactivity of α-factor analogues. A: Binding ability of the peptides was determined by competition binding with [^{3}H]-labelled α-factor for Ste2p. B: Growth arrest assay was used to check activation of Ste2p signaling pathway.

A competition binding assay was performed to determine the binding affinity of α-factor analogues (Figure 5.3A). The modification and addition of lysine, biotin, and DHPA on α-factor decreased binding affinity of the peptides so a shift toward higher concentrations was observed for competition, due to lower binding efficacy of Bio-DHPA^7 α-factor. The growth arrest assay was performed to check biological activity of α-factor analogues. As shown in Figure 5.3B, Bio-DHPA^7 α-factor formed smaller halos when compared with α-factor. When the concentration of peptide was increased by 4 fold, distinct halos were observed. When compared with α-factor, attachment of DHPA

at Lys^{7} decreased binding affinity 30 fold and biological activity by 50%; whereas the addition of biotin decreased binding affinity 18 fold and biological activity by 75%. Through competition binding and halo assay, we know that Bio-DHPA^{7} α-factor is able to bind and activate Ste2p signaling pathway, even though the binding affinity is lower than that of α-factor.

Bio-DHPA^{7} α-factor Crosslink into Ste2p

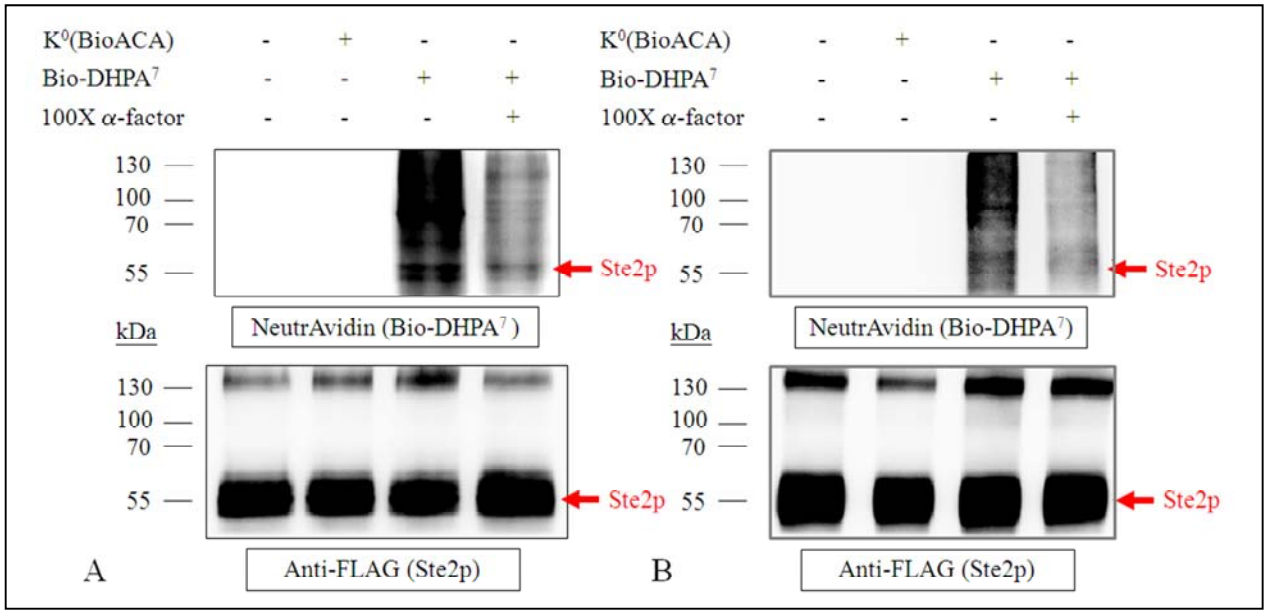

Figure 5.4 Western blot analysis of Bio-DHPA^{7} α-factor crosslinked with Ste2p. Crosslinked product of Bio-DHPA^{7} α-factor and Ste2p appeared before (A) and after (B) His-Nickle purification on western blots probed with NeutrAvidin-HRP conjugate (upper panels). K^{0}(BioACA) α-factor was used as a negative control for crosslinking; an excess amount of α-factor was used to compete with the crosslinking of Bio-DHPA^{7} α-factor.

Western blots at lower panels were probed with FLAG antibody to show total loading of Ste2p.

Since Bio-DHPA^7 α-factor was able to bind Ste2p and activate the signaling pathway, chemical crosslinking with $NaIO_4$ was carried out in the presence of DHPA peptide (10 μM) and Ste2p membrane protein (500 μg). As shown in Figure 5.4A, Bio-DHPA^7 α-factor was crosslinked with Ste2p, and the signal was decreased in the presence of excess α-factor (1 mM), which means the crosslinking is specific for binding pocket of Ste2p. Notably, when Bio-DHPA^7 α-factor was used as a negative control for crosslinking, it showed no signal in NeutrAvidin Western blot, which proves that $NaIO_4$ crosslinking is very specific to DHPA side chain. After crosslinked samples were purified with His-Nickel resin, background signal was reduced and Ste2p-DHPA α-factor crosslink became more distinct (Figure 5.4B). Non-specific background signal can be further reduced by using less peptide in the crosslinking reaction or by more diluted primary antibody (NeutrAvidin-HRP) for immunoblot analysis (data not shown).

In order to identify a specific Ste2p residue that crosslinked with Bio-DHPA^7 α-factor, binding with Bio-DHPA^7 α-factor (20 μM) on a large scale membrane preparation (10 mg) was performed to enrich crosslinked product for His-Nickel and NeutrAvidin purification and cyanogen bromide (CNBr) digestion. Crosslinked product was purified separately with His-Nickel resin to pull down Ste2p by its His tag at the C-terminal and with NeutrAvidin resin to capture Bio-DHPA^7 α-factor. After His-Nickel purification, a distinct band representing Ste2p appeared at approximate 55 kDa position in a Western

blot probed with FLAG antibody (Figure 5.5). The same band at 55 kDa also showed up when the Western blot was probed with NeutrAvidin-HRP conjugate, which suggested that the band is a crosslinked product of Ste2p and Bio-DHPA^7 α-factor. Furthermore, after NeutrAvidin purification, a distinct band also showed up at the size corresponding to Ste2p when Western blot was probed with NeutrAvidin. The same band appeared in anti-FLAG Western blot as well, which indicated the crosslinked product of Bio-DHPA^7 α-factor and Ste2p was purified.

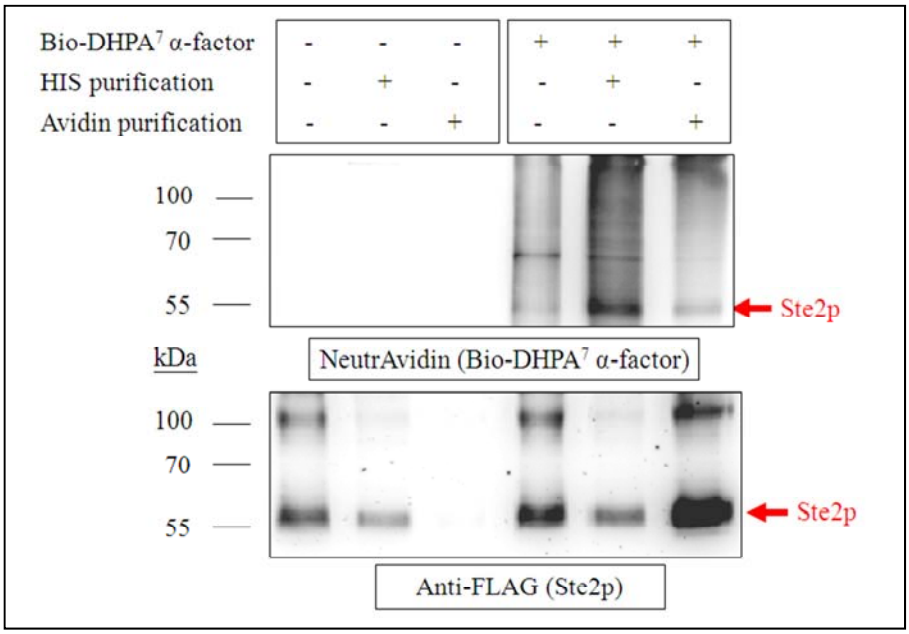

Figure 5.5 Western blot analysis of Bio-DHPA^7 α-factor and Ste2p crosslink after His-Nickel and NeutrAvidin purification. After treatment with 1 mM $NaIO_4$, crosslinked samples were lysed and purified with His-Nickel and NeutrAvidin resins. Eluted protein were separated in SDS-PAGE for Western blot analysis probed with NeutrAvidin-HRP conjugate and FLAG antibody.

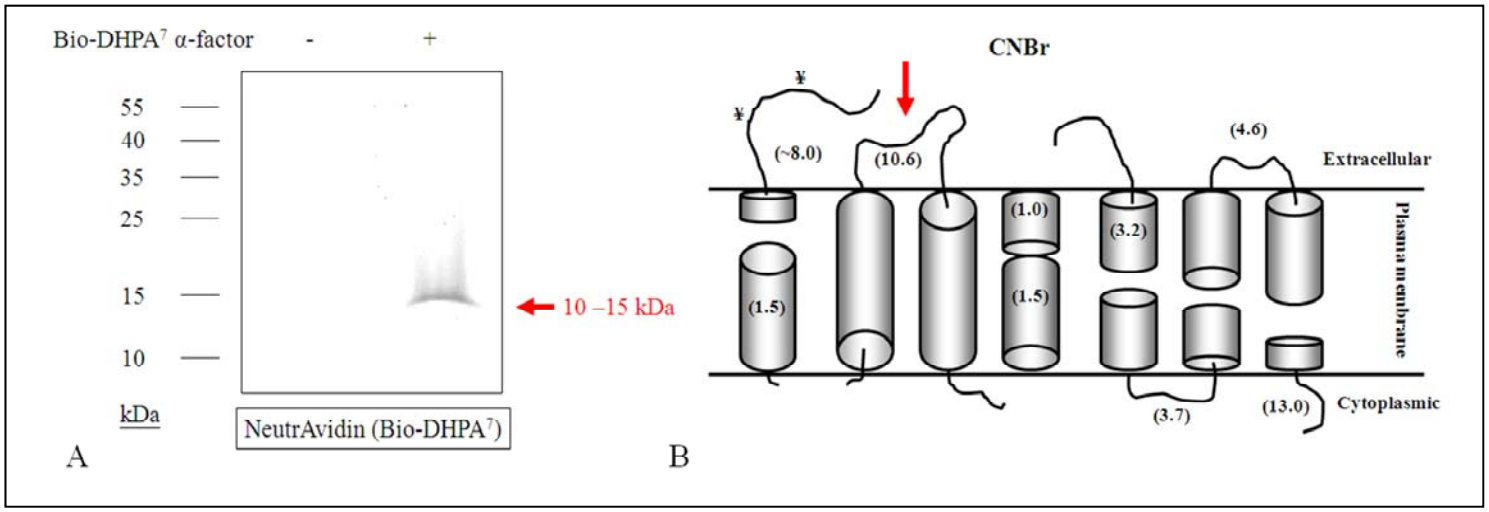

Figure 5.6 Western blot analysis of purified Bio-DHPA^7 α-factor and Ste2p crosslink after cyanogen bromide digestion. His-Nickel and NeutrAvidin purified Bio-DHPA^7 α-factor and Ste2p crosslink was subjected to cyanogen bromide digestion. Digested peptide was then separated in SDS-PAGE for Western blot analysis and probed with NeutrAvidin-HRP (A). Cyanogen bromide cut at methionine residues of Ste2p and generates eight digested fragments (B).

After His-Nickel and NeutrAvidin purification, cyanogen bromide (CNBr) was then used to digest the crosslinked product of Bio-DHPA^7 α-factor and Ste2p. CNBr hydrolyzes peptide bonds at the C-terminus of methionine residues and generated eight digested fragments of Ste2p. Digested sample was then separated in SDS-PAGE for Western blot analysis. After probing with NeutrAvidin-HRP (Figure 5.6A), a crosslinked fragment appeared at the size between 10-15 kDa. Therefore, according to the predicted digestion of Ste2p (Figure 5.6B), transmembrane domain 2-extracellular loop 1-transmembrane domain 3 (TM2-EL1-TM3) (~10.6 kDa) is very likely to be the fragment

that interacts with Bio-DHPA^{7} α-factor (~2 kDa). Matrix-assisted laser desorption/ionization (MALDI) mass spectrometric analysis was performed to ionize the fragment and generate a monoisotopic spectrum (Figure 5.7). A peak appeared at mass-to-charge ratio (m/z) of 12404.046, which is close to the expected size of the crosslinked fragment.

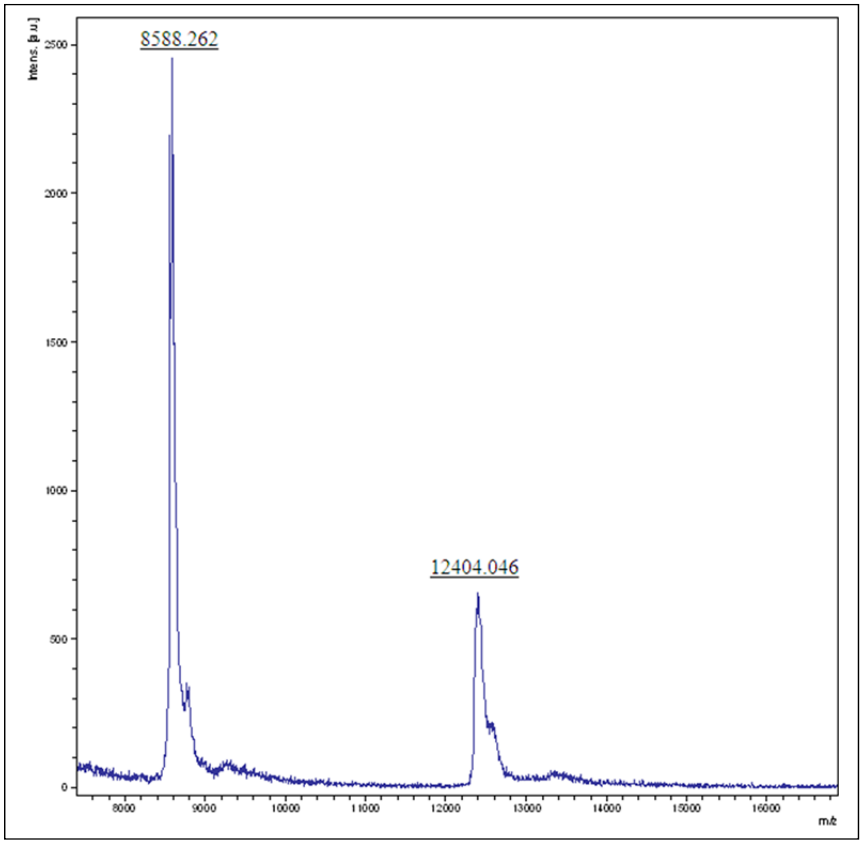

Figure 5.7 Mass spectrum of MALDI-TOF analysis for crosslinked fragment of Bio-DHPA^{7} α-factor and Ste2p. Crosslinked product of Bio-DHPA^{7} α-factor and Ste2p was purified with His-Nickel and NeutrAvidin resins and digested with cyanogen bromide. Expected molecular mass is at 12895.232 Da and the monoisotopic peak appeared at 12404.046 (m/z).

Because DHPA forms crosslinked complex with certain favored amino acids (cysteine, lysine, histidine) when they are in close proximity, according to the protein sequence of Ste2p, there are six residues (K^{77}, H^{94}, K^{100}, H^{126}, K^{151}, and K^{160}) in TM2-EL1-TM3 that would be favored to interact with Bio-DHPA^{7} α-factor (Figure 5.8). Among the six residues, H^{94}, K^{100}, and H^{126} are more likely to be near the binding pocket of Ste2p because they are either close to the transmembrane domain or in the extracellular loop. Therefore, site-directed mutagenesis of K^{100} and H^{126} was carried out. We constructed two alanine mutants (K100A and H126A). The results indicated, however, that these mutants still crosslinked with Bio-DHPA^{7} α-factor. Mutation at the other residues is required to determine the exact binding site and tandem mass spectrometry (MS/MS) may be a better alternative to identify crosslinked residue.

Chapter 4

Discussion

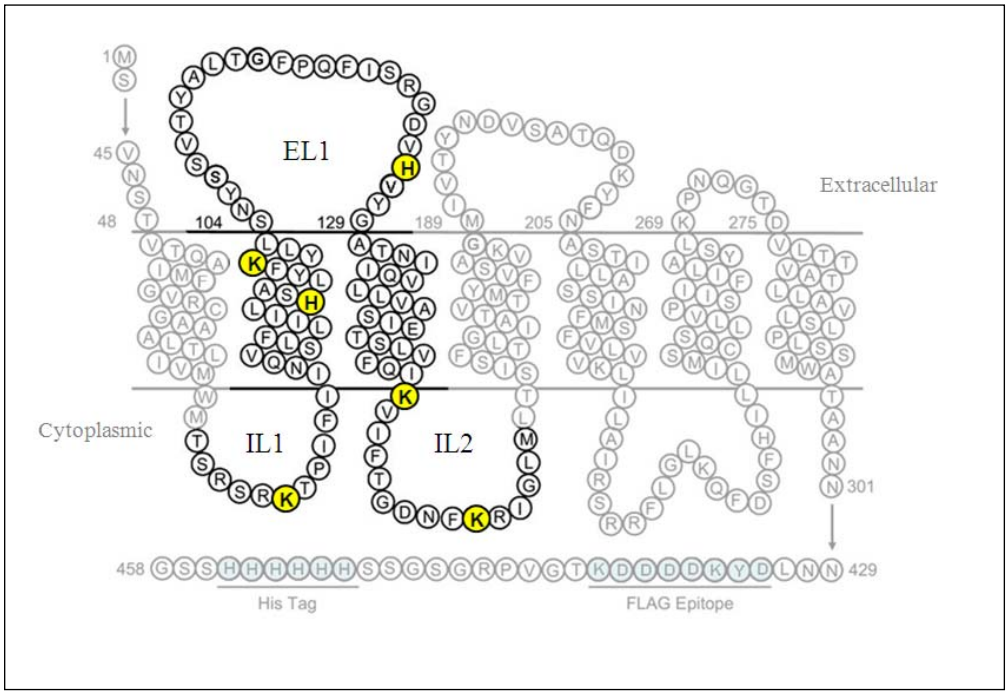

Figure 5.8 Diagram of Ste2p. The residues from intracellular loop 1 (IL1) to intracellular loop 2 (IL2) was highlighted. Six residues (K^{77}, H^{94}, K^{100}, H^{126}, K^{151}, and K^{160}) in TM2-EL1-TM3 region are the candidates to interact with Bio-DHPA^{7} α-factor.

Labeling the ligand with DOPA (3,4-dihydroxyphenylalanine) to serve as a crosslinker has been used to identify interacting residues of Ste2p with the N-terminal and C-terminal ends of α-factor (*10, 12*). This is the first study to use a DOPA-like compound, DHPA (3,4-dihydroxyphenylacetyl), as a crosslinker to investigate whether lysine at the center (seventh amino acid) of the ligand binds with Ste2p. DOPA and DHPA share the dihydroxyl ring, which can be oxidized by $NaIO_4$ to form an *ortho*-

quinone intermediate. This activated product has the tendency to react with the side chain of cysteine, histidine, and lysine (*24*) and therefore can be used to map peptide ligand-protein interaction. According to the results presented, adding DHPA to the epsilon-amine of the lysine residue at position 7 of α-factor decreased binding affinity of the peptide about 30 fold. However, with an adequate amount of Bio-DHPA^{7} α-factor present in the binding reaction, it was able to compete with the binding of α-factor, and Bio-DHPA^{7} α-factor triggered downstream growth arrest activity, even though the halos were smaller than those formed in the presence of α-factor. Therefore, we conclude that Bio-DHPA^{7} α-factor is likely to interact with the same binding pocket of Ste2p because of its ability to compete with α-factor and transduce a downstream signal.

After crosslinking, His-Nickel and NeutrAvidin purification enriched for the Ste2p-DHPA crosslinked product. Cyanogen bromide hydrolysis indicated a crosslinked band at 10-15 kDa as detected in a Western blot probed with NeutrAvidin, which corresponded to the TM2-EL1-TM3 fragment (T^{72}-M^{165}, ~10.6 kDa). The monoisotopic mass of TM2-EL1-TM3 fragment after CNBr digestion is expected to be 10613.811 Da and Bio-DHPA^{7} α-factor is 2282.032 Da. The expected size of TM2-EL1-TM3 and Bio-DHPA^{7} α-factor complex was expected to be about 12895 Da, but the measured peak after MALDI-TOF fractionation indicated a molecular of 12404.046 m/z. The reason for the mass difference of ~491 Da needs to be further studied. The mass spectrum from MALDI-TOF analysis (Figure 5.7) showed the monoisotopic peak at 12404.046 (m/z) within a broad band ranging from 12000 to 13000 (m/z). It is possible that the true crosslinked peak was overshadowed by the broad band.

References for Part V

1. Rosenbaum, D. M., Rasmussen, S. G., and Kobilka, B. K. (2009) The structure and function of G-protein-coupled receptors, *Nature 459*, 356-363.
2. Thomsen, W., Frazer, J., and Unett, D. (2005) Functional assays for screening GPCR targets, *Current opinion in biotechnology 16*, 655-665.
3. Klabunde, T., and Hessler, G. (2002) Drug design strategies for targeting G-protein-coupled receptors, *Chembiochem : a European journal of chemical biology 3*, 928-944.
4. Ratnala, V. R., and Kobilka, B. (2009) Understanding the ligand-receptor-G protein ternary complex for GPCR drug discovery, *Methods Mol Biol 552*, 67-77.
5. Lin, J. C., Parrish, W., Eilers, M., Smith, S. O., and Konopka, J. B. (2003) Aromatic residues at the extracellular ends of transmembrane domains 5 and 6 promote ligand activation of the G protein-coupled alpha-factor receptor, *Biochemistry 42*, 293-301.
6. Lin, J. C., Duell, K., and Konopka, J. B. (2004) A microdomain formed by the extracellular ends of the transmembrane domains promotes activation of the G protein-coupled alpha-factor receptor, *Molecular and cellular biology 24*, 2041-2051.
7. Lee, B. K., Khare, S., Naider, F., and Becker, J. M. (2001) Identification of residues of the Saccharomyces cerevisiae G protein-coupled receptor contributing to alpha-factor pheromone binding, *The Journal of biological chemistry 276*, 37950-37961.

8. Lee, B. K., Lee, Y. H., Hauser, M., Son, C. D., Khare, S., Naider, F., and Becker, J. M. (2002) Tyr266 in the sixth transmembrane domain of the yeast alpha-factor receptor plays key roles in receptor activation and ligand specificity, *Biochemistry 41*, 13681-13689.

9. Son, C. D., Sargsyan, H., Naider, F., and Becker, J. M. (2004) Identification of ligand binding regions of the Saccharomyces cerevisiae alpha-factor pheromone receptor by photoaffinity cross-linking, *Biochemistry 43*, 13193-13203.

10. Umanah, G. K., Huang, L., Ding, F. X., Arshava, B., Farley, A. R., Link, A. J., Naider, F., and Becker, J. M. (2010) Identification of residue-to-residue contact between a peptide ligand and its G protein-coupled receptor using periodate-mediated dihydroxyphenylalanine cross-linking and mass spectrometry, *The Journal of biological chemistry 285*, 39425-39436.

11. Henry, L. K., Khare, S., Son, C., Babu, V. V., Naider, F., and Becker, J. M. (2002) Identification of a contact region between the tridecapeptide alpha-factor mating pheromone of Saccharomyces cerevisiae and its G protein-coupled receptor by photoaffinity labeling, *Biochemistry 41*, 6128-6139.

12. Umanah, G. K., Son, C., Ding, F., Naider, F., and Becker, J. M. (2009) Cross-linking of a DOPA-containing peptide ligand into its G protein-coupled receptor, *Biochemistry 48*, 2033-2044.

13. Hauser, M., Kauffman, S., Lee, B. K., Naider, F., and Becker, J. M. (2007) The first extracellular loop of the Saccharomyces cerevisiae G protein-coupled

receptor Ste2p undergoes a conformational change upon ligand binding, *The Journal of biological chemistry 282*, 10387-10397.

14. Huang, L. Y., Umanah, G., Hauser, M., Son, C., Arshava, B., Naider, F., and Becker, J. M. (2008) Unnatural amino acid replacement in a yeast G protein-coupled receptor in its native environment, *Biochemistry 47*, 5638-5648.
15. Turcatti, G., Nemeth, K., Edgerton, M. D., Meseth, U., Talabot, F., Peitsch, M., Knowles, J., Vogel, H., and Chollet, A. (1996) Probing the structure and function of the tachykinin neurokinin-2 receptor through biosynthetic incorporation of fluorescent amino acids at specific sites, *The Journal of biological chemistry 271*, 19991-19998.
16. Sherman, F. (1991) Getting started with yeast, *Methods in enzymology 194*, 3-21.
17. Raths, S. K., Naider, F., and Becker, J. M. (1988) Peptide analogues compete with the binding of alpha-factor to its receptor in Saccharomyces cerevisiae, *The Journal of biological chemistry 263*, 17333-17341.
18. David, N. E., Gee, M., Andersen, B., Naider, F., Thorner, J., and Stevens, R. C. (1997) Expression and purification of the Saccharomyces cerevisiae alpha-factor receptor (Ste2p), a 7-transmembrane-segment G protein-coupled receptor, *The Journal of biological chemistry 272*, 15553-15561.
19. Burdine, L., Gillette, T. G., Lin, H. J., and Kodadek, T. (2004) Periodate-triggered cross-linking of DOPA-containing peptide-protein complexes, *Journal of the American Chemical Society 126*, 11442-11443.

20. Kraft, P., Mills, J., and Dratz, E. (2001) Mass spectrometric analysis of cyanogen bromide fragments of integral membrane proteins at the picomole level: application to rhodopsin, *Analytical biochemistry 292*, 76-86.

21. Son, C. D., Sargsyan, H., Hurst, G. B., Naider, F., and Becker, J. M. (2005) Analysis of ligand-receptor cross-linked fragments by mass spectrometry, *The journal of peptide research : official journal of the American Peptide Society 65*, 418-426.

22. Beavis, R., and Fenyo, D. (2004) Finding protein sequences using PROWL, *Current protocols in bioinformatics / editoral board, Andreas D. Baxevanis ... [et al.] Chapter 13*, Unit 13 12.

23. Bauer, A., and Kuster, B. (2003) Affinity purification-mass spectrometry. Powerful tools for the characterization of protein complexes, *European journal of biochemistry / FEBS 270*, 570-578.

24. Liu, B., Burdine, L., and Kodadek, T. (2006) Chemistry of periodate-mediated cross-linking of 3,4-dihydroxylphenylalanine-containing molecules to proteins, *Journal of the American Chemical Society 128*, 15228-15235.

PART VI

General Conclusions and Future Studies

Chapter 1

General Conclusions and Discussion

Unnatural Amino Acid Replacement in a Yeast G Protein-Coupled Receptor in its Native Environment (Incorporation of *p*-benzoyl-$_L$-phenylalanine, Bpa, into Ste2p)

In this study, we demonstrated site-specific incorporation of Bpa into Ste2p, a yeast GPCR, by using an orthologous tRNA/aminoacyl-tRNA synthetase pair. Eight mutant STE2 constructs ($F55^{TAG}$, $S107^{TAG}$, $G115^{TAG}$, $V127^{TAG}$, $G188^{TAG}$, $Y193^{TAG}$, $F204^{TAG}$, and $Y266^{TAG}$) were created by engineering the amber TAG stop codon at specific sites within the open-reading frame. An advantage of using the orthologous tRNA/aminoacyl-tRNA synthetase pair to incorporate Bpa into Ste2p in the yeast cell is that the GPCR remains in its native environment and is therefore able to interact with downstream effector molecules, such as the heterotrimeric G proteins, thus allowing assessment of both ligand binding and signal transduction pathway. The incorporation was verified by mass spectrometry, and our result indicates that, once incorporated, the photo-reactive Bpa in Ste2p in certain positions can be used to crosslink with the ligand. We demonstrated that Bpa incorporated into both the F55 (located in transmembrane domain 1, TM1) and Y193 (located in extracellular loop 2, EL2) receptors was able to capture biotinylated α-factor. Photo-reactive crosslinking can be largely competed out by the presence of excess nonbiotinylated α-factor. While F55 is positioned in the binding pocket of the receptor and was expected to interact with the pheromone (*1*), the ability of Bpa in Y193 to capture the ligand suggests a possible role for EL2 in ligand binding. We also used a novel method to supply Bpa to yeast cells via the di/tripeptide transport

system that is common to many eukaryotes (*2, 3*). Expression of the $Y193^{TAG}$ receptor as well as the $F55^{TAG}$ and $G188^{TAG}$ receptors was noticeably enhanced when the cells were grown in the presence of Met-Bpa at 0.1-0.5 mM when compared to Bpa. Because peptide transporters are ubiquitous in living cells (*3*), this method can be used to increase the delivery of unnatural amino acids and extend this approach to amino acids that are impermeable to yeast cells. These results set a stage for the use of unnatural amino acid technology in exploring the structure and interaction of integral membrane proteins in their native environment.

Changes in Conformation at the Cytoplasmic Ends of the Fifth and Sixth Transmembrane Helices of a Yeast G Protein-Coupled Rreceptor in Response to Ligand Binding (Cysteine mutations for disulfide crosslinking of residues in Ste2p)

The third intracellular loop of Ste2p has been shown to play an important role in signal transduction and is involved in Gpa1p (Gα protein in *S. cerevisiae*) activation (*4-6*). Transmembrane domain 5 (TM5) and 6 (TM6) that flank the intracellular loop 3 (IL3) have also been shown to interact with each other and have been suggested to play a critical role in signaling (*7*). In this study, we have used cysteine mutation and disulfide crosslinking analysis to determine conformational changes of residues in IL3 and the ends of TM5 and TM6 transmembrane domains of Ste2p during ligand-induced activation. The result showed strong dimer formation occurred in the IL3 Cys mutants, which is consistent with the conclusion in rhodopsin where IL3 was identified to play a role in receptor oligomerization (*8-10*). Dimer formations observed in our study were

also detected in intact cells, indicating that the disulfide bond formation between the two monomers of Ste2p occurs in the native environment of the receptor. The pattern of disulfide formation in our study, with R233C, L236C, and K239C mutant receptors having the highest percent of disulfide formation, suggests that the residues in IL3 (R^{233}–Q^{240}) may form a 3_{10} helix. Disulfide formation involving residues in the middle of IL3 was not sensitive to ligand binding, implying that residues in the IL3 loop do not change conformation or availability during receptor activation. In contrast, addition of α-factor affected the levels of disulfide formation in Cys-substituted receptors at the boundaries of TM5 and TM6, suggesting that activation of Ste2p involved ligand-induced conformational changes in the cytoplasmic ends of TM5 and TM6. A proposed model according to our experimental data would be: upon ligand binding the two dimer interfaces (TM5/TM5 and TM6/TM6) of Ste2p at the cytoplasmic end shift away from each other or become less flexible so they cannot form the disulfide bond linkage. The reduction of dimer at the cytoplasmic end of TM5 and TM6 was not observed in the presence of an α-factor antagonist, suggesting that antagonist binding to Ste2p does not induce the conformational change or alter the flexibility at the TM5 and TM6. In conclusion, we showed for the first time changes in receptor conformation or flexibility that influence disulfide formation in the region of IL3 of Ste2p close to the TM5 and TM6 boundaries. The hydrophilic residues located in the middle of the IL3 loop (R^{231}–Q^{240}) do not change conformation/availability during receptor activation, whereas many hydrophobic residues at the TM5 and TM6 cytoplasmic ends do. These conformational changes require ligand-induced activation of Ste2p and appear to depend on Ste2p–Gα

protein interactions. The pattern of disulfide formation observed is consistent with a 3_{10} helical structure in the center of IL3 and suggests that the IL3 loop of two Ste2p subunits remain close in proximity both in the active and inactive states of the receptors. Since Ste2p has been shown to have structure–function relationships similar to the physiologically and pharmacologically important rhodopsin-like GPCR family (*11*), the role of IL3 observed in this study has implications not only for Ste2p but also other GPCR systems.

Residue-to-Residue Interactions between a G Protein-Coupled Receptor (GPCR) and its Gα Protein in the *Saccharomyces cerevisiae* Model System (Cysteine mutation for disulfide crosslinking of residues in Ste2p and Gpa1p)

Several studies have shown that GPCR activation results in conformational changes at the TM5-TM6 cytoplasmic ends that appear to be essential for G protein activation in all GPCRs (*12-15*). Studies on the interactions between Ste2p and Gpa1p, its Gα protein, indicate that the Ste2p third intracellular loop (IL3) is involved in Gpa1p activation (*4-6, 16*). Like other Gα proteins in mammals, the region of Gpa1p that has been most commonly predicted to interact with Ste2p is the C-terminus (*17-19*). We have applied cysteine mutation and disulfide crosslinking to determine specific residue-to-residue interactions between Ste2p and Gpa1p. Using combinatorial expression and assay of 242 Ste2p and Gpa1p cysteine mutants, five Ste2p residues (L228C, S243C, L247C, L248C, and I249C) located at the cytoplasmic ends of the transmembrane domain 5 (TM5) and 6 (TM6) were identified to interact with five residues (Q463C, N465C,

K467C, I469C, and G470C) of the C-terminus of Gpa1p. The patterns of Gpa1p interaction with Ste2p in the presence and absence of α-factor suggest that the C-terminus of Gpa1p is closer to TM6 than TM5 in the inactive state of Ste2p. Upon α-factor binding, TM5 and TM6 of Ste2p should undergo ~30° of rotation in counterclockwise and clockwise directions, respectively, and TM6 would shift closer to TM5 as observed in other GPCRs (*2, 43*). The C-terminus of Gpa1p also undergoes two possible changes, rotational and "withdrawal" movements that are required for proper Ste2p coupling and Gpa1p activation. A rotation of the helix (C-terminus) of Gpa1p for ~120° is required for the change of interaction from Ste2p-L247C/Gpa1p-N465C in the inactive state to Ste2p-247C/Gpa1p-467C in the active state. Since TM6 is likely to undergo ~30° clockwise rotation upon ligand binding , Gpa1p may not have to rotate a full ~120° after activation; a ~90° of counterclockwise rotation in Gpa1p would be sufficient. The second conformational change consistent with our disulfide crosslinking results is what we call the "withdrawal" movement. There is a switch of interaction from Ste2p-I249C/Gpa1p-N465C in the inactive state to Ste2p-I249C/Gpa1p I469C in the active state. This switch requires the C-terminus of Gpa1p to move a distance that is approximately the height of an α-helix (~5.4 Å) and undergo a horizontal translation, which may result in about 5 Å withdrawal movement of Gpa1p from Ste2p after activation. Concerted rotational and translational movements between Ste2p and Gpa1p upon ligand binding are proposed whereby the C-terminus of Gpa1p shifts from the TM6 cytoplasmic end towards the inner core of the receptor closer to TM5 and other TMs, such as TM3. Overall, we have proposed the conformational changes in TM5 and TM6 of Ste2p upon ligand binding,

which induces rotational and translational withdrawal movements at the C-terminus of the Gpa1p. This proposed model is similar to the "translational" movement predicted by the helix-switch mechanism derived from kinetic modeling (*20*). This study is the first to identify specific residue-to-residue interactions between a GPCR and its cognate Gα protein in its active and inactive states.

Crosslinking of an α-factor Analog [K^0(BioACA), K^7(DHPA), Nle^{12}]α-factor (Bio-DHPA^7-α-factor) into its G Protein-Coupled Receptor, Ste2p (Incorporation of 3,4-dihydroxyphenylacetyl, DHPA, into α-factor and its crosslinking to Ste2p)

Besides utilizing photo-reactive crosslinking with Bpa-labeled ligand (*1, 21*) to probe the binding domain of Ste2p, we have also applied a periodate-mediated crosslinking with 3,4-dihydroxyphenylalanine (DOPA) labeled α-factor to identify specific interacting residues in Ste2p (*22, 23*). In this study, we used a DOPA-like compound, DHPA (3,4-dihydroxyphenylacetyl), as a crosslinker to investigate where lysine at the center (seventh amino acid) of α-factor binds with Ste2p. DOPA and DHPA share the dihydroxyl ring, which can be oxidized by $NaIO_4$ to form an *ortho*-quinone intermediate. This activated product has the tendency to interact with the side chains of cysteine, histidine, and lysine (*24*) and therefore can be used to map peptide ligand-protein interactions. Chemically synthesized [K^0(BioACA), K^7(DHPA), Nle^{12}]α-factor (Bio-DHPA^7 α-factor) with a DHPA attached to lysine at position 7 and biotin attached to lysine added to the amino-terminus of α-factor was used to bind to Ste2p. Even though attachment of DHPA at Lys^7 decreased binding affinity about 30 fold, it was able to

activate growth arrest in the yeast cell. With an adequate amount of Bio-DHPA^{7} α-factor present in the binding reaction, it was able to compete with the binding with α-factor. Therefore, we conclude that Bio-DHPA^{7} α-factor is likely to interact with the same or similar pocket of Ste2p because of its ability to compete with α-factor and transduce a downstream signal. Bio-DHPA^{7}-α-factor was crosslinked into Ste2p as demonstrated by a Western blot probed with NeutrAvidin-HRP conjugates to detect Bio-DHPA^{7} and Ste2p crosslinked product. The Ste2p-ligand crosslinked complex was then purified with His-Nickel to pull down Ste2p with its His tag at the C-terminus and with avidin beads to capture biotin-labeled ligand and its crosslinked products. Cyanogen bromide digestion was applied and a crosslinked fragment at the size of ~13 kDa was detected in the Western blot probed with NeutrAvidin-HRP and also by MALDI-TOF mass spectrometry. Due to the size of the crosslinked fragment we suggest that Bio-DHPA^{7} α-factor was crosslinked with transmembrane domain 2 to 3 (T^{72}-M^{165}, ~10.6 kDa) flanking extracellular loop 1 (TM2-EL1-TM3) region. Site-directed mutagenesis and tandem mass spectrometry of this region are currently being carried out in order to identify the exact crosslinked residue of Ste2p with Bio-DHPA^{7} α-factor. This study is the first to investigate the interacting residues between Ste2p and position 7 of α-factor. By determination of the Ste2p residues that interact with the first, last, and middle residues of the ligand, we expect to be able to build a better model for the interaction pocket of Ste2p and α-factor.

Summary for the structure and activation of Ste2p

The inactive, or resting, form of Ste2p serves as a restraint function to keep G proteins in the basal state and to prevent activation of pheromone response signaling in the absence of α-factor. Several pairs of residue interactions within the transmembrane domains (N^{84}-Q^{149}, V^{223}-L^{247}, Q^{253}-S^{288}, Q^{253}-S^{292}, and N^{205}-Y^{266}) (*25, 26*) have been identified to maintain inactive state of Ste2p. In addition, site-directed mutagenesis (*26-29*) has also revealed that certain residues (S^{141}, I^{153}, I^{169}, and L^{222}, P^{258}, A^{281}, and T^{282}) are essential to limit constitutive activity of Ste2p. These residues and interactions among transmembrane domains are crucial to hold the inactive confromation of Ste2p in order to avoid unnecessay cellular response.

When the ligand α-factor appears, suggested by mutagenesis studies of Ste2p (*29-34*), many residues (S^{47}, T^{48}, T^{50}, F^{55}, F^{99}, Y^{101}, L^{102}, Y^{128}, F^{204}, N^{205}, Y^{266}, D^{275}, L^{277}, A^{281}, and T^{282}) at the extracellular transmembrane boundaries of the receptor have effects on binding affinity and interactions with α-factor. According to the photo-reactive and chemical crosslinking results from our lab (*1, 22, 23, 35, 36*), several residues (F^{55}, R^{58}, C^{59}, Y^{193}, and K^{269}) of Ste2p have been identified to interact directly with the ligand and possibly reside at the binding pocket of of Ste2p for α-factor. We have also developed some preliminary evidence that a residue (or residues) in extracellular loop 1 flanking transmembrane domain 2 and transmembrane domain 3 interacts with the seventh residue of α-factor. Overall, α-factor binds or interacts with a number of residues on its receptor Ste2p to induce changes in the structure of the receptor from the inactive state to an active conformation.

After the ligand binds, confromational changes occur in Ste2p to "loosen" the resting structure to an active form. Many residues (L^{102}, N^{105}, S^{108}, Y^{111}, T^{114}, N^{132}, M^{180}, Y^{203}, F^{204}, N^{205}, L^{264}, Y^{266}, and D^{275}) have been observed to play critical roles in Ste2p activation (*29, 37, 38*). According to the preliminary data from our lab, we have discovered possible interactions between residues at the transmembrane domains (R^{58}-Q^{135} and H^{94}-E^{143}) when the receptor is in its active conformation. Through cysteine mutation and disulfide crosslinking of Ste2p in the absence and presence of α-factor, we have also determined a rotational and transitional movement in transmembrane domain 5 and 6 of actived Ste2p in concert with the activation of heterotrimeric G proteins (Gpa1p and $G_{\beta\gamma}$ subunits).

The intracellular loop 3 (*6*) and C-terminus (*39*) of Ste2p modulate the activities of the G protein complex. We identified five Ste2p residues (L^{228}, S^{243}, L^{247}, L^{248}, and I^{249}) at the cytoplasmic ends of transmembrane domain 5 and 6 that interact with five residues (Q^{463}, N^{465}, K^{467}, I^{469}, and G^{470}) at the C-terminus of Gpa1p. After the activation of Ste2p, the conformational changes of the receptor leads to a rotational and tarnsitional shift of Gpa1p, this results in about 5 Å withdrawal movement of Gpa1p away from the transmembrane core of Ste2p. The resultant conformational change of Gpa1p allows dissociation of GDP in exchange of GTP (*40*). The $G_{\beta\gamma}$ subunits then dissociate from GTP-activated Gpa1p and transmit the signal to the MAP kinase cascade (*41*) and downstream effectors, which leads to transcriptional activation of response genes, changes in morphology, and cell growth arrest.

Chapter 2

Future Studies

In these studies, we have applied three different crosslinking techniques in order to understand structure of a G protein-coupled receptor in *Saccharomyces cerevisiae* (Ste2p) and its interaction with the ligand (α-factor) and G_α protein (Gpa1p). First, *p*-benzoyl-$_L$-phenylalanine (Bpa) was incorporated into extracellular part of Ste2p as a means to capture α-factor (*36*). Bpa-labeled Ste2p was expressed successfully and two constructs was able to crosslink with α-factor. Second, cysteine mutation and disulfide bond cross-linkage were introduced to intracellular loop 3 (IL3) of Ste2p and C-terminus of Gpa1p to investigate possible interactions. IL3 appeared to be at dimer interface (*42*) and was associated with Gpa1p for conformational changes upon ligand binding. Third, chemical crosslinker 3,4-dihydroxyphenylacetyl (DHPA) was used to label lysine residue at position 7 of α-factor for crosslinking with Ste2p for determination of the binding domain. DHPA peptide bound to Ste2p specifically and was able to trigger downstream signaling. A region of Ste2p spanning from transmembrane domain 2-extracellular loop 1-transmembrane domain 3 (TM2-EL1-TM2) is likely to interact with the DHPA labeled α-factor. Here in this chapter, I am going to talk about possible applications of these techniques for future studies in order to understand the structure of Ste2p in both the resting and activated state and its interaction with its ligand and with other proteins including its Galpha-protein, intracellular regulatory proteins, and other membrane proteins.

Incorporation of *p*-benzoyl-$_L$-phenylalanine (Bpa) into Ste2p

In order to understand the interaction between a peptide ligand and its cognate GPCR, Ste2p had been used as a model system to study its binding pocket for α-factor. Site-directed mutagenesis has been carried out in many studies (*29-34*) to determine possible residues that are important for α-factor binding. Mutation of several residues at the extracellular boundaries of TMs (S^{47}, T^{48}, T^{50}, L^{102}, F^{204}, N^{205}, Y^{266}, D^{275}, L^{277}, A^{281}, and T^{282}) of Ste2p have shown to affect binding activity with the ligand after mutagenesis. Alpha-factor labeled with photo-reactive crosslinker (Bpa) and chemical crosslinker (DOPA) has been applied in our lab to capture Ste2p (*1, 21-23*), and residues R^{58}, C^{59}, and K^{269} were identified to be in close proximity to the binding pocket of the receptor. For this particular aspect of studies, the method of incorporating unnatural amino acid (Bpa) into Ste2p can be applied to substitute for these candidate residues to capture α-factor. Bpa crosslinking is very specific to amino acids within close range (3 Å) to Bpa and therefore has the advantage to define binding pocket of the receptor.

However, there are some disadvantages of Bpa incorporation. For example in our study, we chose to incroporate Bpa into residues with similar aromatic functional group or residues known to be tolerant to amino acid substitution. The side chain of Bpa may be too large to substitute for some smaller amino acids in the receptor so that those receptors will not yield natural interactions with the ligand. Also the system of unnatural amino acid replacement with TAG stop codon mutation we used in our research is not perfect since we encountered problems with "readthrough" expression and target protein degradation. Nevertheless, new approaches to improve the efficiency of unatural amino

acid incroporation has been developed (*43*), which should be very useful for studies of protein-protein interactions.

According to previous studies from our lab, the functional role of residues in the first extracellular loop (EL1) of Ste2p has been investigated by cysteine scanning mutagenesis (*37*). Five mutants were identified to be either partially (L102C and T114C) or severely (N105C, S108C, and Y111C) compromised in signaling. Furthermore, solvent accessibility of residues Y101C and Y106C decreased dramatically upon ligand binding (*44*). It was proposed that EL1 plays an important role in conformational switch that activates Ste2p and initiates signal transduction pathway. Similar to the active states of other GPCRs (bovine rhodopsin and dopamine D_2 receptor) (*45, 46*), upon ligand binding, there might be a shift in position of the helical region of EL1 that forms an activation pocket with the transmembrane (TM) domains. In addition, mutagenesis study from Konopka's group (*26*) has shown that some mutants (S141P, I153F, I169K, and L222P) of Ste2p that contained substitution within the TM domains displayed a significant increase in constitutive activity that was α-factor independent. These residues on the contrary are important to hold the receptor in inactive state, possibly through interacting with other residues in different TM domains. In order to identify possible interactions between EL1 and other TM domains and within TM-TM domains in active and inactive states, incorporation of Bpa into EL1 and suggested TM residues can be applied for photoaffinity crosslinking. With the addition of chemical or enzymatic digestion, Bpa crosslinking has great potential to determine possible binding domains.

For another application of Bpa-labeled Ste2p, intracellular interacting proteins may be identified. After ligand binds, Ste2p receptor is phosphorylated, ubiquitinated, and internalized by actin-based endocytic machinery. The intracellular proteins involved in these regulatory interactions can be "captured" by Ste2p labeled in the C-terminus or intracellular loops. Enrichment and mass spectrometry of these crosslinked proteins can lead to determination of the intracellular "interactome" both in the resting and activated (α-factor addition) states. Also, clathrin (Chc1p), which is associated with formation of internalizing cargo for endocytosis, was found to co-localize with Ste2p (*47*). It is possible that clathrin interacts with Ste2p and forms an endocytic complex for trafficking inside the cell.

A novel application of Bpa-labeled Ste2p would be to apply Bpa-mediated crosslinking to capture other membrane-bound proteins that are associated with Ste2p during ligand-mediated cell signaling or during mating. There is a pheromone-dependent interaction between Ste2p and Ste3p (the a-factor receptor) in later stages of fusion between opposite mating types of *S. cerevisiae* that may be probed with a Bpa-labeled Ste2p (*48*).

Finallly, Bpa-labeled Ste2p may be useful to identify TM-TM interactions of the resting or activated state of Ste2. Transmembrane domains 1 (TM1), 4 (TM4) and 7 (TM7) of Ste2p were identified previously to be at the dimer/oligomer interface (*49, 50*). The method of Bpa incorporation can be applied in Ste2p to confirm protein-protein interaction with other proteins and to identify potential residue-to-residue binding sites.

Cysteine Mutation for Disulfide Crosslinking of Residues in Transmembrane Domains

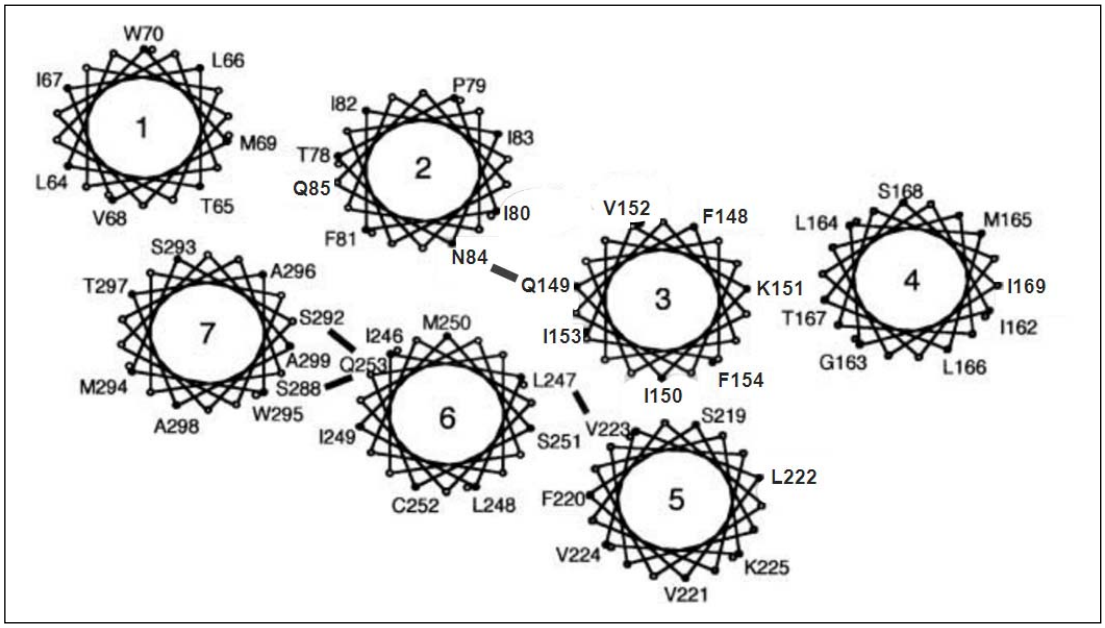

Figure 6.1 Two-dimensional structural model of the transmembrane region of the α-factor receptor (*26*). The seven helices are arranged according to the structure of rhodopsin. Solid lines between Asn84 and Gln149, Val223 and Leu247, and among Gln253, Ser288, and Ser292 indicate intramolecular interactions suggested by mutagenesis studies (*7*, *26*, *51*).

Comparison of functional equivalent regions between rhodopsin and Ste2p has revealed that there are several similarities of the polar amino acids in the transmembrane (TM) domains which might play essential roles for TM helix interaction and helix folding (*11*). According to mutagenesis and molecular modeling studies (Figure 6.1), possible interactions within the core of TM helix bundle have been predicted (*26, 51*). Residue

Asn84 in TM2 is likely to interact with Gln149 in TM3 (N^{84}-Q^{149}) based on the observation that mutants in both residues displayed strong constitutive activity (*26*). Cysteines substitution at position Val223 in TM5 and position Leu247 (V^{223}-L^{247}) in TM6 formed a disulfide bond indicating an interaction between TM5 and TM6 (*7*). Residue Gln253 in TM6 was proposed to interact with Ser288 and Ser292 in TM7 (Q^{253}-S^{288} and Q^{253}-S^{292}) also based on constitutively active mutants (*51*). The structural model shows possible orientation of Ste2p in inactive state according to the interactions bewteen TM2-TM3, TM5-TM6, and TM6-TM7 domains.

On the other hand, according to preliminary data from our lab of residue swapping in TM domains, some residue interactions in TM domains occurs after ligand binding, which suggests that interfering with TM interaction in the active conformation might lead to loss of function for Ste2p activation. In the active state of Ste2p, Arg58 in TM1 was found to potentially interact with Gln135 in TM3 (R^{58}-Q^{135}); His94 in TM2 is likely to interact with Glu143 (H^{94}-E^{143}). In conclusion, the polar residues in TM domains play important roles either to hold Ste2p in the inactive state (N^{84}-Q^{149}, V^{223}-L^{247}, Q^{253}-S^{288} and Q^{253}-S^{292}) or to promote conformational switch of Ste2p that initiates signal transduction pathway (R^{58}-Q^{135} and H^{94}-E^{143}). In order to test these proposed interactions of polar residues in TM helix of Ste2p, cysteine mutation for disulfide crosslinking can be applied to examine these TM residues. This method has been applied successfully to capture the interaction of polar residues between Asn205 at TM5 bounday and Tyr266 in TM6 (N^{205}-Y^{266}) (*25*). Cysteine mutation has the advantage to substitute specific residues

of interest and disulfide crosslinking can determine whether they are close enough (2-3 Å) for possible interaction to occur.

Incorporation of 3,4-dihydroxyphenylacetyl (DHPA) into α-factor and Ste2p

In Part V of this dissertation, I have presented the crosslinking result of 3,4-dihydroxyphenylacetyl (DHPA) labeled α-factor and Ste2p. After digestion with cyanogen bromide, a crosslinked band at 10-15 kDa was detected in the Western blot probed with NeutrAvidin, which was concluded to be at the region between transmembrane domain 2 and 3 flanking extracellular loop 1 (TM2-EL1-TM3, T^{72}-M^{165}). The band was purified and confirmed by matrix-assisted laser desorption/ionization (MALDI) mass spectrometric analysis. Until now, the exact binding residue of this fragment with Bio-$DHPA^7$ α-factor has not yet been identified. It was suggested that the position 7 side chain of α-factor is more likely to interact with a pocket formed by extracellular domains of Ste2p (*52*). Therefore, a series of site-directed mutagenesis at TM2-EL1-TM3 region should be performed to identify the exact binding site. Multiple steps of purification (His-Nickel and FLAG resin) and digestion (cyanogen bromide and trypsin) should be considered in order to enrich the crosslinked fragment, which then can be subjected to tandem mass spectrometric analysis (MS/MS) (*22*) for detailed sequencing in order to confirm the exact binding site.

An alanine scanning of α-factor by replacing each residue with Ala amino acid has been performed in order to understand the role of each residue of the peptide (*53*). Residues near the N-terminus (position 2, 3, and 4) are found to be important for receptor

activation and the ones near the C-terminus (position 11, 12, and 13) are important for binding with Ste2p. The center of α-factor contains a Pro-Gly sequence (position 7, 8, 9 and 10), which is likely to promote a β-turn and help to orient the binding and signaling domains of the pheromone. The photoreactive crosslinker *p*-benzoylphenylalanine (Bpa) has been incorporated in to different positions of α-factor (*1, 21*). Bpa-labeled α-factor analogs displayed different affinities when binding with Ste2p and only a few (Bpa1, Bpa3, and Bpa13) of them was used to crosslink with the receptor. Since previous studies from our lab with DOPA and DHPA crosslinking have shown very prominent results (*23, 42*), scanning through every residue of α-factor with chemical crosslinkers DOPA and DHPA should be considered in order to determine where it binds Ste2p. Furthermore, agonists, antagonists, and synergists of Ste2p can also be labeled with DOPA or DHPA, and then the binding site of Ste2p with different peptides can be evaluated.

The translational machinery to incorporate redox-active DHP group (3,4-dihydroxyphenylalanine, DOPA) into proteins in *E.coli* has been optimized (*54*). We anticipate that future efforts from other labs will optimize DOPA or DHPA incorporation into targeted residues of a yeast protein by using orthogonal tRNA-aminoacyl tRNA synthetase pairs. The side chain of DOPA and DHPA has the advantage to crosslink specifically with certain amino acids (cysteine, histidine, and lysine) (*24*) and therefore can be used as an alternative to Bpa crosslinking. According to our previous results, chemical crosslinkers, DOPA and DHPA, normally display stronger crosslinking signal than photo-reactive Bpa. Therefore, development to incorporate DOPA or DHPA into yeast proteins, such as Ste2p, has a great potential to identify residue-to-residue

interactions. In the extracellular side, DHPA-labeled Ste2p can be used to capture the ligand and help define the binding pocket. In the intracellular side, DHPA can crosslink and help to identify Ste2p interacting proteins.

References for Part VI

1. Son, C. D., Sargsyan, H., Naider, F., and Becker, J. M. (2004) Identification of ligand binding regions of the Saccharomyces cerevisiae alpha-factor pheromone receptor by photoaffinity cross-linking, *Biochemistry 43*, 13193-13203.
2. Daniel, H., Spanier, B., Kottra, G., and Weitz, D. (2006) From bacteria to man: archaic proton-dependent peptide transporters at work, *Physiology (Bethesda) 21*, 93-102.
3. Saier, M. H., Jr. (2000) A functional-phylogenetic classification system for transmembrane solute transporters, *Microbiology and molecular biology reviews : MMBR 64*, 354-411.
4. Clark, C. D., Palzkill, T., and Botstein, D. (1994) Systematic mutagenesis of the yeast mating pheromone receptor third intracellular loop, *The Journal of biological chemistry 269*, 8831-8841.
5. Stefan, C. J., and Blumer, K. J. (1994) The third cytoplasmic loop of a yeast G-protein-coupled receptor controls pathway activation, ligand discrimination, and receptor internalization, *Molecular and cellular biology 14*, 3339-3349.
6. Celic, A., Martin, N. P., Son, C. D., Becker, J. M., Naider, F., and Dumont, M. E. (2003) Sequences in the intracellular loops of the yeast pheromone receptor Ste2p required for G protein activation, *Biochemistry 42*, 3004-3017.
7. Dube, P., DeCostanzo, A., and Konopka, J. B. (2000) Interaction between transmembrane domains five and six of the alpha -factor receptor, *The Journal of biological chemistry 275*, 26492-26499.

8. Fotiadis, D., Liang, Y., Filipek, S., Saperstein, D. A., Engel, A., and Palczewski, K. (2003) Atomic-force microscopy: Rhodopsin dimers in native disc membranes, *Nature 421*, 127-128.

9. Liang, Y., Fotiadis, D., Filipek, S., Saperstein, D. A., Palczewski, K., and Engel, A. (2003) Organization of the G protein-coupled receptors rhodopsin and opsin in native membranes, *The Journal of biological chemistry 278*, 21655-21662.

10. Filizola, M., Wang, S. X., and Weinstein, H. (2006) Dynamic models of G-protein coupled receptor dimers: indications of asymmetry in the rhodopsin dimer from molecular dynamics simulations in a POPC bilayer, *Journal of computer-aided molecular design 20*, 405-416.

11. Eilers, M., Hornak, V., Smith, S. O., and Konopka, J. B. (2005) Comparison of class A and D G protein-coupled receptors: common features in structure and activation, *Biochemistry 44*, 8959-8975.

12. Domazet, I., Martin, S. S., Holleran, B. J., Morin, M. E., Lacasse, P., Lavigne, P., Escher, E., Leduc, R., and Guillemette, G. (2009) The fifth transmembrane domain of angiotensin II Type 1 receptor participates in the formation of the ligand-binding pocket and undergoes a counterclockwise rotation upon receptor activation, *The Journal of biological chemistry 284*, 31953-31961.

13. Reynolds, K. A., Katritch, V., and Abagyan, R. (2009) Identifying conformational changes of the beta(2) adrenoceptor that enable accurate prediction of ligand/receptor interactions and screening for GPCR modulators, *Journal of computer-aided molecular design 23*, 273-288.

14. Rosenbaum, D. M., Rasmussen, S. G., and Kobilka, B. K. (2009) The structure and function of G-protein-coupled receptors, *Nature 459*, 356-363.

15. Wess, J., Han, S. J., Kim, S. K., Jacobson, K. A., and Li, J. H. (2008) Conformational changes involved in G-protein-coupled-receptor activation, *Trends in pharmacological sciences 29*, 616-625.

16. Gladue, D. P., and Konopka, J. B. (2008) Scanning mutagenesis of regions in the Galpha protein Gpa1 that are predicted to interact with yeast mating pheromone receptors, *FEMS yeast research 8*, 71-80.

17. Kallal, L., and Kurjan, J. (1997) Analysis of the receptor binding domain of Gpa1p, the G(alpha) subunit involved in the yeast pheromone response pathway, *Molecular and cellular biology 17*, 2897-2907.

18. Cabrera-Vera, T. M., Vanhauwe, J., Thomas, T. O., Medkova, M., Preininger, A., Mazzoni, M. R., and Hamm, H. E. (2003) Insights into G protein structure, function, and regulation, *Endocrine reviews 24*, 765-781.

19. Rasmussen, S. G., DeVree, B. T., Zou, Y., Kruse, A. C., Chung, K. Y., Kobilka, T. S., Thian, F. S., Chae, P. S., Pardon, E., Calinski, D., Mathiesen, J. M., Shah, S. T., Lyons, J. A., Caffrey, M., Gellman, S. H., Steyaert, J., Skiniotis, G., Weis, W. I., Sunahara, R. K., and Kobilka, B. K. (2011) Crystal structure of the beta2 adrenergic receptor-Gs protein complex, *Nature 477*, 549-555.

20. Scheerer, P., Heck, M., Goede, A., Park, J. H., Choe, H. W., Ernst, O. P., Hofmann, K. P., and Hildebrand, P. W. (2009) Structural and kinetic modeling of an activating helix switch in the rhodopsin-transducin interface, *Proceedings of*

the National Academy of Sciences of the United States of America 106, 10660-10665.

21. Henry, L. K., Khare, S., Son, C., Babu, V. V., Naider, F., and Becker, J. M. (2002) Identification of a contact region between the tridecapeptide alpha-factor mating pheromone of Saccharomyces cerevisiae and its G protein-coupled receptor by photoaffinity labeling, *Biochemistry 41*, 6128-6139.

22. Umanah, G. K., Huang, L., Ding, F. X., Arshava, B., Farley, A. R., Link, A. J., Naider, F., and Becker, J. M. (2010) Identification of residue-to-residue contact between a peptide ligand and its G protein-coupled receptor using periodate-mediated dihydroxyphenylalanine cross-linking and mass spectrometry, *The Journal of biological chemistry 285*, 39425-39436.

23. Umanah, G. K., Son, C., Ding, F., Naider, F., and Becker, J. M. (2009) Cross-linking of a DOPA-containing peptide ligand into its G protein-coupled receptor, *Biochemistry 48*, 2033-2044.

24. Liu, B., Burdine, L., and Kodadek, T. (2006) Chemistry of periodate-mediated cross-linking of 3,4-dihydroxylphenylalanine-containing molecules to proteins, *Journal of the American Chemical Society 128*, 15228-15235.

25. Lee, Y. H., Naider, F., and Becker, J. M. (2006) Interacting residues in an activated state of a G protein-coupled receptor, *The Journal of biological chemistry 281*, 2263-2272.

26. Parrish, W., Eilers, M., Ying, W., and Konopka, J. B. (2002) The cytoplasmic end of transmembrane domain 3 regulates the activity of the Saccharomyces cerevisiae G-protein-coupled alpha-factor receptor, *Genetics 160*, 429-443.

27. Konopka, J. B., Margarit, S. M., and Dube, P. (1996) Mutation of Pro-258 in transmembrane domain 6 constitutively activates the G protein-coupled alpha-factor receptor, *Proceedings of the National Academy of Sciences of the United States of America 93*, 6764-6769.

28. Stefan, C. J., Overton, M. C., and Blumer, K. J. (1998) Mechanisms governing the activation and trafficking of yeast G protein-coupled receptors, *Molecular biology of the cell 9*, 885-899.

29. Lin, J. C., Duell, K., Saracino, M., and Konopka, J. B. (2005) Identification of residues that contribute to receptor activation through the analysis of compensatory mutations in the G protein-coupled alpha-factor receptor, *Biochemistry 44*, 1278-1287.

30. Bajaj, A., Connelly, S. M., Gehret, A. U., Naider, F., and Dumont, M. E. (2007) Role of extracellular charged amino acids in the yeast alpha-factor receptor, *Biochimica et biophysica acta 1773*, 707-717.

31. Lee, B. K., Khare, S., Naider, F., and Becker, J. M. (2001) Identification of residues of the Saccharomyces cerevisiae G protein-coupled receptor contributing to alpha-factor pheromone binding, *The Journal of biological chemistry 276*, 37950-37961.

32. Lee, B. K., Lee, Y. H., Hauser, M., Son, C. D., Khare, S., Naider, F., and Becker, J. M. (2002) Tyr266 in the sixth transmembrane domain of the yeast alpha-factor receptor plays key roles in receptor activation and ligand specificity, *Biochemistry 41*, 13681-13689.

33. Lin, J. C., Duell, K., and Konopka, J. B. (2004) A microdomain formed by the extracellular ends of the transmembrane domains promotes activation of the G protein-coupled alpha-factor receptor, *Molecular and cellular biology 24*, 2041-2051.

34. Lin, J. C., Parrish, W., Eilers, M., Smith, S. O., and Konopka, J. B. (2003) Aromatic residues at the extracellular ends of transmembrane domains 5 and 6 promote ligand activation of the G protein-coupled alpha-factor receptor, *Biochemistry 42*, 293-301.

35. Abel, M. G., Lee, B. K., Naider, F., and Becker, J. M. (1998) Mutations affecting ligand specificity of the G-protein-coupled receptor for the Saccharomyces cerevisiae tridecapeptide pheromone, *Biochimica et biophysica acta 1448*, 12-26.

36. Huang, L. Y., Umanah, G., Hauser, M., Son, C., Arshava, B., Naider, F., and Becker, J. M. (2008) Unnatural amino acid replacement in a yeast G protein-coupled receptor in its native environment, *Biochemistry 47*, 5638-5648.

37. Akal-Strader, A., Khare, S., Xu, D., Naider, F., and Becker, J. M. (2002) Residues in the first extracellular loop of a G protein-coupled receptor play a role in signal transduction, *The Journal of biological chemistry 277*, 30581-30590.

38. Dosil, M., Giot, L., Davis, C., and Konopka, J. B. (1998) Dominant-negative mutations in the G-protein-coupled alpha-factor receptor map to the extracellular ends of the transmembrane segments, *Molecular and cellular biology 18*, 5981-5991.

39. Yi, T. M., Kitano, H., and Simon, M. I. (2003) A quantitative characterization of the yeast heterotrimeric G protein cycle, *Proceedings of the National Academy of Sciences of the United States of America 100*, 10764-10769.

40. Wall, M. A., Coleman, D. E., Lee, E., Iniguez-Lluhi, J. A., Posner, B. A., Gilman, A. G., and Sprang, S. R. (1995) The structure of the G protein heterotrimer Gi alpha 1 beta 1 gamma 2, *Cell 83*, 1047-1058.

41. Dowell, S. J., Bishop, A. L., Dyos, S. L., Brown, A. J., and Whiteway, M. S. (1998) Mapping of a yeast G protein betagamma signaling interaction, *Genetics 150*, 1407-1417.

42. Umanah, G. K., Huang, L. Y., Maccarone, J. M., Naider, F., and Becker, J. M. (2011) Changes in conformation at the cytoplasmic ends of the fifth and sixth transmembrane helices of a yeast G protein-coupled receptor in response to ligand binding, *Biochemistry 50*, 6841-6854.

43. Wang, Q., and Wang, L. (2008) New methods enabling efficient incorporation of unnatural amino acids in yeast, *Journal of the American Chemical Society 130*, 6066-6067.

44. Hauser, M., Kauffman, S., Lee, B. K., Naider, F., and Becker, J. M. (2007) The first extracellular loop of the Saccharomyces cerevisiae G protein-coupled

receptor Ste2p undergoes a conformational change upon ligand binding, *The Journal of biological chemistry 282*, 10387-10397.

45. Palczewski, K., Kumasaka, T., Hori, T., Behnke, C. A., Motoshima, H., Fox, B. A., Le Trong, I., Teller, D. C., Okada, T., Stenkamp, R. E., Yamamoto, M., and Miyano, M. (2000) Crystal structure of rhodopsin: A G protein-coupled receptor, *Science 289*, 739-745.

46. Shi, L., and Javitch, J. A. (2004) The second extracellular loop of the dopamine D2 receptor lines the binding-site crevice, *Proceedings of the National Academy of Sciences of the United States of America 101*, 440-445.

47. Newpher, T. M., Smith, R. P., Lemmon, V., and Lemmon, S. K. (2005) In vivo dynamics of clathrin and its adaptor-dependent recruitment to the actin-based endocytic machinery in yeast, *Developmental cell 9*, 87-98.

48. Shi, C., Kaminskyj, S., Caldwell, S., and Loewen, M. C. (2007) A role for a complex between activated G protein-coupled receptors in yeast cellular mating, *Proceedings of the National Academy of Sciences of the United States of America 104*, 5395-5400.

49. Wang, H. X., and Konopka, J. B. (2009) Identification of amino acids at two dimer interface regions of the alpha-factor receptor (Ste2), *Biochemistry 48*, 7132-7139.

50. Kim, H., Lee, B. K., Naider, F., and Becker, J. M. (2009) Identification of specific transmembrane residues and ligand-induced interface changes involved in homo-

dimer formation of a yeast G protein-coupled receptor, *Biochemistry 48*, 10976-10987.

51. Dube, P., and Konopka, J. B. (1998) Identification of a polar region in transmembrane domain 6 that regulates the function of the G protein-coupled alpha-factor receptor, *Molecular and cellular biology 18*, 7205-7215.

52. Ding, F. X., Lee, B. K., Hauser, M., Patri, R., Arshava, B., Becker, J. M., and Naider, F. (2002) Study of the binding environment of alpha-factor in its G protein-coupled receptor using fluorescence spectroscopy, *The journal of peptide research : official journal of the American Peptide Society 60*, 65-74.

53. Naider, F., and Becker, J. M. (2004) The alpha-factor mating pheromone of Saccharomyces cerevisiae: a model for studying the interaction of peptide hormones and G protein-coupled receptors, *Peptides 25*, 1441-1463.

54. Alfonta, L., Zhang, Z., Uryu, S., Loo, J. A., and Schultz, P. G. (2003) Site-specific incorporation of a redox-active amino acid into proteins, *Journal of the American Chemical Society 125*, 14662-14663.

VITA

Li-Yin Huang was born in Chiayi, Taiwan. She graduated from National Yang-Ming University and received her Bachelor of Science degree in Medical Radiation Technology. She received her Master of Science degree in Biomedical Engineering from National Cheng Kung University. After her Master degree, she worked as a research assistant in the Department of Medical Laboratory Science and Biotechnology in National Cheng Kung University. She was accepted to the Ph.D. program in Microbiology Department at the University of Tennessee, Knoxville. She did her graduate work in Dr. Jeffrey M. Becker's laboratory. Throughout the course of her time in this program, she served as a graduate teaching and research assistant. She received her Doctor of Philosophy degree in Microbiology.